A Hydrodynamic Model of the North and South Rivers Estuary using RMA-10

by

Cameron K. Tana

B.S., Civil and Environmental Engineering
A.B., Economics
Stanford University, 1998

Submitted to the Department of Civil and Environmental Engineering in partial fulfillment of the requirements for the degree of

Master of Engineering in Civil and Environmental Engineering

at the

MASSACHUSETTS INSTITUTE OF TECHNOLOGY

June 1999

Author.....
Department of Civil and Environmental Engineering
May 14, 1999

Certified by.....
Dr. M. Llewellyn Thatcher
Lecturer in Civil and Environmental Engineering
Thesis Supervisor

Accepted by.....
Andrew J. Whittle
Chairman, Departmental Committee on Graduate Studies

A Hydrodynamic Model of the North and South Rivers Estuary using RMA-10

by

Cameron K. Tana

Submitted to the Department of Civil and Environmental Engineering
On May 13, 1999 in Partial Fulfillment of the
Requirements for the Degree of Master of Engineering in
Civil and Environmental Engineering

ABSTRACT

This study details the development of a hydrodynamic model for the North and South Rivers estuary in Massachusetts. Tidal influence dominates freshwater inflow in this small estuary. Other complicating factors for hydrodynamics include the presence of tidal flats, marshlands, and the confluence between the two rivers and Massachusetts Bay.

RMA-10, a finite element hydrodynamics program, is used to model the estuary. The model is transient – allowing for the resolution of the tidal cycle. This application of the program uses depth-averaged elements to represent the system.

Three schemes are used for the system. The first scheme is essentially one-dimensional with a constant Manning's n friction coefficient over the estuary. The failure of this scheme to calibrate with pressure and velocity data shows that friction characteristics vary with location in the estuary. The second scheme is a similar representation of the geometry as the first scheme, but Manning's n varies with distance. By using a higher than typical value of Manning's n at the mouth and more typical values upstream, this scheme calibrates and verifies well with pressure and velocity data. The variation of Manning's n in this scheme shows that features near the estuary's mouth are important for adding drag to the system. The third scheme represents tidal flats, whereas the first two schemes do not. This scheme is a better representation of the physics of the flow at the mouth than the first two schemes.

The output of the hydrodynamics model can be used as an input to a water quality model of the North and South Rivers estuary. The calibrated and verified second scheme is appropriate for use in modeling water quality. The third scheme is currently unable to model water quality, because numerical approximations for scalar transport using this scheme do not converge.

Thesis Supervisor: M. Llewellyn Thatcher
Title: Lecturer in Civil and Environmental Engineering

Acknowledgements

First and foremost, I would like to thank Lew Thatcher for his kind and generous guidance in acting as my thesis supervisor. Not only did he travel from his home on the North River to meet with me twice a week to discuss the project, he was always available for support in figuring out the mysteries that RMA-10 sometimes presents.

Eric Adams also deserves heartfelt props. Besides being available as a resource to discuss the hydrodynamics issues of the rivers, he always had good ideas for making the work better. His occasionally different point of view challenged me and I appreciate it.

In many ways, the work of Rocky Geyer of Woods Hole Oceanographic Institute on the North River in the summer of 1997 allowed my work to be legitimate. His time series data set of pressure and salinity in the North River formed the basis for the model's calibration and verification. I thank him for allowing me to use his unpublished data. I am hoping his work does not remain unpublished for long.

Thanks to Ian King for letting me use the RMA family of models free of charge.

Sylvia Lee was a great teammate to have on this project. Her work makes my work worthwhile and I appreciate her dedication and support. Also, she laughed at my jokes.

I would also like to thank Steve Ivas of the North and South Rivers Watershed Association for his unflagging enthusiasm for what I was doing. I would be remiss not to thank the Association for allowing me to raid their library. I would also like to say thanks for caring; you have a beautiful estuary and I am glad somebody is watching over it.

Others at MIT helped me out quite a bit. Heidi Nepf gave me a working understanding of flow through vegetation. Kathy MacLaughlin helped formulate our project goals. The rest of the M.Eng. group was in the same boat so I always had an understanding ear for my articulation of the project's challenges. Finally, I'd like to thank my roommates Ivan and Brian for being great guys.

Also, thanks to the Department of Civil and Environmental Engineering for their financial support, especially for the rental car. Also, I give appreciation to the Stanford athletics program and KZSU-FM, for paving the way to the Sears Graduate Scholarship.

Of course, my education would not be possible without the Tana Family Scholarship. But way beyond that, my family's emotional support has always been there. Thanks to dad for writing two letters a week, mom for caring a lot, and my brother Evan for being excited about life.

In closing, I would like to thank my future wife. I don't know who she is, but I'm sure she'll be easier to find now that I have completed this thesis.

Table of Contents

List of Figures

List of Tables

1. Background

1.1 Location

The North and South Rivers, located approximately 30 miles south of Boston, Massachusetts (Figure 1.1), wind through several suburban towns and discharge to Massachusetts Bay (Figure 1.2). The rivers are tidal; the tidal head of the North River is 20 kilometers upstream and the tidal head of the South River is about 10 kilometers upstream. The two rivers share an inlet, known as New Inlet, located in Scituate, Massachusetts. The rivers form a complex estuary with changing geometry and flows, or hydrodynamics. In addition, marshland and wetland areas border the rivers.

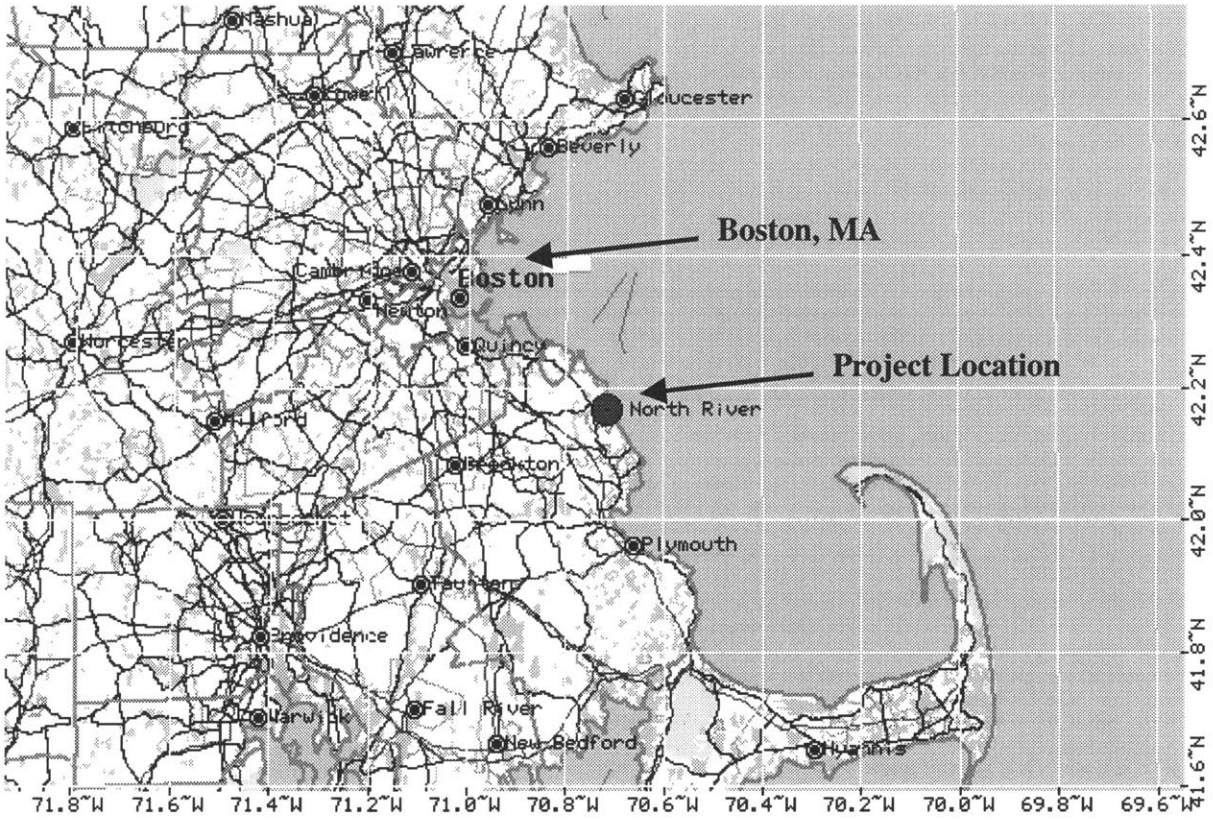

Figure 1.1 Location of North and South Rivers

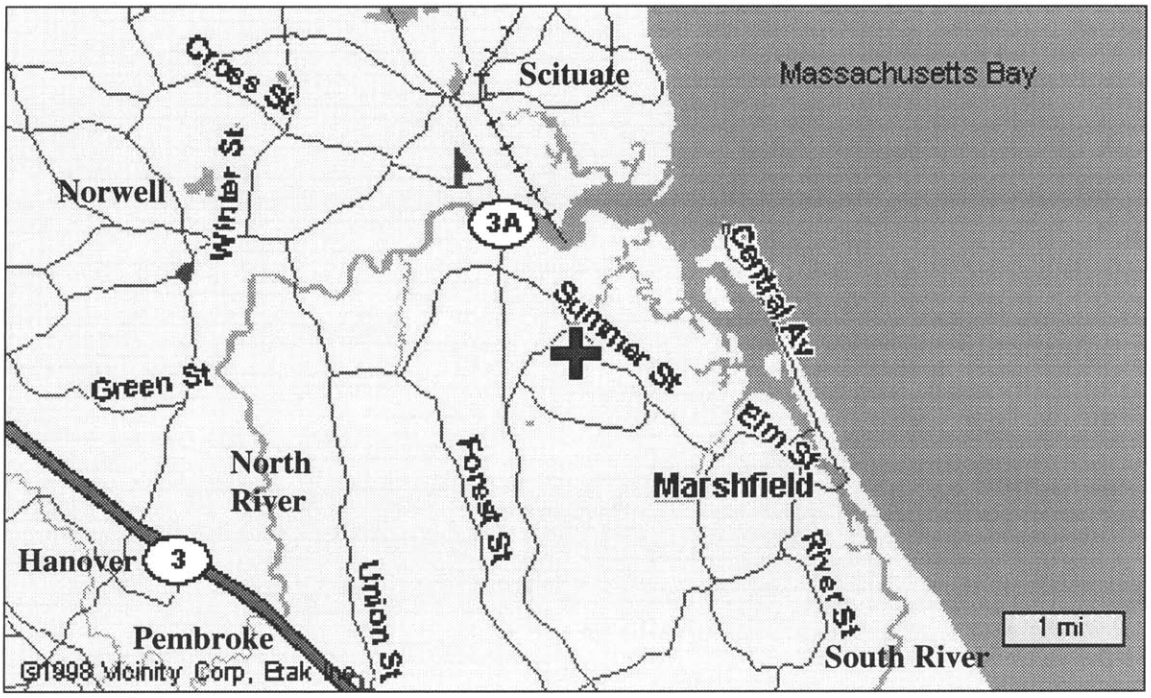

Figure 1.2 Map of North and South Rivers

1.2 Values of the Watershed

The North and South Rivers provide many intrinsic benefits. The locals take pride in the history of the North River as an important center of shipbuilding. Presently, recreational benefits include boating and swimming. The rivers also have the potential to support fishing and shellfish harvesting. Perhaps most importantly, the rivers provide a rich habitat for wildlife and a beautiful natural setting for residents and visitors.

1.3 The North and South Rivers Watershed Association

The North and South Rivers Watershed Association, Inc. (NSRWA) is a group of local citizens who are concerned with improving and preserving the unique watershed in which they live. In

addition to organizing recreational events such as boating events and nature walks, NSRWA is active in evaluating water quality issues in the watershed. For example, NSRWA has commissioned water quality reports for the North River by Baystate Environmental Consultants (1990,1991). Currently, NSRWA is implementing the South River Initiative, which will focus attention on the water quality of the little studied South River. NSRWA also administers RiverWatch, which is a summertime water quality monitoring program.

1.4 Water Quality Concerns

NSRWA is concerned with several water quality problems in the watershed. First, the Department of Marine Fisheries has closed shellfish harvesting beds due to high fecal coliform counts. Second, high quantities of fecal coliform present a health hazard to recreational users of the rivers. In general, NSRWA is concerned with how changes in water quality affect the ecological health of the rivers. These water quality concerns include other pollutants besides fecal coliform, such as nutrients.

1.5 Project Scope

To address the concerns of NSRWA, computer models capable of interpreting the complicated hydrodynamics and water quality issues of the North and South Rivers have been developed (Lee and Tana, 1999). NSRWA will be able to use the models as tools to evaluate the response of the North and South Rivers to point and non-point pollution sources and identify areas of the rivers that are most susceptible to pollution.

This particular study uses the developed models to characterize fecal coliform contamination in the rivers (Lee, 1999; Lee and Tana, 1999). This involves quantifying the sources of fecal coliform in the watershed. The developed models calculate the effects of these estimated coliform loads on water quality in the rivers during the summertime. The summertime is the period of concern because recreational usage of the rivers is highest in the summer and past

sampling activity has shown that pollutant concentrations are higher in the summer than during other seasons.

1.6 Future uses of the models

NSRWA can use the models for proactive decision making in the management of the watershed such as:

- Warning residents and recreational users under what conditions the concentrations of pollutants may be high.
- Characterizing water quality in sensitive areas of the watershed including areas containing threatened species.
- Evaluating different pollution management plans and characterizing the resulting water quality improvements in the rivers due to the policies.
- Using the model as a visual educational tool to help residents, recreational users, business owners and developers understand the effect they have on the rivers.

1.7 Report Organization

This thesis details the development of a hydrodynamic model for the North and South Rivers. This hydrodynamic model serves as a necessary input for the fecal coliform water quality model of the North and South Rivers developed by Lee (1999). In addition, the work extends the investigation of the hydrodynamics beyond the input used by Lee for water quality.

Chapter 2 describes the hydrodynamic characteristics of the North and South Rivers. Chapter 3 introduces RMA-10, the hydrodynamic modeling program used for application to this estuary. Chapter 4 discusses how the model represents the North and South Rivers in space and time with different schematizations. Chapter 5 outlines the treatment of boundary conditions. Chapters 6-9 discuss model calibration for three different model schemes against data for velocity, depth changes, and salinity. Chapter 10 discusses the marshlands, a main feature of the estuary that is

not modeled, and how the marshlands might be modeled in the future. Chapter 11 gives final conclusions.

2. North and South Rivers Hydrodynamic Characteristics

The North and South Rivers estuary has several characteristics that complicate the hydrodynamics. These complications increase the importance of creating a highly resolved hydrodynamics input to a water quality model for the estuary. The changing flows in the rivers have a great effect on the changing water quality of the rivers. These hydrodynamic characteristics include the large tidal range relative to freshwater input, the shared confluence of the North and South Rivers, and the presence of tidal flats and marshlands. There have apparently been few modeling studies of hydrodynamics in small estuaries of this type.

2.1 Tidal Range

The influence of the tide of the North and South Rivers system is large relative to the influence of freshwater flow. The depths are very low at low tide and increase greatly at high tide – changing the character of the hydrodynamics. At the mouth, the tidal range is nearly 3 meters (NOS Tidal Bench Marks, 1991), and the mean depth is about 5 meters. In reaches approximately 8 km upstream of the mouth on the North River, the mean depth is about 2 meters (Geyer, 1997). Dr. W.R. Geyer of the Woods Hole Oceanographic Institute measured changes of depth at Route 3 with a pressure gage (Figure 2.1). The measured tidal range at these upstream locations is between 1.5 – 2 meters. Low water is around one meter deep, but high water is nearly three meters deep. Near the South River head, the low water depth is less than 1 meter and the tidal range is approximately 2 meters.

Comparison of the tidal prism volume to the freshwater inflow over a tidal cycle further emphasizes the importance of the tide. Assuming the average characteristics of the rivers in Table 2.1, the tidal prism for the North River is 800,000 cubic meters and the prism for the South River is 400,000 cubic meters. USGS stream gage values at Curtis Crossing on Indian Head River at the North River tidal head represent about 80 km^2 of drainage area.

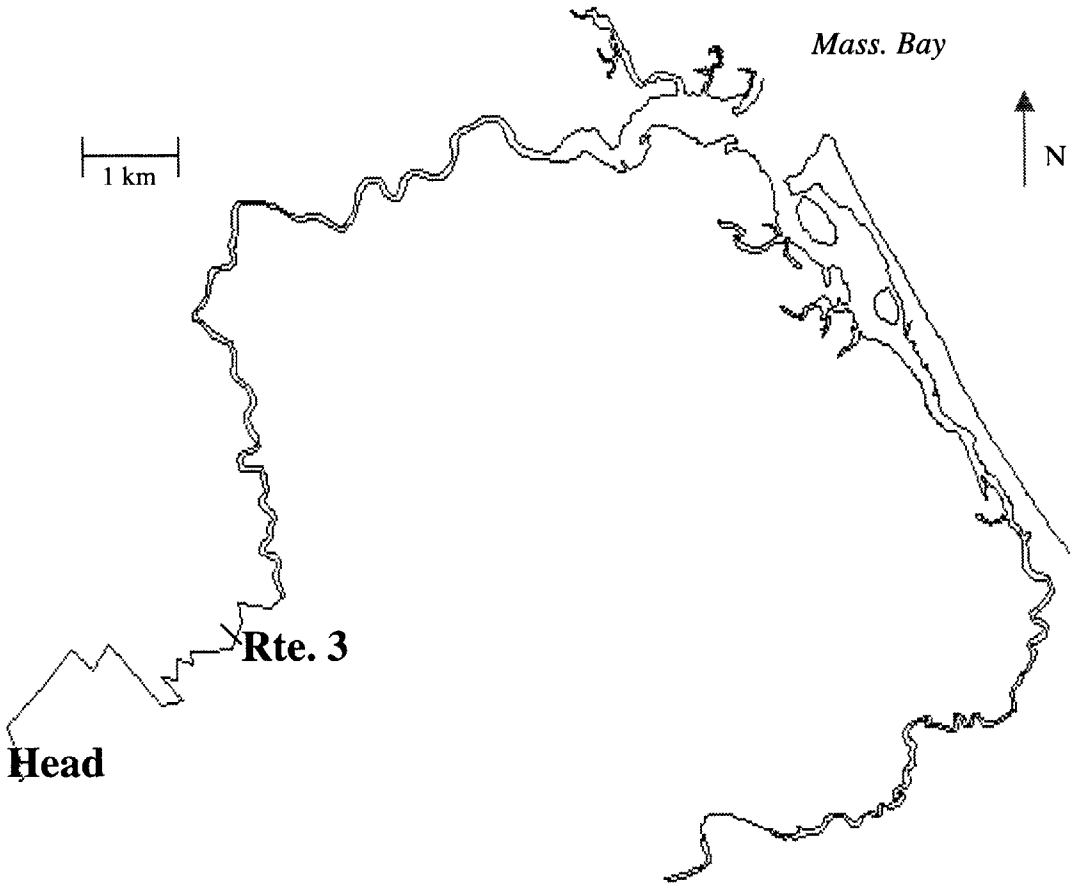

Figure 2.1 Location of Upstream Pressure Gauge Station and North River Tidal Head

Extrapolating these values for the entire drainage area as given by Wandle and Morgan (1984), we can calculate the total freshwater inflow volume over a tidal cycle. In the summer, average Curtis Crossing flows are less than 0.75 m^3/s; this translates to 72,900 m^3 of North River freshwater and 24,300 m^3 of South River freshwater in a tidal cycle. The tidal prism volume is over 10 times the freshwater volume in the summer. Although most water quality concerns take

place during the summer and the summer is the focus of this study, the tidal prism still dominates during high inflows in the winter and spring. The average flow in months with high flow is about 3 m^3 of inflow at Curtis Crossing (Figure 2.2), but the tidal prism volume is still more than two times the freshwater volume entering over a tidal cycle.

River	Length to Tidal Head (km)	Avg. Width (m)	Average Tidal Range (m)	Total Drainage Area (km^2)
North	20	40	2	180
South	10	20	2	60

Table 2.1 Estimated Average Characteristics of North and South Rivers

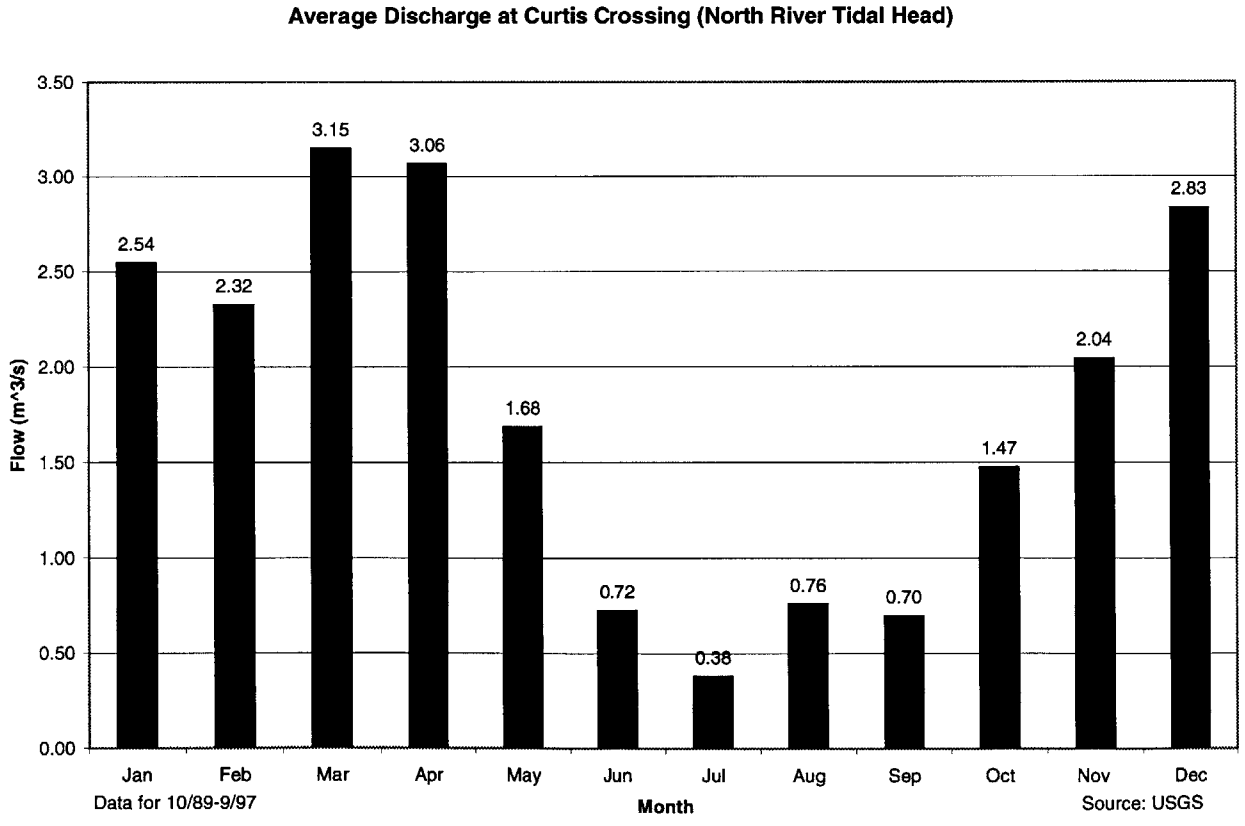

Figure 2.2 Monthly Average Inflow at North River Tidal Head (USGS Station 01105730)

2.2 Shared Confluence

Two rivers form this estuary and they share an inlet to Massachusetts Bay. New Inlet (Figure 2.3) splits into the North and South Rivers between Third and Fourth Cliffs of Scituate, MA. An example of the dynamics of this confluence is the fact that the mouth used to be about six kilometers southeast of the current confluence. The Portland Gale of 1898 closed off the Old Mouth and created New Inlet (NSRWA, 1997). In addition, local boaters recount stories of frequent capsizes in the confluence area and the North and South Rivers Watershed Association warns that New Inlet is hazardous to all watercraft (NSRWA, 1997).

2.3 Tidal Flats

In the North and South Rivers system, a main channel conveys water over the whole tidal cycle. However, the large tidal range results in flooding of areas adjacent to the main channel at high tide. The first areas that flood are tidal flats that generally inundate every tidal cycle (rivers' shaded areas in Figure 2.3). These areas are void of plants and surround the main (low water) channel up to the Route 3A bridge (three kilometers from the mouth) on the North River and the Julian St. Bridge (five kilometers from the mouth) on the South River. These tidal flats cause the river near the mouth to widen considerably and quickly at high tide. The tidal flats more than double the width of the channel in some areas near the mouth.

2.4 Marshlands

Behind the tidal flats near the mouth and bordering the main channel further upstream are salt marshes and freshwater wetlands (white areas with blue markings in Figure 2.3). These wetlands frequently flood during high tide and provide additional spreading of the water in the same manner as the tidal flats. In addition, the marshes provide two other complicating factors to the flow. First, many narrow (1 meter wide) ditches are cut through the marshes originally for the purpose of mosquito control. Second, the dense plant growth significantly changes the physics of flow resistance.

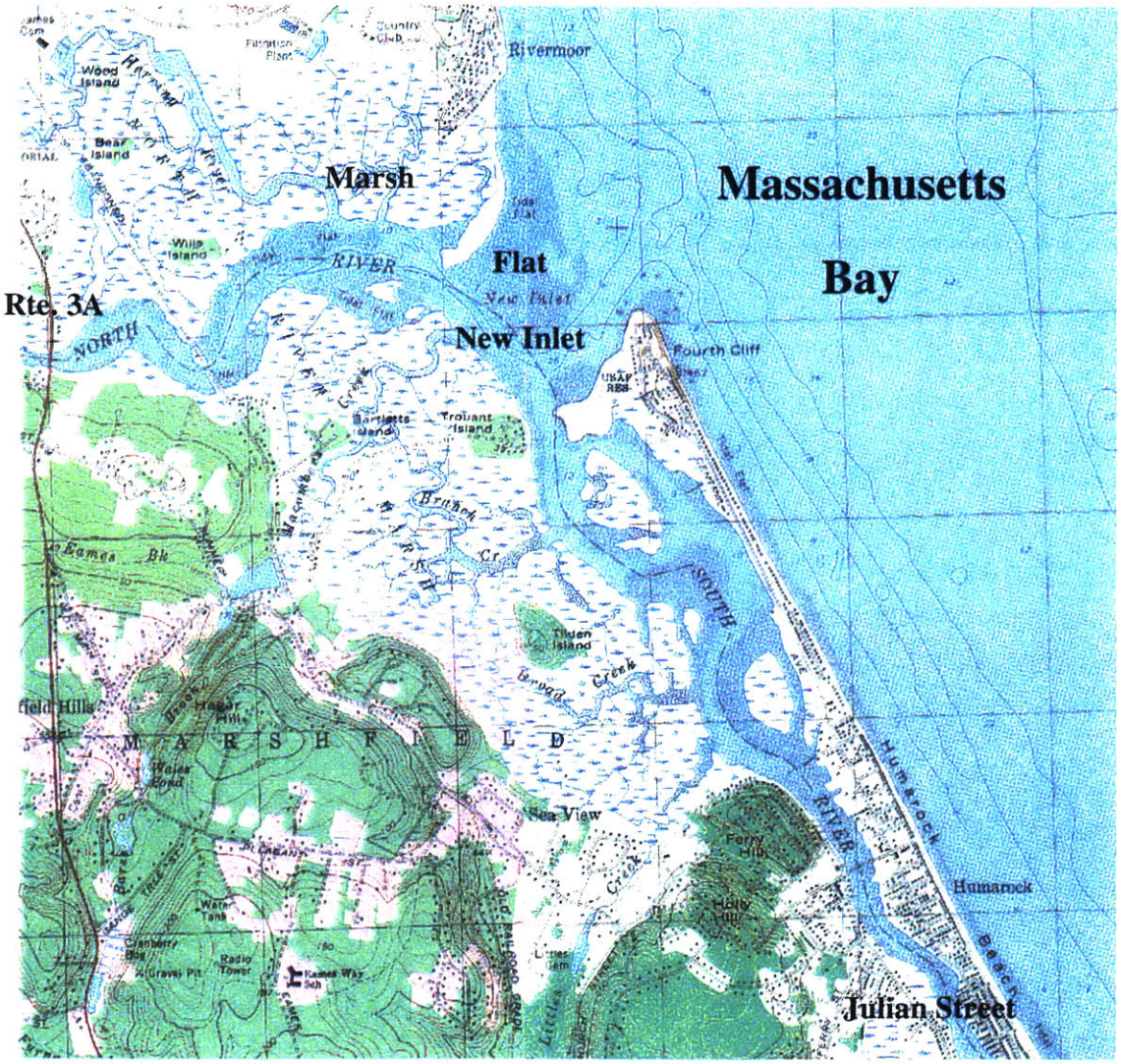

Figure 2.3 USGS Topographic Map of New Inlet, Tidal Flats, and Marshlands

3. RMA-10 Model

In order to model the hydrodynamics of the North and South Rivers estuary, the study uses RMA-10 (King, 1993), a FORTRAN program that numerically approximates solutions to the equations governing fluid flow. In addition, RMA-10 solves the transport equation for modeling the salinity distribution in a water body. RMA-10 is a transient model – allowing for the model to resolve the changes over the tidal cycle. RMA-10 is a finite element model so the complex geometry of the estuary can be represented to a high resolution. In addition, RMA-10 allows for one-dimensional, two-dimensional, and three-dimensional elements. This application of the program uses two-dimensional elements exclusively, but the expansion of the model to three-dimensional elements is possible where necessary.

3.1 Governing Equations

The equations that RMA-10 solves in order to model the hydrodynamics and salinity are the conservation equation, the momentum equations, and the transport equation.

3.1.1 Conservation Equation

The conservation equation says that the net mass inflow into a control volume must equal the change in the storage of mass in the volume. If this concept is applied to an infinitesimal control volume and an incompressible fluid, the governing conservation equation used by RMA-10 is derived (Equation 3.1).

$$\frac{\partial u}{\partial x}+\frac{\partial v}{\partial y}+\frac{\partial w}{\partial z}=0 \tag{3.1}$$

where x,y,z = the Cartesian coordinate system with z in the vertical upward direction
u,v,w = corresponding velocities in the Cartesian direction

For two-dimensional depth averaged flow, which is used in this model of the North and South Rivers, the equation reduces to the following (Equation 3.2) with the inclusion of water depth.

$$h(\frac{\partial u}{\partial x}+\frac{\partial v}{\partial y})+u\frac{\partial h}{\partial x}+v\frac{\partial h}{\partial y}+\frac{\partial h}{\partial t}-q_A=0 \qquad (3.2)$$

where h = water depth
q_A = element inflow per unit area

3.1.2 Momentum Equations

The equations for the conservation of momentum are based on the following concept: a change of momentum in a control volume is equal to the net flux of momentum in and out of the control volume plus any impulse applied to the volume. These equations (Equations 3.3), also known as the Navier-Stokes equations, are derived when the above concept is applied to an infinitesimal control volume for an incompressible fluid.

$$\frac{\partial u}{\partial t}+u\frac{\partial u}{\partial x}+v\frac{\partial u}{\partial y}+w\frac{\partial u}{\partial z}-fv-\frac{\partial}{\partial x}(\varepsilon_{xx}\frac{\partial u}{\partial x})-\frac{\partial}{\partial y}(\varepsilon_{yx}\frac{\partial u}{\partial y})-\frac{\partial}{\partial z}(\varepsilon_{zx}\frac{\partial u}{\partial z})+\frac{1}{\rho}\frac{\partial p}{\partial x}=0 \qquad (3.3a)$$

$$\frac{\partial v}{\partial t}+u\frac{\partial v}{\partial x}+v\frac{\partial v}{\partial y}+w\frac{\partial v}{\partial z}+fu-\frac{\partial}{\partial x}(\varepsilon_{xy}\frac{\partial v}{\partial x})-\frac{\partial}{\partial y}(\varepsilon_{yy}\frac{\partial v}{\partial y})-\frac{\partial}{\partial z}(\varepsilon_{zy}\frac{\partial v}{\partial z})+\frac{1}{\rho}\frac{\partial p}{\partial y}=0 \qquad (3.3b)$$

$$\frac{\partial w}{\partial t}+u\frac{\partial w}{\partial x}+v\frac{\partial w}{\partial y}+w\frac{\partial w}{\partial z}-\frac{\partial}{\partial x}(\varepsilon_{xz}\frac{\partial w}{\partial x})-\frac{\partial}{\partial y}(\varepsilon_{yz}\frac{\partial w}{\partial y})-\frac{\partial}{\partial z}(\varepsilon_{zz}\frac{\partial w}{\partial z})+g+\frac{1}{\rho}\frac{\partial p}{\partial z}=0 \qquad (3.3c)$$

where ρ = density
g = downward acceleration due to gravity
p = water pressure
ε = kinematic turbulent eddy coefficients
f = Coriolis factor=$2\omega\sin\phi$
$\omega = 7.3 \times 10^{-5}$ radians/sec
ϕ = Latitude (positive north of the equator)

For two-dimensional depth averaged flow, the three equations (Equations 3.3) reduce to two equations since all derivatives with respect to z become zero. In terms of water depth, the two remaining equations (Equations 3.4) that RMA-10 solves are:

$$\frac{\partial u}{\partial t}+u\frac{\partial u}{\partial x}+v\frac{\partial u}{\partial y}-fv-\frac{1}{h}\frac{\partial}{\partial x}(h\varepsilon_{xx}\frac{\partial u}{\partial x})-\frac{1}{h}\frac{\partial}{\partial y}(h\varepsilon_{xy}\frac{\partial u}{\partial y})+g\frac{\partial \eta}{\partial x}+\frac{1}{\rho}g\eta\frac{\partial \rho}{\partial x}+\frac{1}{\rho}\Gamma_{hx}=0 \quad (3.4a)$$

$$\frac{\partial v}{\partial t}+u\frac{\partial v}{\partial x}+v\frac{\partial v}{\partial y}+fu-\frac{1}{h}\frac{\partial}{\partial x}(h\varepsilon_{yx}\frac{\partial v}{\partial x})-\frac{1}{h}\frac{\partial}{\partial y}(h\varepsilon_{yy}\frac{\partial v}{\partial y})+g\frac{\partial \eta}{\partial y}+\frac{1}{\rho}g\eta\frac{\partial \rho}{\partial y}+\frac{1}{\rho}\Gamma_{hy}=0 \quad (3.4b)$$

where Γ_h = depth averaged external tractions such as bottom friction and wind stress
η = water elevation relative to a fixed horizontal datum

3.1.3 Transport Equation

For modeling transport of scalars such as salt, the advection-diffusion equation is the governing equation. This equation (Equation 3.5) expresses the conservation of mass of a scalar like salt in an infinitesimal control volume.

$$\frac{\partial S}{\partial t}+u\frac{\partial S}{\partial x}+v\frac{\partial S}{\partial y}+w\frac{\partial S}{\partial z}-\frac{\partial}{\partial x}(D_x\frac{\partial S}{\partial x})-\frac{\partial}{\partial y}(D_y\frac{\partial S}{\partial y})-\frac{\partial}{\partial z}(D_z\frac{\partial S}{\partial z})-\theta_s=0 \quad (3.5)$$

where S = salinity
D = the eddy diffusion coefficients
θ_s = source and sink of salinity.

When the equation is vertically averaged, derivatives of z drop out and RMA-10 solves the following (Equation 3.6):

$$\frac{\partial S}{\partial t}+u\frac{\partial S}{\partial x}+v\frac{\partial S}{\partial y}-\frac{1}{h}\frac{\partial}{\partial x}(hD_x\frac{\partial S}{\partial x})-\frac{1}{h}\frac{\partial}{\partial y}(hD_y\frac{\partial S}{\partial y})-\theta_s=0 \quad (3.6)$$

3.2 Finite Element Method

RMA-10 uses the finite element method to numerically approximate solutions to the above equations. The steps of the approach used by RMA-10 is as follows:

1. RMA-10 defines elements by isoparametric approximations.
2. RMA-10 uses the Galerkin Method of Weighted Residuals for the finite element derivation.
3. RMA-10 uses the Newton Raphson method for equation structure and iteration of nonlinear terms.
4. RMA-10 uses a modified Crank Nicholson time stepping scheme for unsteady flow.
5. RMA-10 integrates finite element integrals using Gaussian quadrature.

The reader can find more details in King (1993).

3.3 Grid Generation

The program RMAGEN allows for manual creation of grids consisting of triangular and quadrilateral elements. For depth-averaged models, triangular elements consist of three corner nodes and three mid-side nodes while quadrilateral elements consist of four corner nodes and four mid-side nodes. In RMAGEN, element geometry, nodal bottom elevations, and element types are specified (King, 1994).

3.4 Parameters

In the hydrodynamic model, calibration involves the adjustment of two sets of parameters. These parameters are the external traction of bottom friction and the internal shear stresses of eddy viscosity. For modeling salinity, an additional parameter, the eddy diffusion coefficients, can be adjusted. By far, the most important calibration tool for both hydrodynamics and salinity is the external friction term.

3.4.1 Bottom Friction

Because a two-dimensional depth-averaged model does not resolve changes in velocity over depth, the bottom boundary condition of zero velocities (the no-slip condition) does not apply.

Instead, RMA-10 represents this boundary condition with the Manning's n friction formulation. This formulation applies the shear stress as an average force over the entire depth (King, 1993). The Manning equation was originally developed to represent bottom shear stress in steady and uniform flow. The equation results from the one-dimensional balance between the external stress on the flow provided at the channel bottom and the self-weight of the fluid. For depth averaged flow where the channel is broad enough such that the hydraulic radius is equal to the water depth, the frictional formulation (Equations 3.7) is

$$\Gamma_{hx} = \frac{\rho g n^2 u \sqrt{(u^2 + v^2)}}{h^{\frac{4}{3}}} \tag{3.7a}$$

$$\Gamma_{hy} = \frac{\rho g n^2 v \sqrt{(u^2 + v^2)}}{h^{\frac{4}{3}}} \tag{3.7b}$$

where Manning's n is a coefficient representing the friction.

The model uses this formulation to represent boundary shear for transient and non-uniform flow even though the derivation is based on steady and uniform flow. The assumption that Manning's n is valid in situations other than steady and uniform flow is made for practical considerations and is justified by experience (Koseff, 1997).

Manning's n is a powerful calibration tool. In choosing Manning's n, the modeler must recognize that Manning's n represents all factors that affect boundary shear, and therefore affect the turbulent flow structure (Chow, 1959). As a result, if the model does not resolve factors such as flow separation and marsh vegetation that add drag to the system, the modeler can adjust Manning's n to account for the sum of those factors. Even though the derivation of Manning's n is based on bottom friction, Manning's n can be changed to calibrate the model to the results of the total drag on the system.

3.4.2 Turbulent Eddy Coefficients

The turbulent eddy coefficients represent the flow's internal shear stresses and describe how momentum is transported within the flow. The turbulent eddy coefficients are analogous to molecular viscosity constants. Turbulence closure efforts make this analogy possible. In the depth-averaged model of the North and South Rivers, these terms determine the velocity profile horizontally because the model resolves the estuary in two dimensions.

The turbulent eddy coefficients are not as powerful a tool for calibration as Manning's n. In depth-averaged flow, the self-weight of fluid and the boundary friction represented by Manning's n largely balance each other out – leaving the internal stress terms that include the turbulent eddy coefficients with secondary importance (Adams, 1999). It turns out that adjusting these coefficients has little effect on the resulting flow depth and velocity outputs.

However, these coefficients must be in the right order of magnitude for the numerical solutions in RMA-10 to converge. For two-dimensional tidal flow in a marshy estuary, an appropriate range for the turbulent eddy coefficients is 2,000 Ns/m^2 – 10,000 Ns/m^2 for μ_t in dynamic units and 2 m^2/s – 10 m^2/s for ε in kinematic units (Thomas and McAnally, 1985). If the coefficients are set at orders of magnitude below these values, convergence is only possible with Manning's n friction values too high to adequately represent the estuary's flow field. The velocities are too low with this high representation of drag in the system. With an appropriate order of magnitude of the eddy coefficients, the model can converge with a lower Manning's n and outputs higher and more realistic velocities.

3.4.3 Turbulent Diffusion Coefficients

Turbulent diffusion coefficients describe how scalars such as salt spread in a turbulent flow field. Since the model does not resolve the vertical profile of the velocities and gives a low resolution of the transverse velocity profile in upstream reaches of the river, these coefficients represent

dispersion processes. Coefficients are based on Lee's (1999) calibration of a water quality model that uses the hydrodynamics results as input. Lee uses data from a Woods Hole Oceanographic Institute dye study in the North River (Geyer, 1997) to do this calibration.

For salt, the diffusion coefficients are of secondary importance because advection dominates dispersion in this system. Basically, the salinity gradient is so small and the tidal velocities are so large that, on the average, the advective flux overwhelms the diffusive flux (Equation 3.8).

$$uS >> D\frac{\partial S}{\partial x} \tag{3.8}$$

4. Schematization

The development of the model consists of runs using several different schematizations for representing the rivers. These schematizations range in complexity; the initial schematization is the most simple and succeeding schematizations incrementally add complexity. The runs using the different schematizations are compared in order to gain understanding of the system's hydrodynamics. The first schematization is essentially one-dimensional with each element having the same characteristics. The second schematization is a similar spatial grid to the initial scheme, but allows for the elements to have different characteristics. The third schematization adds additional resolution in a second dimension by representing the tidal flats near the mouth.

4.1 Depth-Averaged

All schematizations use two-dimensional depth-averaged elements to represent the estuary. Geyer (1997) found that scalars such as dye and salinity are fairly well mixed vertically upstream of Route 3A on the North River. Salinity driven density differences may cause vertical stratification at the confluence, but an estimate of the estuarine Richardson number defends the neglect of this vertical effect. The estuarine Richardson number is determined by Equation 4.1.

$$R = \frac{(\rho_{ocean} - \rho_{fresh}) g \dfrac{Q_{fresh}}{B}}{\rho_{ocean} U_T^3} \qquad (4.1)$$

where ρ = density
g = gravitational constant
Q_{fresh} = freshwater flow
B = channel width
U_T = RMS tidal velocity.
and $(\rho_{ocean}-\rho_{fresh})/\rho_{ocean} = 0.03$, $g = 9.8$ m/s^2, $Q_{fresh} = 1$ m^3/s, $B = 70$ m at mouth, and $U_T = 0.4$ m/s

Under summer conditions, the Richardson number for the North and South Rivers is R= 0.07 which is below 0.08, the number above which the estuary becomes partially stratified (Fischer *et al.*, 1979).

4.2 Horizontal Scale and Shape for Schematization

The task of schematizing the river utilizes a digitized map that outlines the high water channel line (Figure 4.1). Obtained from the Topo Depot World Wide Web site (Sylvan Ascent Inc., 1999), the digitized map is scaled based on decimals of longitude and latitude. Aligning the x and y coordinates with the East-West and North-South directions respectively, 1/100 of a longitude degree equals 831 meters in the x-direction and 1/100 of a latitude degree equals 1107 meters in the y-direction. Figure 4.1 shows the digitized map without the original distortion; that is, the scales for the x and y directions are equal.

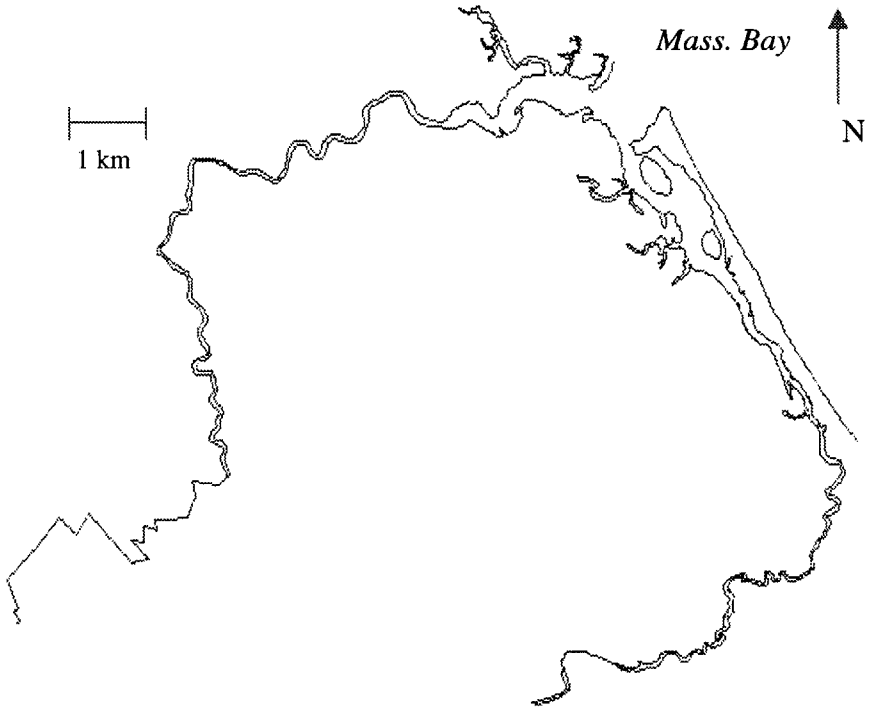

Figure 4.1 Undistorted Digitized Map of High Water Channel

4.3 Bottom Elevation Schematization

The bottom elevations of the channel are relative to mean lower low water. The values of the elevations are based on nautical chart soundings in reaches near the mouth (NOS, 1997),

soundings from the Woods Hole dye study in reaches further upstream of the North River (Geyer, 1997), and six North River cross-sections from a 1966 Division of Marine Fisheries report (Fiske *et al.*, 1966). Upstream of Bridge Street, mean lower low water depth is about 1 meter. There are few soundings available for the South River upstream of Julian Street, but the channel is less than 1 meter at the head of tide during low tide.

4.4 Scheme 1 : Low Water Channel with Spatially Constant Characteristics

The first schematization represents the low water level channel of the rivers (Figure 4.2). This is the main channel of the river that always conveys water. The low water channel line and high water channel lines are similar upstream of Route 3A on the North River and upstream of Julian Street Bridge on the South River. In these stretches, the width of a single two-dimensional element fits the channel delineated by the digitized map. Downstream of these locations, the low water line is estimated from USGS topographic maps that differentiate between tidal flat areas and the main channel. Upstream of the confluence, the channel is represented by one element across the width of the rivers.

In the arms of the two rivers upstream of the confluence, a single two-dimensional element is used across the channel width. The width of the element represents the width of the channel. This scheme is essentially one-dimensional since the purpose of the transverse dimension of the element is to represent the width. The transverse side of the element does have three nodes that can have different values for velocity and depth, but this does a poor job of resolving the transverse variation of the flow.

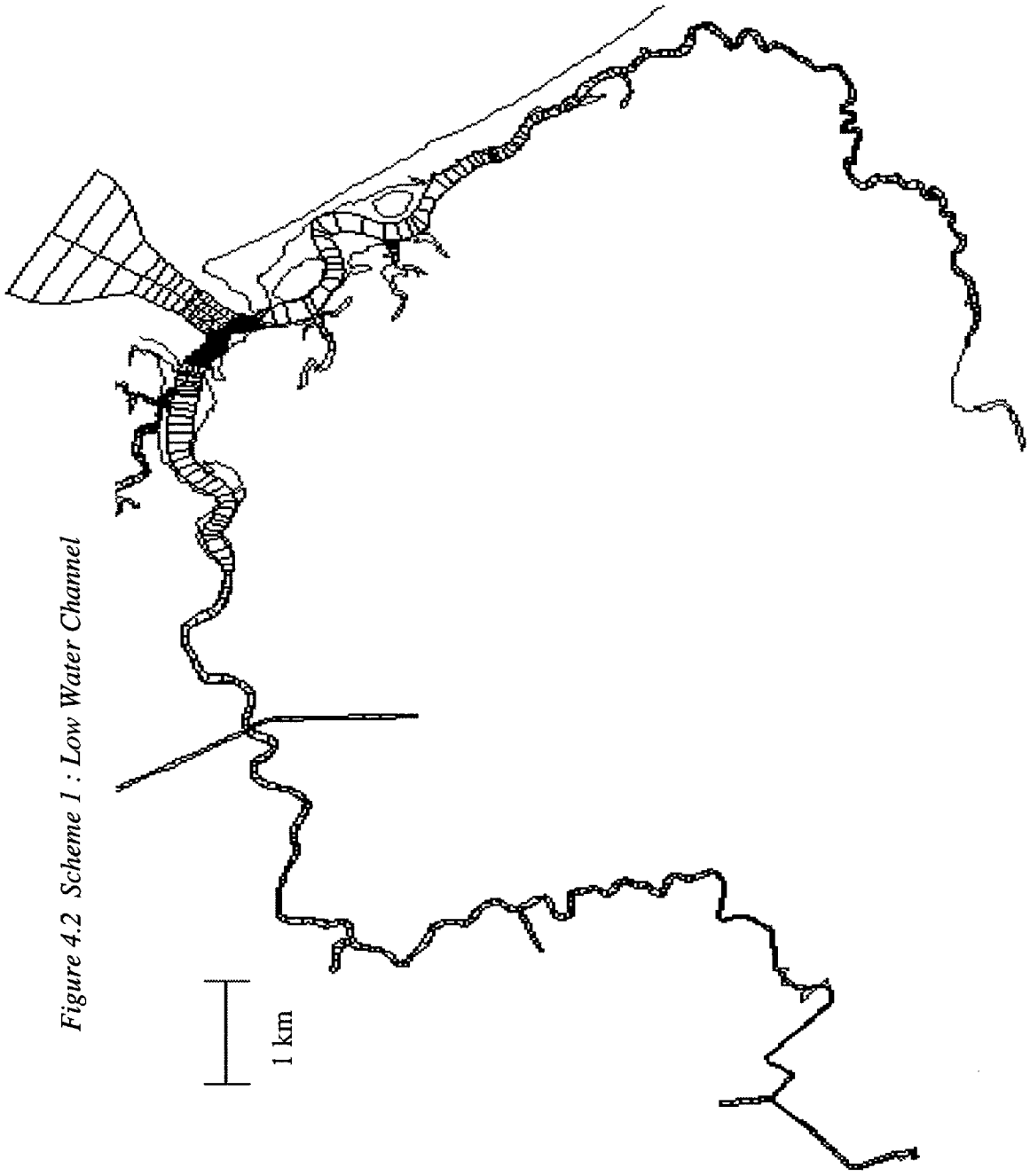

Figure 4.2 Scheme 1 : Low Water Channel

For two-dimensional elements, RMA-10 represents the banks of the channel as vertical planes. Since the low water channel generally has fairly steep banks, it is reasonable to represent the channel cross-section as rectangular. However, this schematization creates a problem when the high tide overtops the banks of the low water channel. In reality, the additional water volume provided by high tide results in increased river width as well as depth. The model will represent the additional water only with an increased depth (Figure 4.3). This is especially problematic when tidal flats line the channel because the width of the river changes fairly continuously in these areas. Areas upstream of the tidal flats do not present the same degree of problem, but the marshlands adjacent to the basically rectangular main channel will flood at high tide.

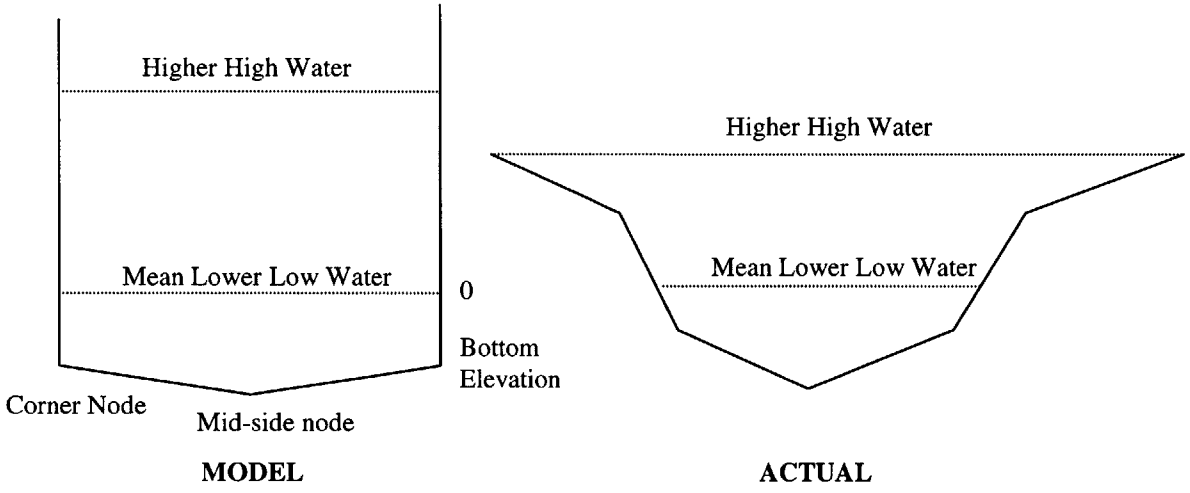

Figure 4.3 Low Water Channel Schematization (Schemes 1 & 2) vs. Actual Cross-section near Mouth

At the confluence, the schematization still only represents the low water channel width but uses more than one element to represent that width (Figure 4.4). Therefore, a fully two-dimensional grid represents the confluence. Eight elements across the width in the mouth area are the highest amount of lateral resolution in the scheme. The scheme makes a transition from the highly defined confluence area to the ocean boundary in Massachusetts Bay that is two elements across. The scheme does not represent islands in the channel or constrictions.

Scheme 1 does not differentiate between types of elements. All elements have the same values for hydrodynamic characteristics such as Manning's n and eddy viscosity.

4.5 Scheme 2 : Low Water Channel with Spatially Variant Characteristics

The first two schemes use essentially the same spatial grid of the lower water level channel. The first two schemes differ in the amount of extension of the refined confluence grid upstream. Scheme 1 (Figure 4.4) transitions to the one element representation of the width near the inlet from Damons Creek on the North River and at the entry to the South River between Fourth Cliff and Trouant Island. Scheme 2 (Figure 4.5) continues the representation of the low water channel width with two elements past the entry to the Herring River on the North and past Branch Creek on the South.

The significant difference between the first two schemes involves the treatment of element characteristics such as friction and viscosity. Scheme 1 constrains characteristics such as Manning's n and eddy viscosity to be spatially constant. Scheme 2 allows these characteristics to vary over the rivers' reaches. In RMA-10, elements can be assigned different types and different element types can represent different characteristics. In Scheme 2, the element type changes over space and each type has variable characteristics for calibration purposes.

4.6 Scheme 3 : Addition of Tidal Flats

The USGS topographic maps identify the flats that are represented in the third scheme (Figure 4.6). Since the elevations of the tidal flats are not well defined, it is assumed that the tidal flat bottom elevations vary from the mean lower low water elevation (0 m) to high water elevation (3 m) moving away from the main channel of low water. The number of elements schematized for this area is based on a trial and error process to avoid strong gradients that can cause the model to fail to converge.

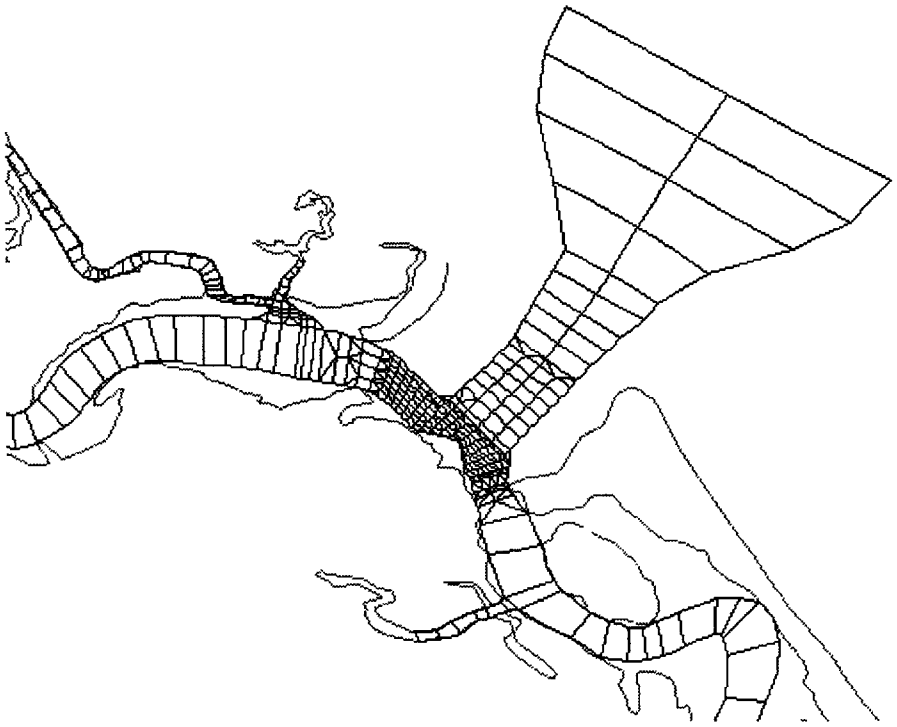

Figure 4.4 Scheme 1 near Mouth

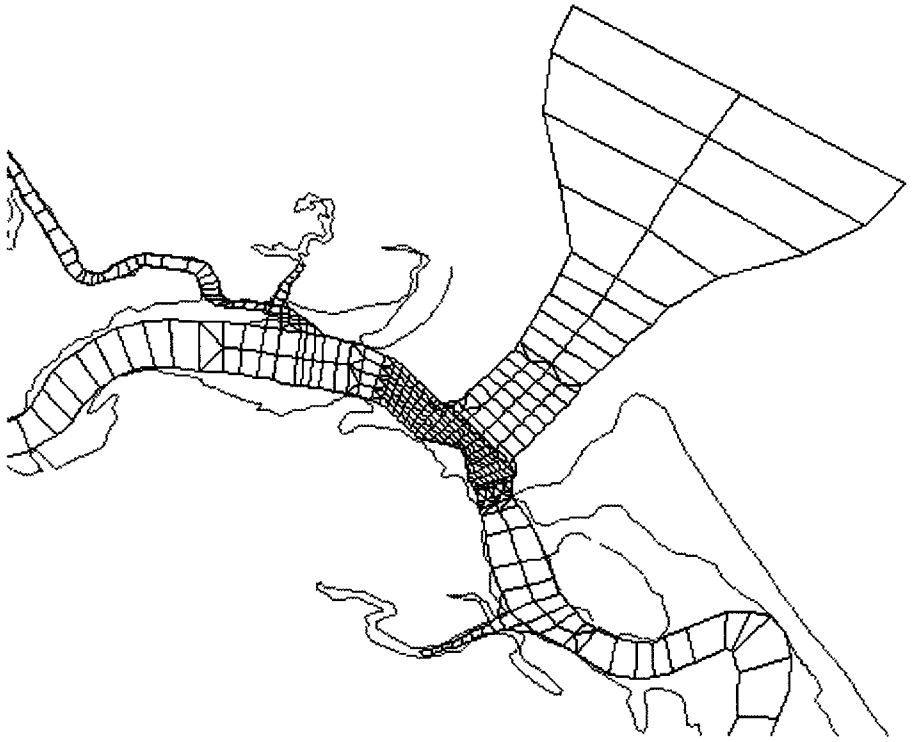

Figure 4.5 Scheme 2 near Mouth

Figure 4.6 Scheme 3 : Addition of Tidal Flats

Figure 4.7 Ocean and Tributary Boundary Locations

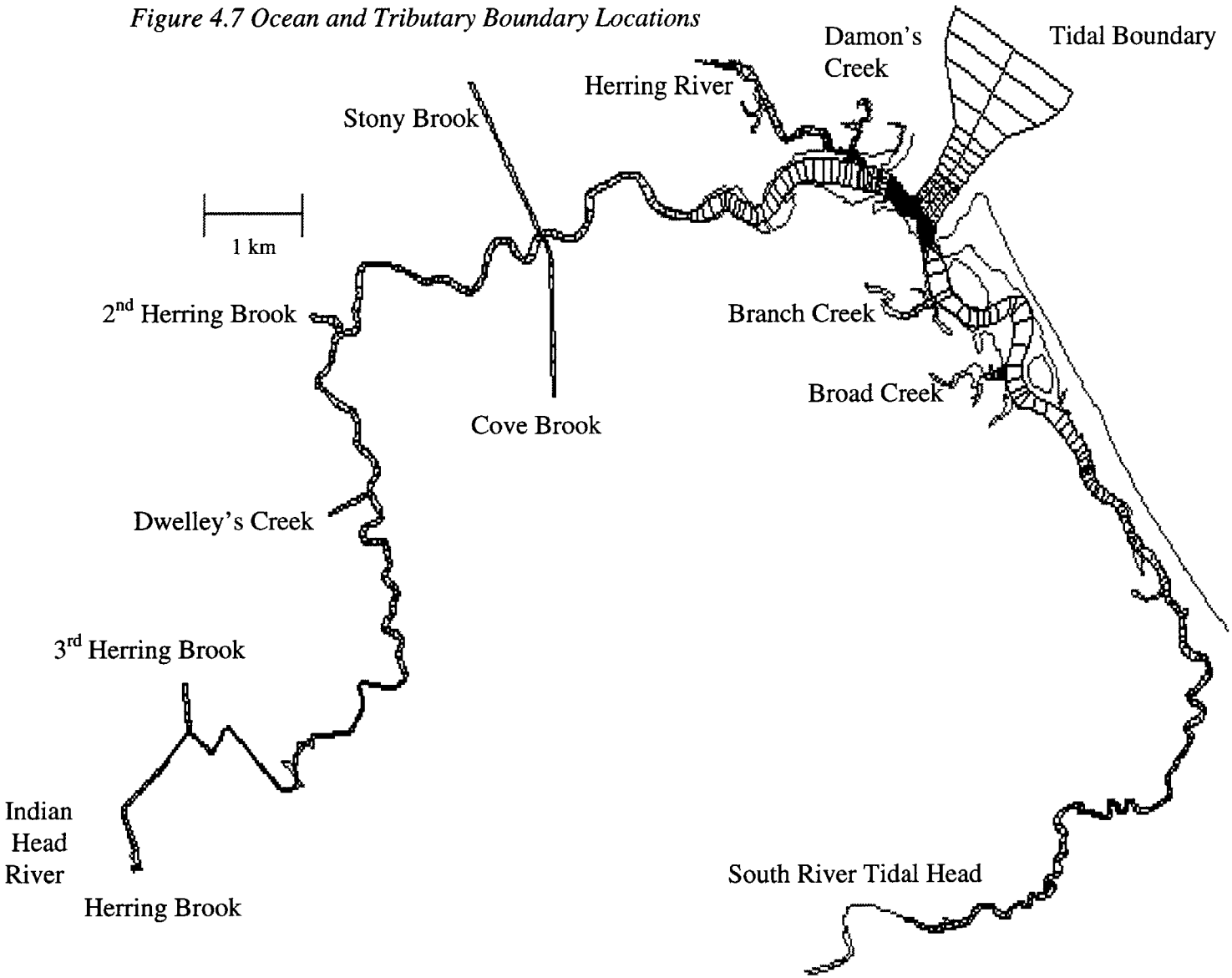

4.7 Tributaries

All schematizations include tributaries that are cataloged in a stream-order listing by the USGS (Wandle and Morgan, 1984) and have an obvious freshwater source based on USGS maps. These tributaries include Herring River, Cove Brook, Stony Brook, Second Herring Brook, Dwelley's Creek, Third Herring Brook, and Herring Brook on the North River (Figure 4.7). The South River has no such tributaries up to the tidal head, but some are schematized for the purpose of modeling tidal flooding. If the digitized map represents the outline of the tributary, as in the case of Herring River, the schematization of the tributary is based on that outline up to the point of the freshwater source. Otherwise, a straight channel represents the length of the tributary from the freshwater source to the main river. In all cases, the transverse dimension of a two-dimensional element represents a tributary's width.

4.8 Time Discretization

This model application uses a time step of 0.05 hours or 3 minutes. The time span simulated ranges from 4-7 days based on calibration needs.

This is well over the amount of time for the hydrodynamics output to eliminate the effects of the flat-water initial condition. To start the model, the estuary is given a constant water elevation -- a condition that never actually occurs. The model eliminates the effects of this condition when the output reaches harmonic steady state given a harmonic input. This harmonic input is formulated by a sinusoidal created by RMA-10 (Equation 4.1):

$$H = a * \cos(\omega * t + \theta) + \overline{H} \qquad (4.1)$$

where H =tidal elevation above mean lower low water
a = amplitude = 1.4 m
ω = M2 harmonic speed (radians/hr) = 0.5076 rad/hr
t = time (hr)
θ = Phase advance at time 0 = $\pi/4$

$\overline{H}$ = Average tidal elevation above mean lower low water = 1.5 m

Given boundary conditions of constant inflow (~0.5 m^3/s) and a steady harmonic tide, the depths upstream reach harmonic steady state well under 4-7 days (Figure 4.8). In fact, the dynamics reach steady state within the first tidal cycle.

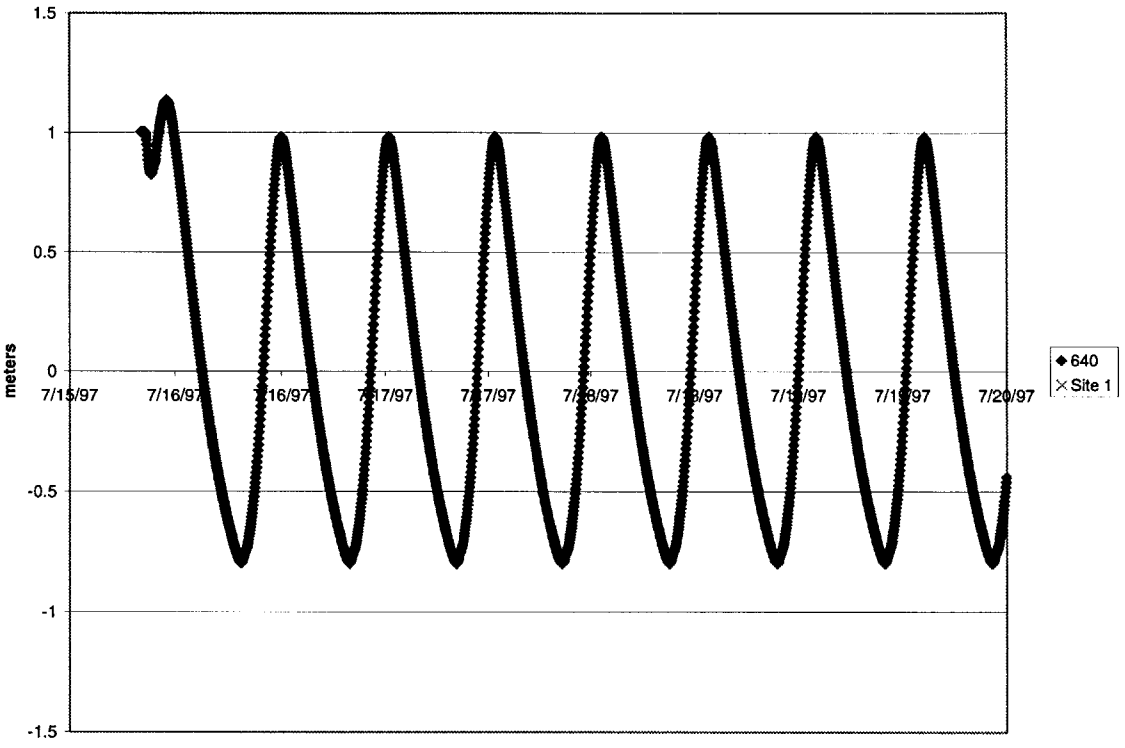

Figure 4.8 Response of Dynamics to Harmonic Boundary Condition : Tidal Range 15 km Upstream

5. Boundary Conditions

Boundary conditions are necessary to set up a numerical model that represents changes over space. Because the geographic area represented by the model schematization is limited to a finite space and the represented system is not isolated, the model needs to account for external effects on the system as boundary conditions. The boundary conditions are introduced into the model as independent variables that affect the flow field within the domain schematized. The boundary conditions that are most important for modeling an estuary are the tides and the tributary inflow.

5.1 Mouth Tidal Heights

In order to simulate the time-varying flow field of an estuary, the tidal boundary condition is the primary concern because the tidal elevation at the mouth of the estuary has a continuously high rate of change. This results in continuously changing water elevations over the estuary. These changing elevations are known as barotropic pressure gradients, which are the highlighted terms in the depth-averaged momentum equations (Equations 5.1). These gradients drive the flow.

$$\frac{\partial u}{\partial t}+u\frac{\partial u}{\partial x}+v\frac{\partial u}{\partial y}-fv-\frac{1}{h}\frac{\partial}{\partial x}(h\varepsilon xx\frac{\partial u}{\partial x})-\frac{1}{h}\frac{\partial}{\partial y}(h\varepsilon xy\frac{\partial u}{\partial y})+\mathbf{g}\frac{\partial \boldsymbol{\eta}}{\partial \mathbf{x}}+\frac{1}{\rho}g\eta\frac{\partial \rho}{\partial x}+\frac{1}{\rho}\Gamma_{hx}=0 \quad (5.1a)$$

$$\frac{\partial v}{\partial t}+u\frac{\partial v}{\partial x}+v\frac{\partial v}{\partial y}+fu-\frac{1}{h}\frac{\partial}{\partial x}(h\varepsilon_{yx}\frac{\partial v}{\partial x})-\frac{1}{h}\frac{\partial}{\partial y}(h\varepsilon_{yy}\frac{\partial v}{\partial y})+\mathbf{g}\frac{\partial \boldsymbol{\eta}}{\partial \mathbf{y}}+\frac{1}{\rho}g\eta\frac{\partial \rho}{\partial y}+\frac{1}{\rho}\Gamma_{hy}=0 \quad (5.1b)$$

where g = acceleration due to gravity
η = water elevation relative to a horizontal datum
x,y = horizontal Cartesian coordinates

In the North and South Rivers, the high tidal range relative to the mean low water depth magnifies the importance of the tidal boundary condition. Although tidal-averaged estuarine models emphasize the importance of freshwater flow (Adams, 1999), the effort to resolve the flow field within a tidal cycle shifts the focus to the tide.

Historical tidal height data represent the tide at the estuary's New Inlet. For validation purposes, data from summer 1997 is used, but any historical time period is possible due to the comprehensive data set available from the National Ocean Service (NOS). In order to make predictions of future hydrodynamics in the North and South Rivers, NOS provides tidal chart predictions. In order to use the predictions, future users need to interpolate a tidal curve between the high tide and low tide predictions provided. In addition, future users should take caution when modeling storm conditions because the predictions are inaccurate when affected by storms.

Due to the small time step of 3 minutes (DT = 0.05 hr) in the model, the finest resolution of data provided by the National Ocean Service, 6 min tidal heights, is most appropriate. RMA-10 has the option of interpolating water elevations from a tidal graph (King, 1998). The interpolated values provide water elevations at a continuity line representing the boundary for each time step. The boundary is a line with a length of two elements outside of the mouth in Massachusetts Bay (Figure 4.7). This is continuity line (CL) 2 in all versions of the model.

Also, the use of this combination of data and time step means that only half the time steps use interpolated values for this boundary condition. The other time steps use values directly from the tidal graph, which is derived from NOS historical data. The fine resolution of the tide data requires 240 lines of data in the tidal graph file for each day simulated; this runs into the maximum amount of lines allowed by RMA-10 if the simulation is for more than two days. This application of the model takes advantage of RMA-10's restart capabilities to run longer simulations.

The extensive tidal data provided by NOS is only available for Boston Harbor (Station 8443970; NOS, 1998), so the model needs to account for the geographical difference between Boston Harbor and New Inlet of the North and South Rivers. First, there is a different tidal range (twice the amplitude) between the two locations. NOS provides information for converting Boston Harbor values to tidal data for Scituate Harbor, which is located near New Inlet. The factor for both high and low tides is 0.92 so the model uses Boston Harbor values multiplied by this factor

(NOS, 1999). These tidal elevations are relative to mean lower low water -- the datum for the channel bottom elevations in the model.

The second difference between Boston Harbor tidal data and values at the North and South Rivers is temporal. The high and low tides arrive at Boston at different times than they do at Scituate. In fact, according to NOS, high tides arrive at Scituate three minutes before Boston and low tides arrive at Scituate two minutes after Boston (NOS, 1999). Extrapolating these temporal differences to the rest of the tidal cycle is complicated and since the differences are relatively small, the model uses the Boston times for setting the phase of the tidal cycle at New Inlet. NOS provides these times in local standard time so either the tidal graph data or the model results must be adjusted to daylight savings time by adding one hour when modeling the estuary from April to October. This application of the model uses the NOS times in the input and adjusts the results.

5.2 Tributary Inflows

If the tidal elevations provide a boundary condition at one end of the estuary, the other end has a boundary impacted by freshwater flow. The North River is tidal for about 20 km up to Curtis Crossing where there is a USGS streamflow gage. The tidal head is about 10 km upstream of New Inlet on the South River. In addition, there are many freshwater tributaries, especially along the North River, that provide inflows to the estuary.

For the North River, daily streamgage data from the USGS measurements at Curtis Crossing on the Indian Head River provide the values for the hydrograph at the tidal head. The flows at the tidal head of the South River and the freshwater tributaries along the North River are calculated based on the Curtis Crossing daily streamflow measurements. An estimate for flow at an ungaged stream included in the model is the product of the flow at Curtis Crossing and a factor related to the drainage area of the stream. This factor is the drainage area of the tributary divided by the drainage area at Curtis Crossing. The USGS provides tributary drainage areas for the following drainage basins: South River head of tide, Herring River (or First Herring Brook),

Second Herring Brook, Third Herring Brook, and Herring Brook at Pembroke (Wandle and Morgan, 1985). Other drainage basins schematized are less than 7.8 km^2 so they are estimated as 5.2 km^2. This applies to the basins of Cove Brook, Stony Brook, and Dwelley's Creek. If the source of the tributary appears to be in a salt marsh, the freshwater inflow is ignored. Figure 4.7 shows the schematized tributaries and Table 5.1 shows the factors used for estimating tributary inflows.

Basin	CLQ/Element	Area (km^2)	Factor for Streamflow	Angle of inflow
Indian Head	CLQ 1	78.5	1.00	0.426
South Head	CLQ 3		0.48	6.106
First Herring	Element 764		37.8	NA
2nd Herring	Element 766	3.5	17.1	NA
3rd Herring	CLQ 6	9.1	0.37	4.785
Herring Br	CLQ 7	14.4	0.50	5.935
Macombers	Not used		0.00	0.666
Damons	CLQ 9		0.00	2.265
Cove	CLQ 10	5.2	0.07	2.492
Stony	Element 94	5.2	0.07	NA
Dwelleys	Element 724	5.2	0.07	NA
Branch	CLQ 13		0.00	1.408
Broad	CLQ 14		0.00	0.250
Clapp	Not used			0.120
Littles	Not used		0.00	0.242

Table 5.1 Tributary Inflows

Similar to the treatment of a tidal graph, RMA-10 can interpolate inflow values from a hydrograph. For the purposes of this interpolation, the daily streamflow values derived from the Curtis Crossing stream gage data are assigned to each day at 12 noon (Julian Day = xxx.5). For all time steps between the successive days at noon, the streamflow values are linearly interpolated (King, 1998).

There are two types of inflow graphs used in this model: the continuity line inflow and the element inflow. The continuity line inflow is a flow at some angle across a line of nodes; this angle should be the angle in radians of the ray perpendicular to the boundary and pointing into the domain. The element inflow is a depositing of flow into a specific element. The choice of which inflow type to use for a modeled tributary is based on salinity considerations.

The continuity line is appropriate where the water is always fresh and the tide does not bring salt to the boundary. However, when there is positive inflow at that continuity line, salt cannot travel up to the boundary. Two factors contribute to this fact. When there is freshwater flow, the continuity line is set to a constant salinity value of zero. Salt cannot travel to the boundary because such a large gradient would be eliminated by diffusion (Figure 5.1). Also, because the continuity line type translates the flow to velocities at the boundary nodes, the inflow has momentum. The momentum constantly pushes the freshwater downstream -- preventing the salt from moving up the stream (Figure 5.2).

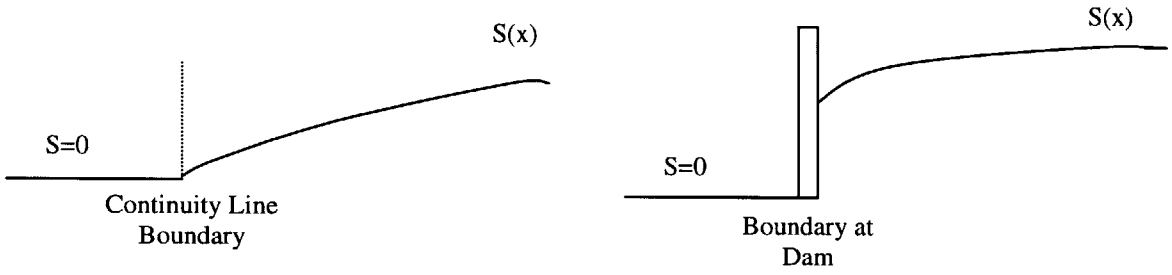

Figure 5.1 Concentration with Distance at Boundary

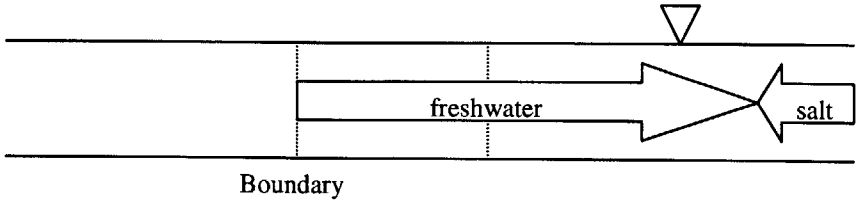

Figure 5.2 Continuity Line Momentum Effects

In this system, a tributary's tidal head is marked by a run of the river dam. At high tide, salt travels up to the dam. Element inflow allows for this high salinity at the boundary because this inflow type does not have a constant concentration. Therefore, this type can simulate the high salt concentrations on the downstream side of the dam while the no salt condition of the upstream side is outside the domain (Figure 5.1). The element inflow also has no momentum. This inflow is the q_A referred to in the continuity equation (Equation 5.2) where q_A is the volumetric inflow rate divided by the element area. No velocities are associated with the inflow and the freshwater inflow can mix with the salt advecting upstream with the tide (Figure 5.3).

$$h\left(\frac{\partial u}{\partial x}+\frac{\partial v}{\partial y}\right)+u\frac{\partial h}{\partial x}+v\frac{\partial h}{\partial y}+\frac{\partial h}{\partial t}-\mathbf{q}_A=0 \tag{5.2}$$

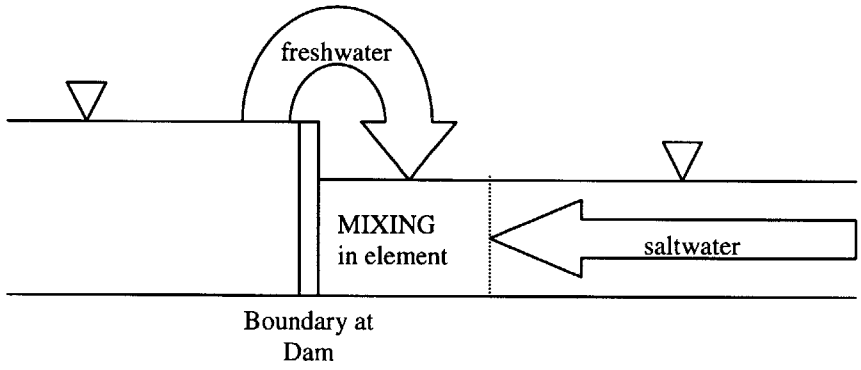

Figure 5.3 Element Inflow Formulation

The choice of continuity line inflow or element inflow results from the character of the tributary's freshwater source. As stated above, if the source, as mapped by the USGS, appears to be in a saltwater marsh, the freshwater is ignored even if the tributary is schematized. Most notable of these salt marsh creeks are Damon's Creek, Branch Creek, and Broad Creek. In the other extreme, when the tributary has a source upstream of freshwater wetlands as delineated by the USGS maps, the source must be completely fresh and a continuity line will work for these tributaries. This applies to the tidal head inflows of both the North and South Rivers and the tributaries near the North River head: Herring Brook and Third Herring Brook. Perhaps surprisingly, Cove Brook, which enters the North River only about 5 km upstream of the mouth, has a freshwater wetland just downstream of the source so the source inflow is represented by a

continuity line. Other streams entering the rivers have freshwater sources, but flow solely through salt marshes. For these sources, dams mark the freshwater source, but also allow for salt to travel up to the dam during high tide. Element inflow simulates this type of inflow accurately and is used for Herring River, Stony Brook, Second Herring Brook, and Dwelley's Creek.

Nonpoint sources of drainage as quantified by the USGS are ignored. This includes 25 square kilometers along the North River and 25 square kilometers along the South River.

6. Scheme 1 : Low Water Channel with Spatially Constant Characteristics

The first scheme is the representation of the channel width as the low water line (see Section 4.4). Tidal flats and marshlands are not included so an increase in river volume only results in an increase in tidal height, not an increase in channel width. In the first scheme, the elements are assumed to have similar hydrodynamic characteristics. The Manning's n friction coefficient, the most important characteristic, does not vary with space in this model scheme.

6.1 Tidal Range Calibration

The primary tool for calibration of the hydrodynamics is a time series data set for the North River obtained from Dr. Rocky Geyer (1997) at Woods Hole Oceanographic Institute (WHOI). The data set includes hourly measurements of pressure, salinity, and temperature at three points along the North River. These three points are near Route 3, Bridge St., and Route 3A (Figure 6.1). The data set runs from July through August 1997. Calibration efforts concentrate on data between July 14 – July 20, which are the dates of the accompanying dye study.

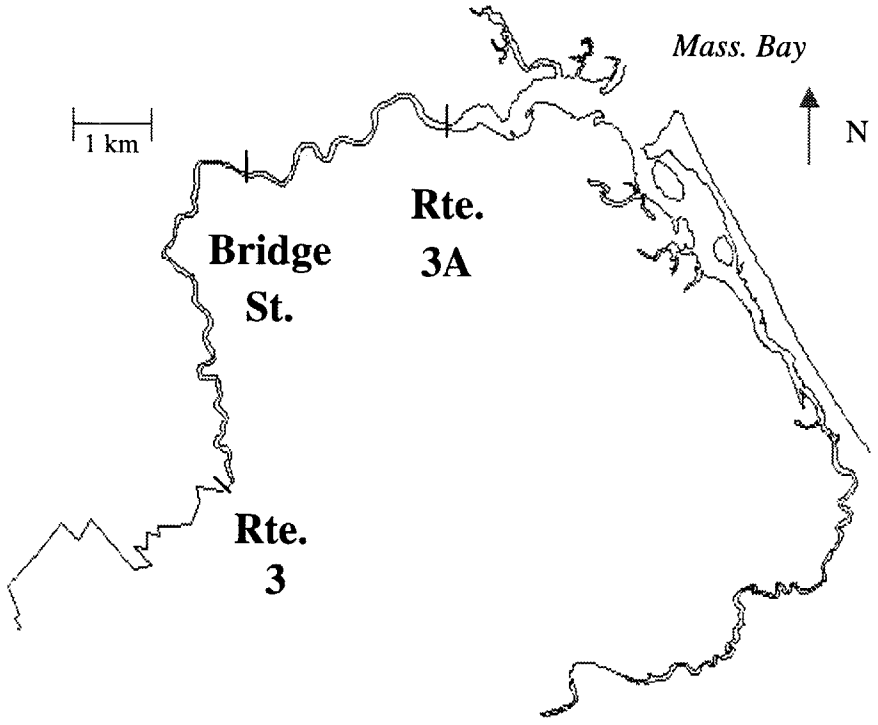

Figure 6.1 Location of North River Pressure Gauge Stations

For calibration of the tidal range, the pressure data converts to equivalent water depths. Since the locations of the pressure gages are unknown, we take the average water depth for the time period of interest and calculate the variation of water depth around that mean for each location. The time series of depths is extracted from the model results for nodes representing each of these three locations (Table 6.1). The variation of these nodal depths around an average is compared to the variation of the data in order to calibrate the model.

Nearby Bridge	Kilometers from mouth	WHOI Site Identification	Model Node
Route 3	14	Site 1	Node 640
Bridge St.	7	Site 2	Node 152
Route 3A	3	Site 3	Node 254

Table 6.1 North River Sampling Station Identification

Several characteristics about the location dependent tidal range are evident when viewing calibration results. The most effective calibration tool is the Manning's n friction coefficient, because friction plays a dominant role in the tidal dynamics of a shallow estuary (Parker, 1984). Adjusting Manning's n does not change the Route 3A tidal range much; trying Manning's n coefficients of 0.020 to 0.080 approximates data for this downstream site. This site is close enough to the tidal boundary that very little damping of the tidal amplitude can take place. The upstream sites of Bridge Street and particularly Route 3 are especially sensitive to adjustment. With low Manning's n, the tidal range whips up the river with little damping. With high Manning's n, the velocities turn around before the full maximum and minimum tidal elevations can reach the upstream sites. Figure 6.2 shows a comparison of the average tidal ranges from models with Manning's n ranging from 0.040 to 0.060. In order to make a best match of the tidal ranges of each of the sites, we need to supply a Manning's n of 0.050 (Figures 6.3-6.5).

A second look at Figure 6.2 also shows that it is very difficult to get a close match for both upstream sites: Bridge St. and Route 3. None of the model runs displayed do a very good job of calibrating to the Bridge St. tidal range, but n=0.040 does better than n=0.050. However, n=0.050 clearly does better than n=0.040 for the Route 3 tidal range.

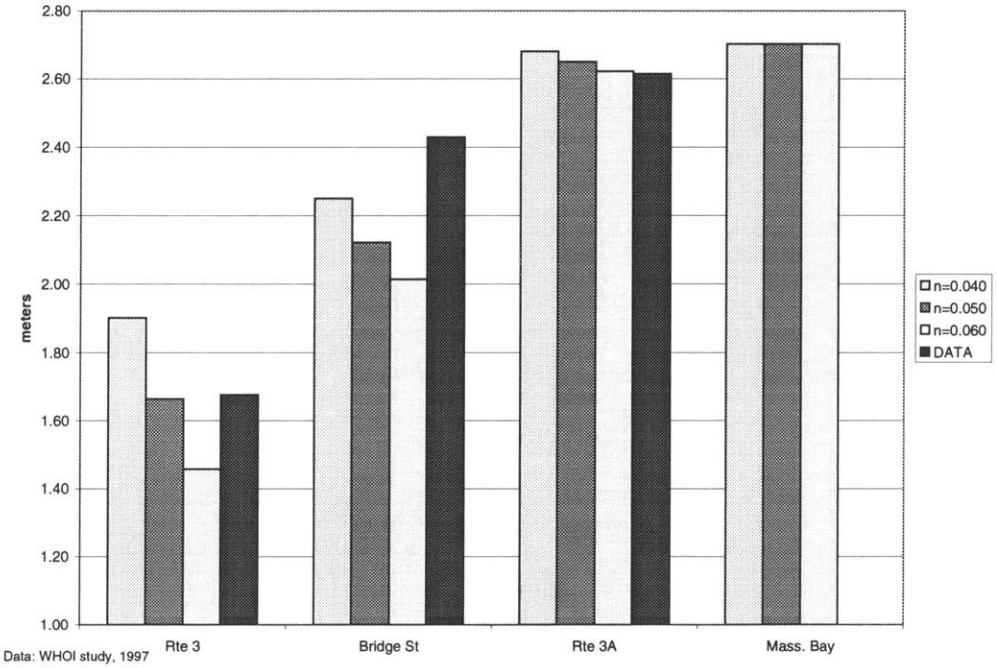

Figure 6.2 Comparison of Average Tidal Range for Manning n of 0.040, 0.050, and 0.060

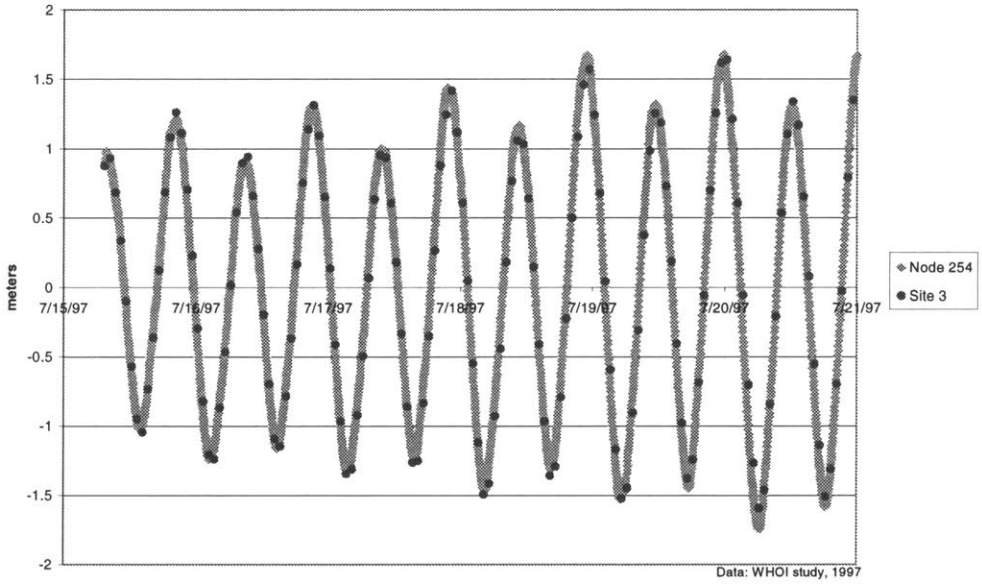

Figure 6.3 Tidal Range Calibration near Rte. 3A for Scheme 1 : Manning's n=0.050

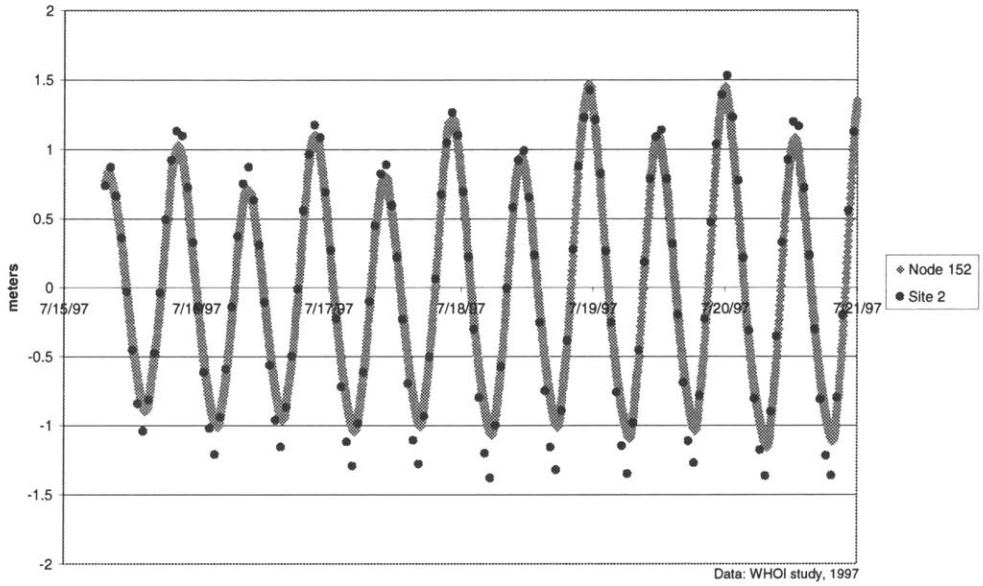

Figure 6.4 Tidal Range Calibration near Bridge St. for Scheme 1 : Manning's n=0.050

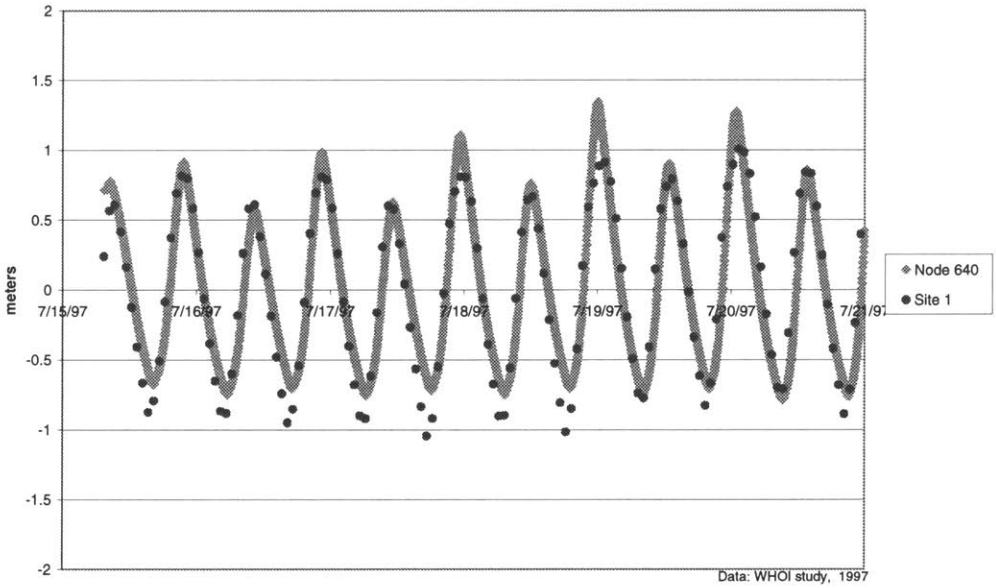

Figure 6.5 Tidal Range Calibration near Rte. 3 for Scheme 1 : Manning's n = 0.050

6.2 Velocity Calibration

The hydrodynamic input to a water quality model consists of water depths and velocities at every node in the grid. Therefore, it is necessary to calibrate not just the depths, but the velocities as well. Unfortunately, there are few data sets available giving measurements of velocity in the system. A Metcalf and Eddy report gives velocity data over ten hours on two summer 1989 days. This data set has five to seven data points per day at three locations in the Herring River and at Damon's Point on the North River (Metcalf and Eddy II, 1995). The other data set is Geyer's velocity measurements taken at the same time as his dye study. Geyer took velocity readings from his surveying boat on July 17, 1997. The boat followed the dye patch up and down the North River from about Route 3 to Bridge St. In order to be consistent with the model runs for tidal range calibration, Geyer's velocity data (1997) are used.

Since the exact location of the boat over time is unknown, we can only use this data as a general check of velocities in the North River. We select a single mid-stream node in the North River and compare the velocity output to the velocity data. For the calibration of Scheme 1, we use the velocities of node 1472 (Figure 6.6) about ten kilometers upstream of the mouth.

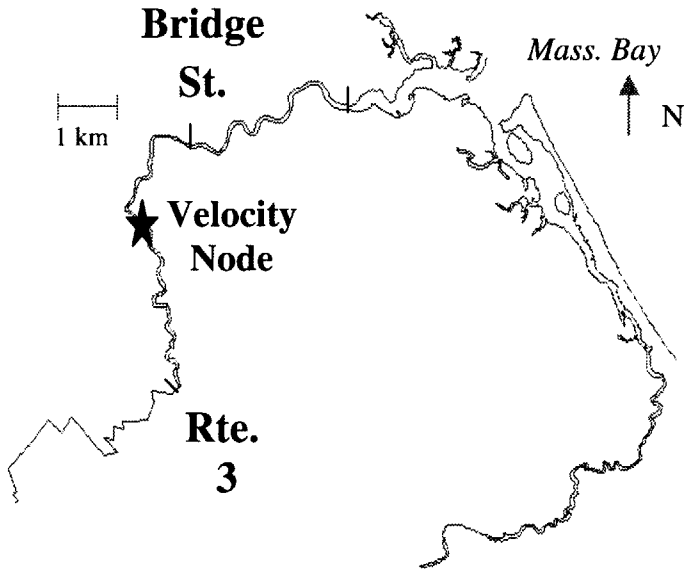

Figure 6.6 Location of Model Node Used for Velocity Calibration

Comparisons of the velocity output over time with the data show that the model gives velocities that are too low (Figure 6.7). At flood tide, the peak velocity is less than 40 cm/s, when the bulk of the measurements for the flood tide are over 40 cm/s. The Manning's n of 0.050 does not adequately represent the flows in the upstream stretches of the river. This Manning's n is higher than typical Manning's n values for natural river channels. Natural river channels that are windy with pools and shoals have values of 0.033-0.040 (Henderson, 1966). It is found that Manning's n values of 0.020-0.030 give upstream velocities in the ballpark of the data, but these values do not allow for calibration of the tidal range.

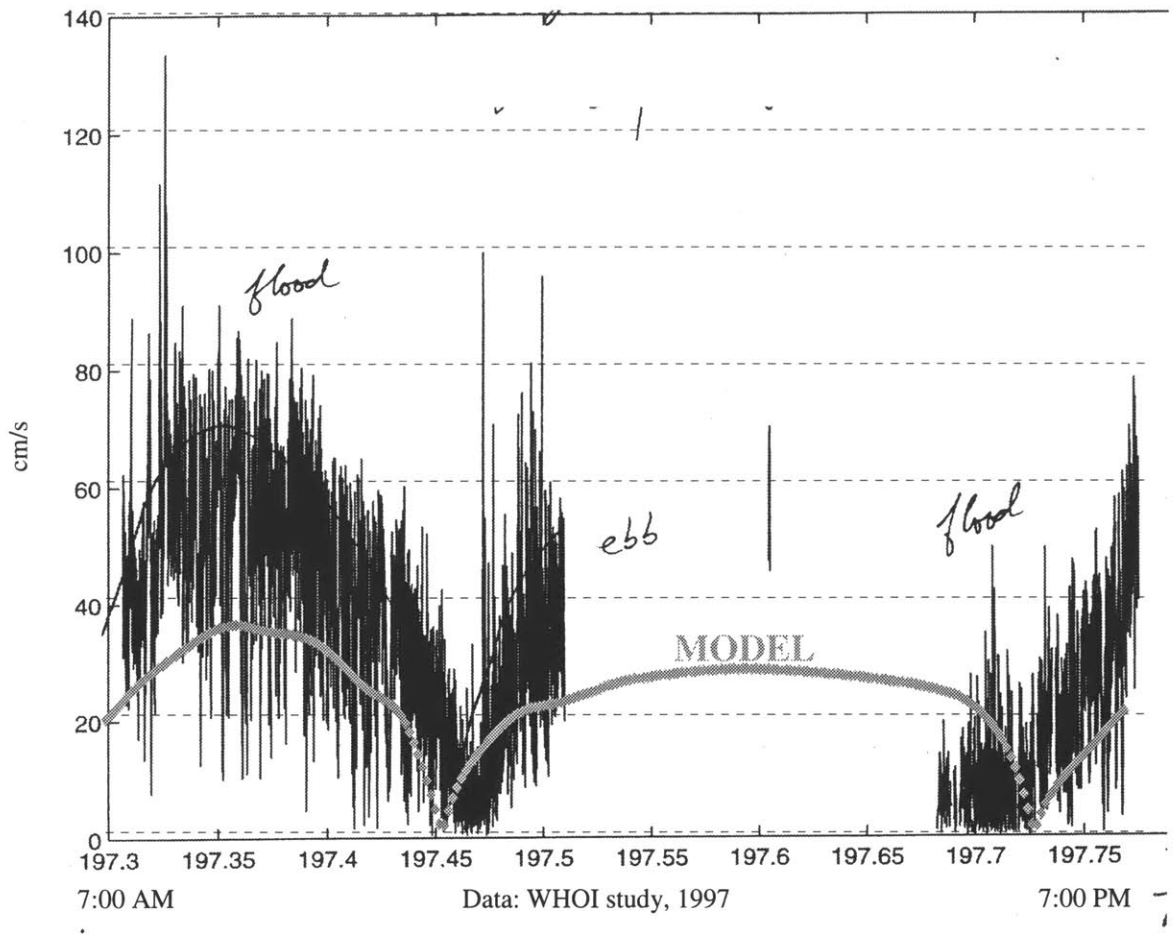

Figure 6.7 Velocity Calibration for July 17, 1997 between Bridge St. and Route 3 for Scheme 1

6.3 Scheme 1 Discussion

There are two main problems with Scheme 1, which only schematizes the low water channel and treats the Manning's n coefficient as spatially constant. First, it is difficult to calibrate the tidal ranges at both Bridge Street and Route 3. Since the low water channel is similar to the high water channel between these two sites, the difficulty in calibrating both sites with one Manning's n coefficient seems to go against the assumption that Manning's n coefficient is the same along the river.

Second, the velocities in the upstream reaches represented by the model with a Manning's n of 0.050 are much too small to calibrate with reality. Lower Manning's n results in model depths that do not align with the actual tidal range variation along the river. The water quality model (Lee, 1999) takes the depth and velocity output from the hydrodynamics model as independent variable input so the output from Scheme 1 cannot be justifiably used for the water quality model.

A lower Manning's n must be used in the upstream stretch of the river, but the average damping of the tidal range represented by the Manning's n of 0.050 must be represented somewhere in the river. Using lower Manning's n upstream and higher Manning's n downstream is the essence of Scheme 2.

7. Scheme 2 : Low Water Channel with Spatially Variant Characteristics

Clearly, the constant roughness throughout the estuary used in Scheme 1 does not adequately represent the hydrodynamics. In Scheme 2, we use essentially the same geometry and allow for different elements to have different hydrodynamic characteristics. The main characteristic that varies over the estuary grid is the Manning's n roughness coefficient. Near the mouth, the grid is more refined with longer reaches of the river defined by more than one element across the channel's width. The channel width still represents the low water channel, but the transverse variation in cross-section is slightly more resolved (see Section 4.5).

7.1 Roughness Coefficients

As discussed in Chapter 6, total tidal damping at the upstream site of Route 3 is represented by the constant Manning's n of 0.050 in the first scheme. However, such a high Manning's n does not depict the upstream velocities well at all. Therefore, lower and more typical Manning's n values are used in the upstream river-like channels. In order to account for the damping of the tidal range, the model uses a high Manning's n near the mouth. At the mouth, neither Scheme 1 nor Scheme 2 represents the changing geometry of the channel well. Both schemes use the low water channel line as the constant width of the channel. Tidal flats, marshlands, and other features are not represented by the first two schemes. Using a higher Manning's n is meant to account for the lack of resolution of features near the mouth.

7.2 Tidal Range Calibration

Using the same procedure as in Scheme 1, we calibrate the model against tidal range data (Geyer, 1997) by changing Manning's n for reaches around the measurement sites. As in Scheme 1, the model's tidal range calibrates with data at the Rte. 3A site for a large range of Manning's n values used at the mouth. Therefore, the calibration concern is with the sites further upstream. Since the upstream sites need to be within the typical range of values for this parameter, the major calibration tool for the upstream sites is the downstream Manning's n near

the mouth (Figure 7.1). A Manning's n of 0.080 works well for the tidal range at Rte. 3A (Figure 7.2) and getting the tidal ranges damped appropriately upstream. As found in the calibration of Scheme 1, calibration of Scheme 2 against tidal range data requires a different treatment for the stretch around Bridge Street than around Route 3 (Figure 7.1). For the mid-stream site at Bridge St., a Manning's n of 0.020 for the surrounding reach calibrates well (Figure 7.3). For the upstream site at Rte. 3, a Manning's n of 0.025 for the reach from the Bridge St. area to the tidal head is appropriate (Figure 7.4). These latter values for the roughness coefficients are similar to typical values for clean and straight natural river channels. Comparison of Figure 7.5 with Figure 6.4 shows the similar tidal range calibration results between Scheme 1 and Scheme 2.

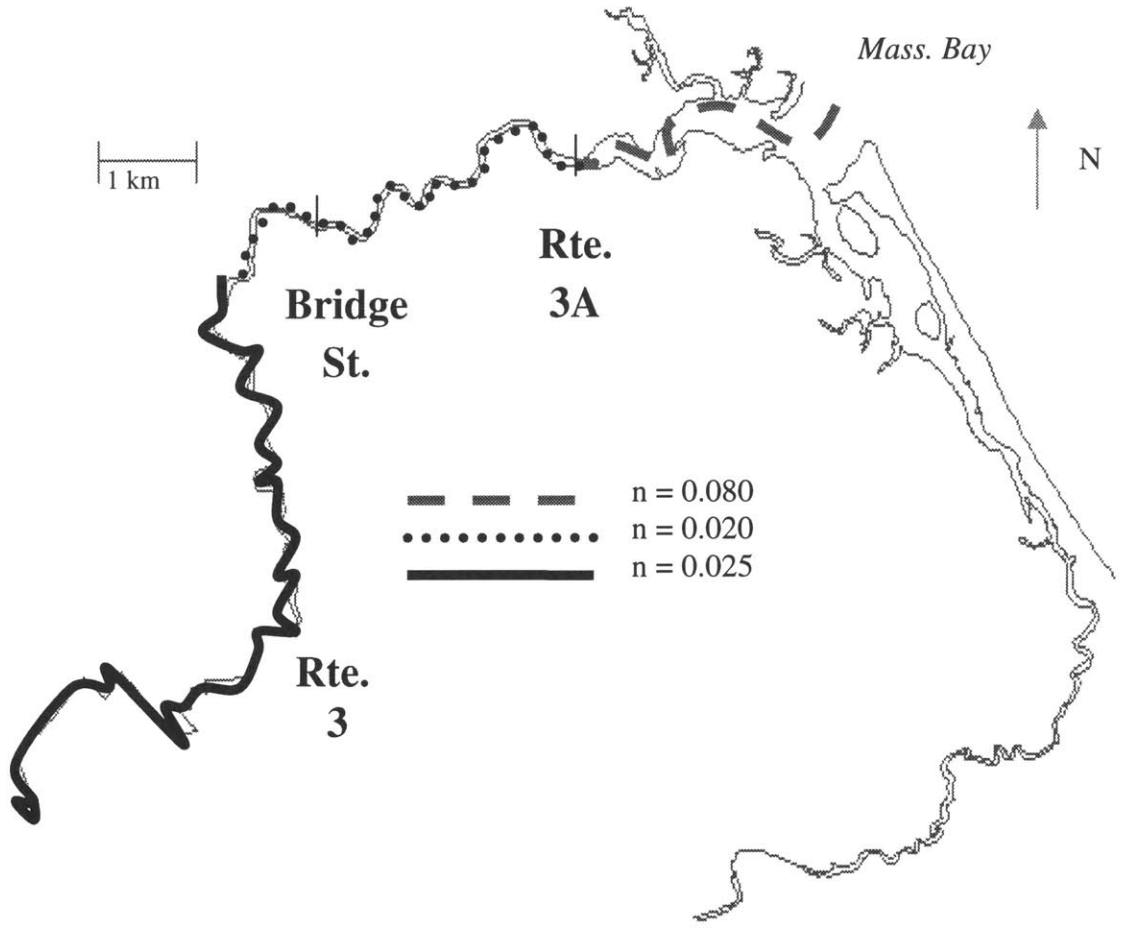

Figure 7.1 Reaches of North River with different Manning's n coefficients for Scheme 2

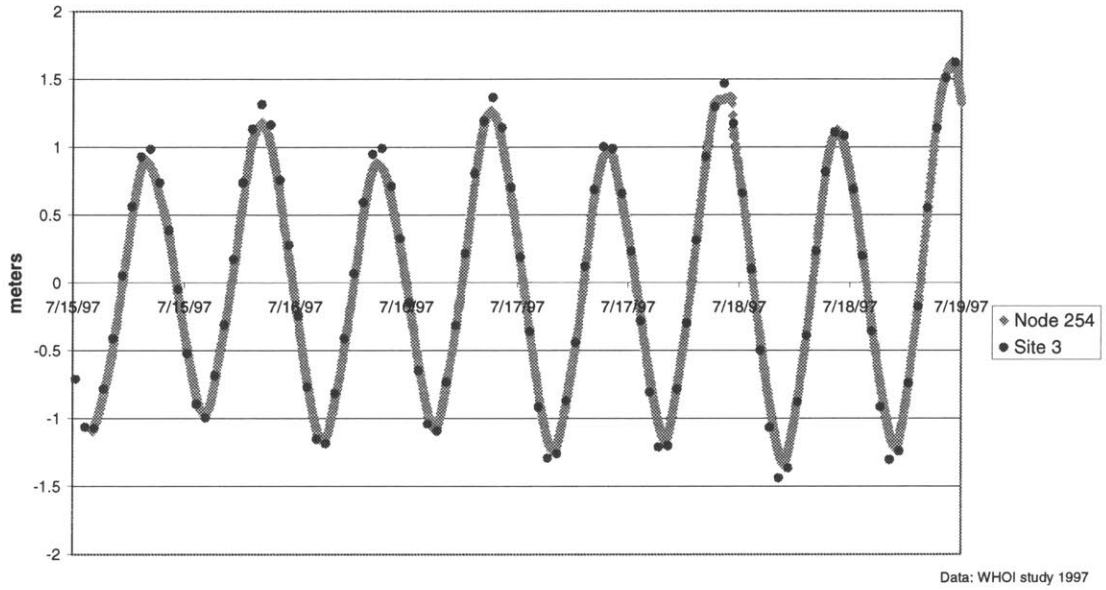

Figure 7.2 Tidal Range Calibration near Rte. 3A for Scheme 2 : Manning's n = 0.080

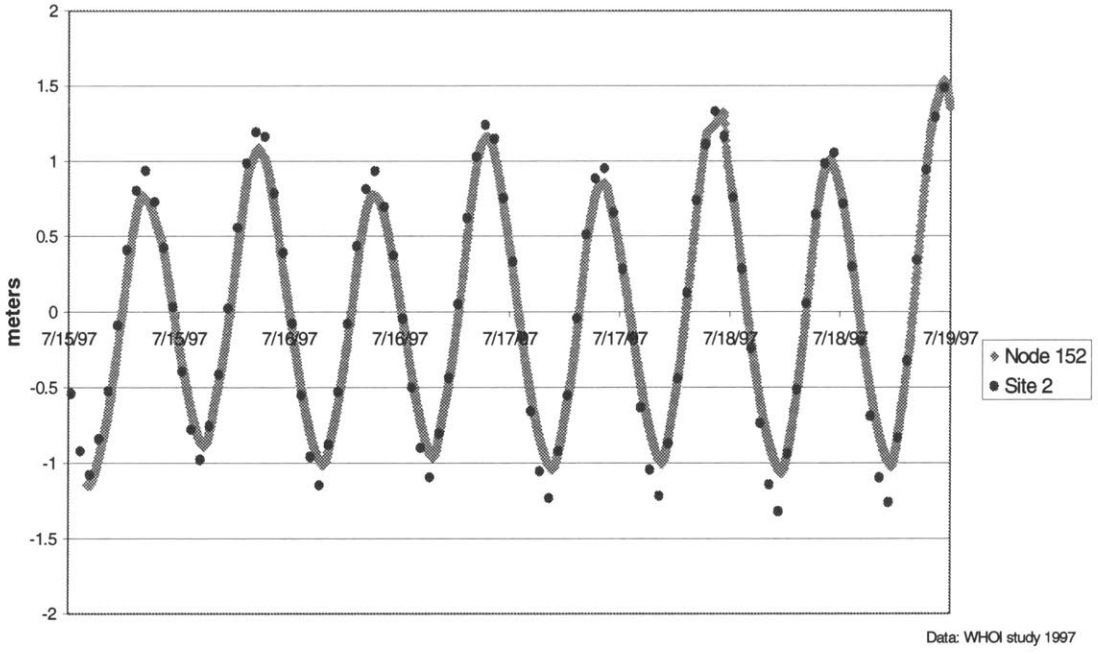

Figure 7.3 Tidal Range Calibration near Bridge St. for Scheme 2 : Manning's n = 0.020

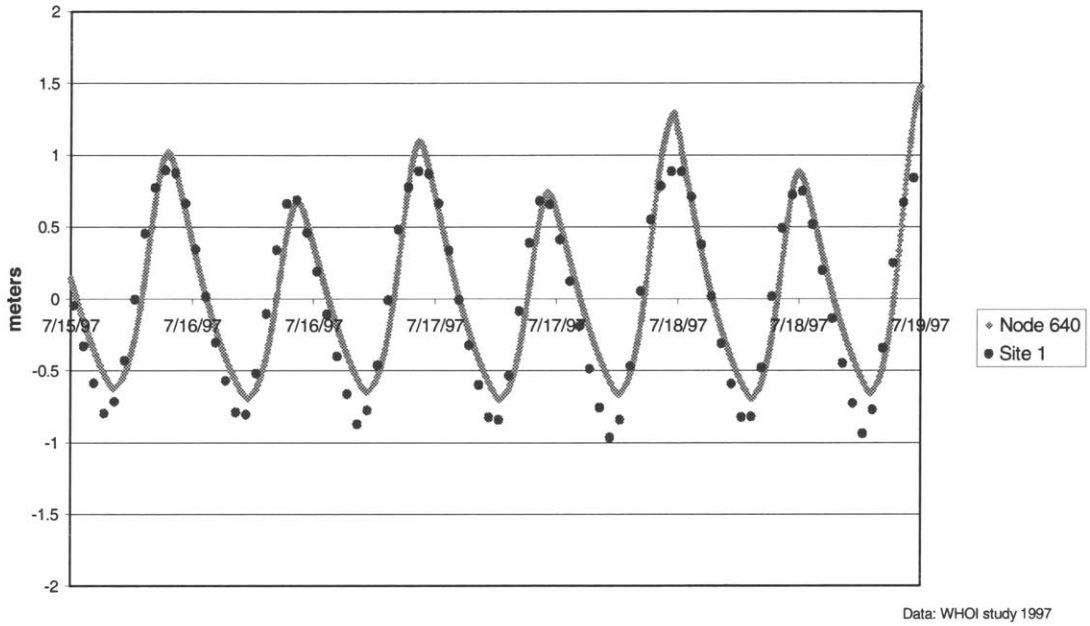

Figure 7.4 Tidal Range Calibration near Rte. 3 for Scheme 2 : Manning's n = 0.025

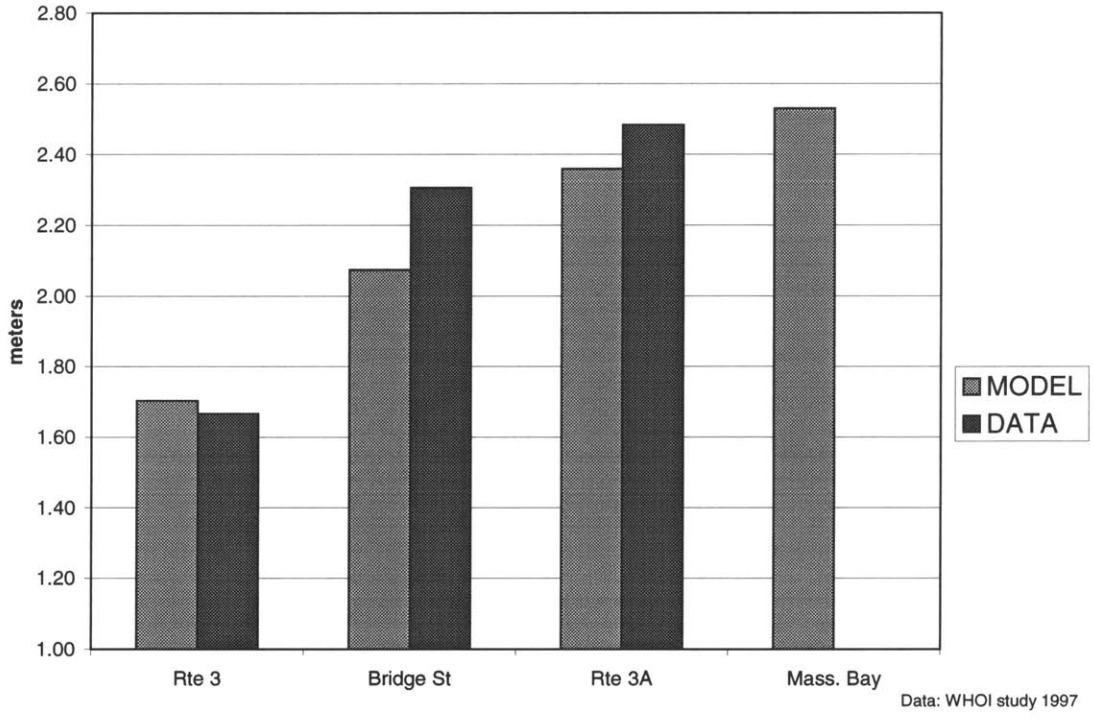

Figure 7.5 Average Tidal Range July 15-18, 1997 for Scheme 2 : Manning's n varies spatially

7.3 Velocity Calibration

The first two schemes give similar results for tidal ranges, but the velocity calibration results tell a different story. In Scheme 2, the Manning's n coefficients in the upstream stretch are at most half the value of the single coefficient used in Scheme 1. This allows for higher velocities in Scheme 2 than in Scheme 1 for the upstream stretches where Geyer took velocity measurements. The time series results for velocity at midstream node 1472 (Figure 7.6) approximate the velocities measured along the North River between Bridge St. and Route 3 by Geyer (Figure 7.7).

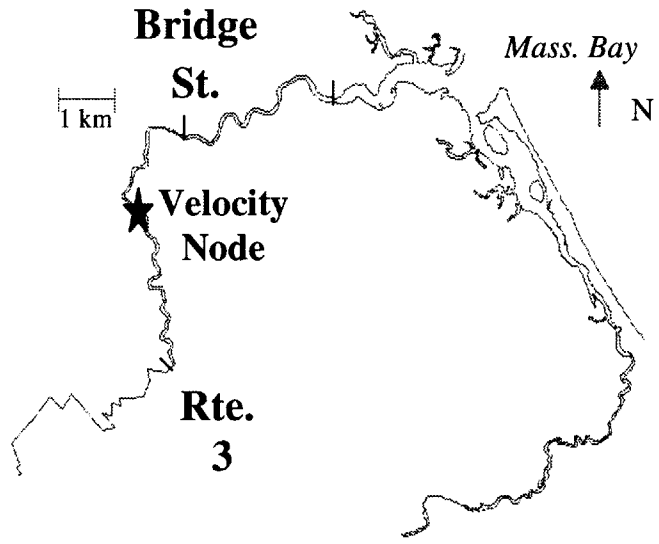

Figure 7.6 Location of Model Node Used for Velocity Calibration

An exact match of the model results and the data is not possible, because the data do not represent velocities at a single point like the model results do. However, the velocity results from Scheme 2 resemble the data for velocity in this stretch, while Scheme 1 (Figure 6.7) does not. Scheme 2 clearly outperforms Scheme 1 with respect to velocity and is more suitable as an input to a water quality model.

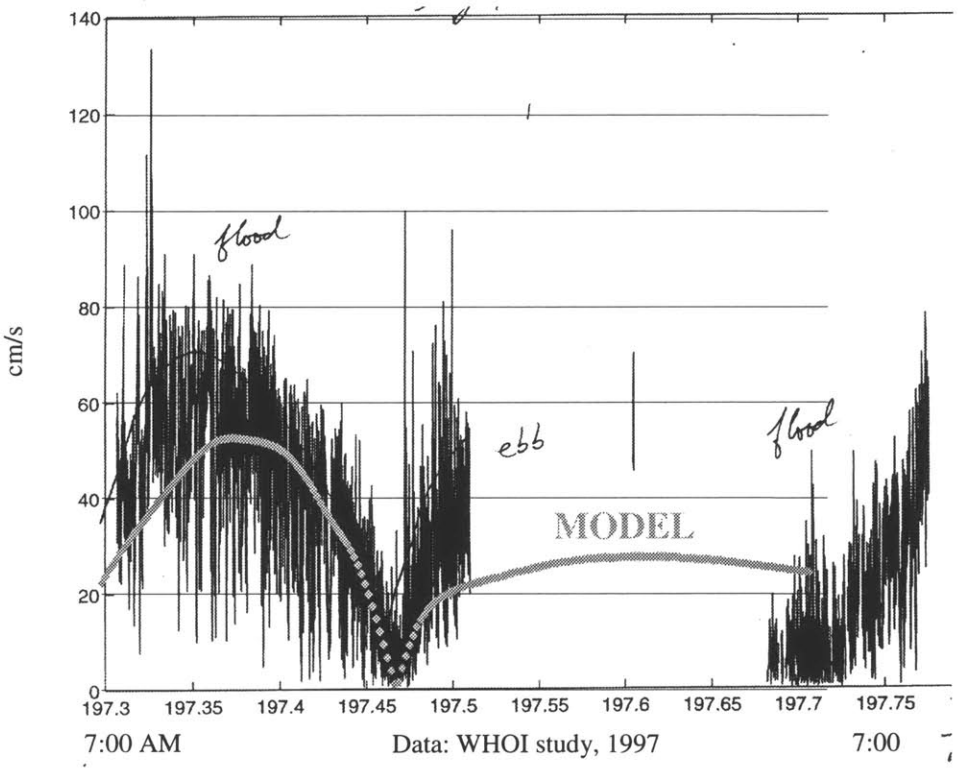

Figure 7.7 Velocity Calibration for July 17, 1997 between Bridge St. and Route 3 for Scheme 2

7.4 Tidal Lag Calibration

We are also concerned about the phasing of the tide in the model. To test this problem, we extract the times when the water depth is highest at the three locations and subtract the high tide time at the mouth to obtain a high tide lag at the three locations. This is done for both the data and the model results. We repeat the process for low tide in order to quantify the low tide lag. The model appears to do better for the high tide lag (Figure 7.8) than for the low tide lag (Figure 7.9). However, the data are only resolved to hourly data so that presents potential error in identifying when the high tide and low tide actually reach the measurement site. The resulting differences in lags are well within this error.

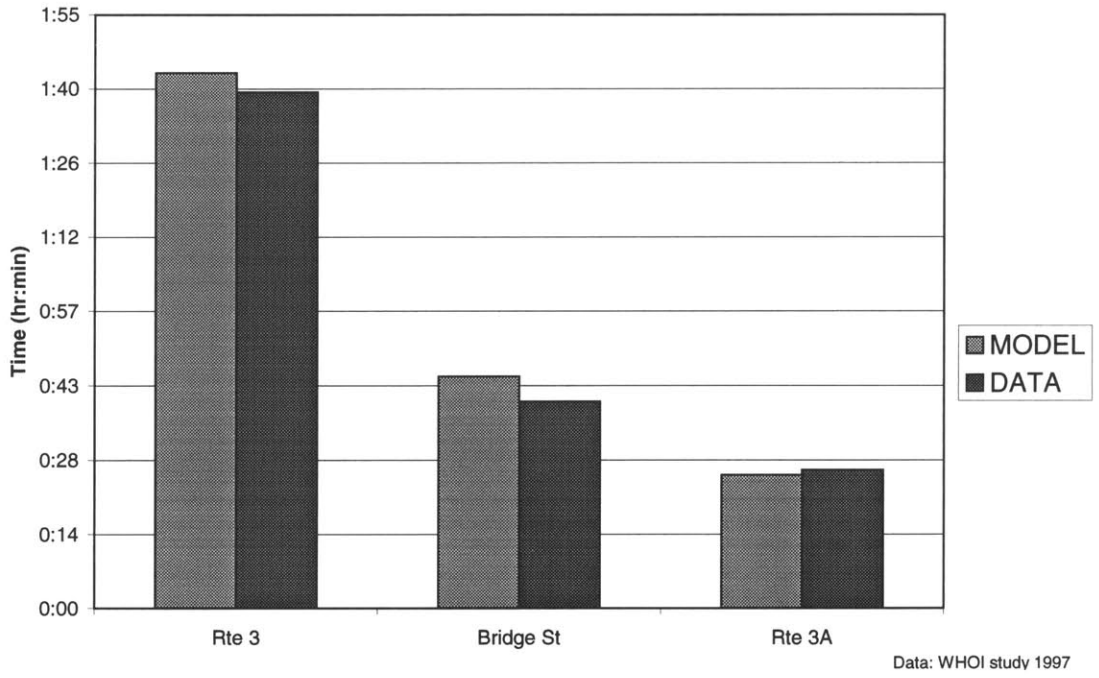

Figure 7.8 Average High Tide Lag July 15-18, 1997 for Scheme 2: Manning's n varies spatially

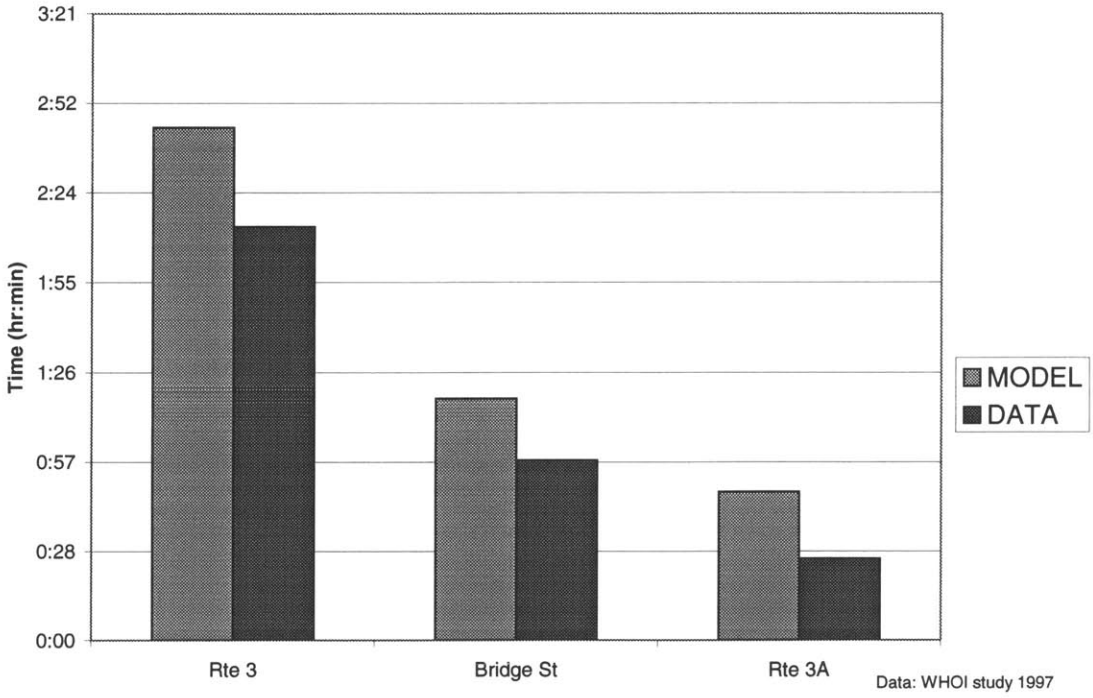

Figure 7.9 Average Low Tide Lag July 15-18, 1997 for Scheme 2: Manning's n varies spatially

7.5 South River Tidal Lags

The time series data are only available for three sites along the North River; there are no equivalent data for the South River. However, local knowledge provides approximate tide differentials from the mouth at Sea St. Bridge, Julian St. Bridge, and Willow St. Bridge along the South River (NSRWA; Figure 7.10). The model approximates the roughness coefficients in the South River in a similar fashion to the North River. In the mouth area, Manning's n is 0.080 and upstream, it is a more realistic 0.025 (Figure 7.8). Using the same method for checking the tidal lag as in the North River, we compare the average South River tidal lags from the model with the approximate lags provided (Table 7.1).

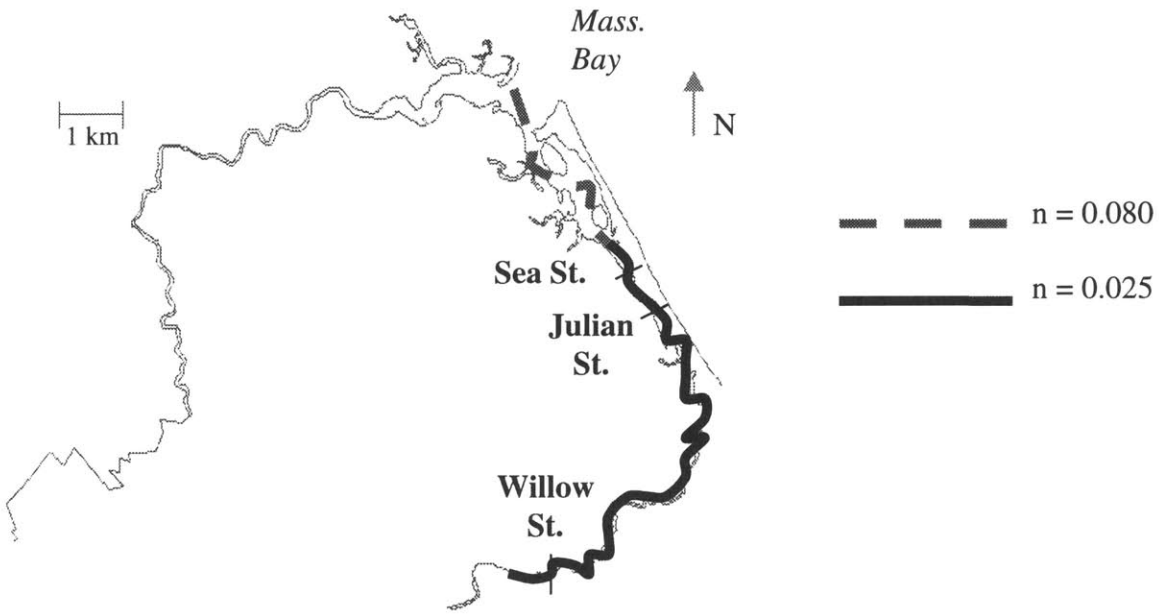

Figure 7.10 Locations for South River Tidal Lag Approximations and Manning's n estimates along different reaches of South River

Location	km from mouth	Model High Tide Lag	Model Low Tide Lag	NSRWA Approximation
Sea St. Bridge	4	0:16	1:01	0:30
Julian St. Bridge	5	0:26	1:25	0:45
Willow St. Bridge	9.5	0:40	2:24	1:00-2:00

Table 7.1 South Rivers Tidal Lags

The high tide lag and the low tide lag averages bracket the approximation and an average of the model's high tide and low tide lag is similar to the NSRWA approximation. The high tide should travel faster than the low tide because the average effect of bottom friction on the flow is less when the water is deeper. A look at the model's formulation of the friction, the Manning's equation (Equations 7.1) demonstrates this. Increasing the depth h decreases the external

traction on the system, which increases velocities and allows for faster propagation of the high tide than the low tide. However, the model may overestimate the difference between the high tide and low tide lags. Using tidal gages at specific points along the South River to measure changes in depths over the tidal cycle would enable this comparison.

$$\Gamma_{hx} = \frac{\rho g n^2 u \sqrt{(u^2 + v^2)}}{\mathbf{h}^{\frac{4}{3}}} \tag{7.1a}$$

$$\Gamma_{hy} = \frac{\rho g n^2 v \sqrt{(u^2 + v^2)}}{\mathbf{h}^{\frac{4}{3}}} \tag{7.1b}$$

where Γ_h = depth averaged external traction
ρ = density
g = acceleration due to gravity
u,v = velocities in horizontal Cartesian directions
h = water depth
Manning's n is a coefficient representing friction

7.6 Scheme 2 Verification

In order to test whether the model is robust, the model must be verified. Verification, sometimes referred to as validation, is the comparison of model results to data. This data set must not be the same data set used for calibration purposes (Ditmars *et al.*, 1987). Since Geyer's pressure data set extends through the middle of August 1997 and the calibration data set is confined to July 1997, a data set suitable for verification is available. Ideally, the verification data set represents different conditions from the calibration data set. The tidal boundary conditions are different between the July 15-20 calibration data and the August 9-14 verification data. The calibration tide rises from a neap tide condition toward the spring tide, while the verification data is at neap tide (Figure 7.11).

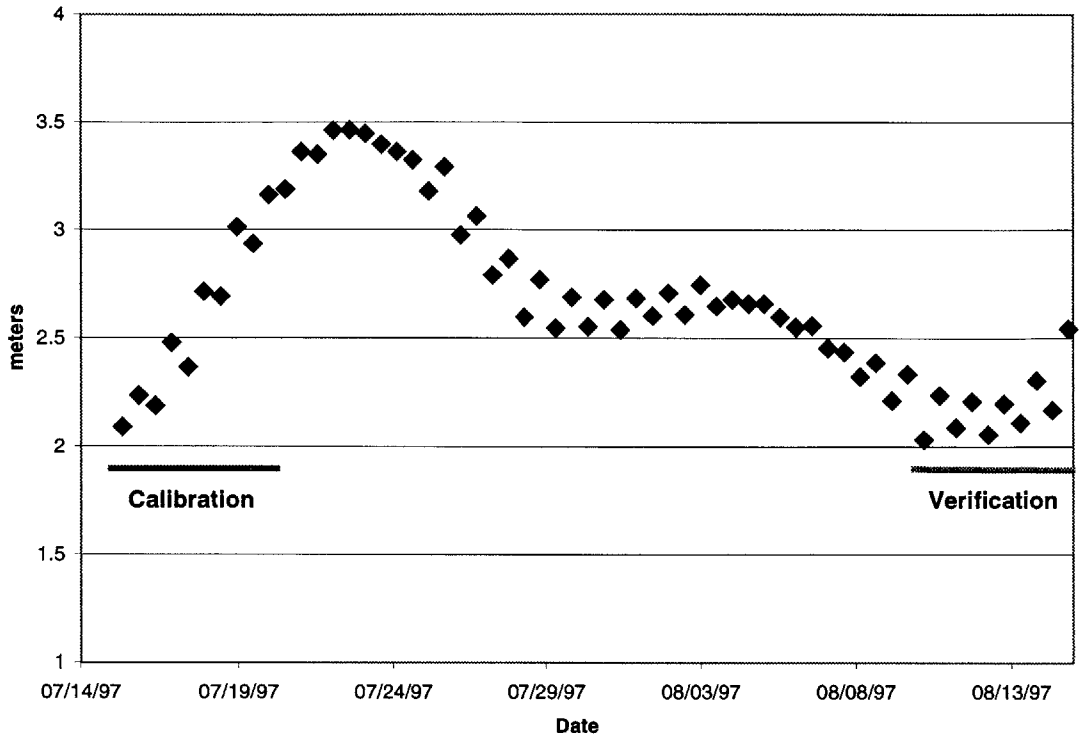

Figure 7.11 Tidal Range for Tidal Cycles from July 15 to August 14

Unfortunately, the freshwater inflow condition is similar for these two data sets. The average Indian Head Brook discharge into the North River at Curtis Crossing is only 14 m^3/s in the July period and 16 m^3/s in the August period. This summer is particularly dry; the average inflow in the 1990s has been 38 m^3/s in July and 76 m^3/s in August. To fully verify the model, we would want to use a springtime data set when the freshwater inflow is up to ten times greater. Since such a data set is not available, verification of the model is only possible for the summer condition. However, the water quality concerns take place during the summer and a model that is verified to work during the summer is adequate for the purpose of modeling the estuary's water quality.

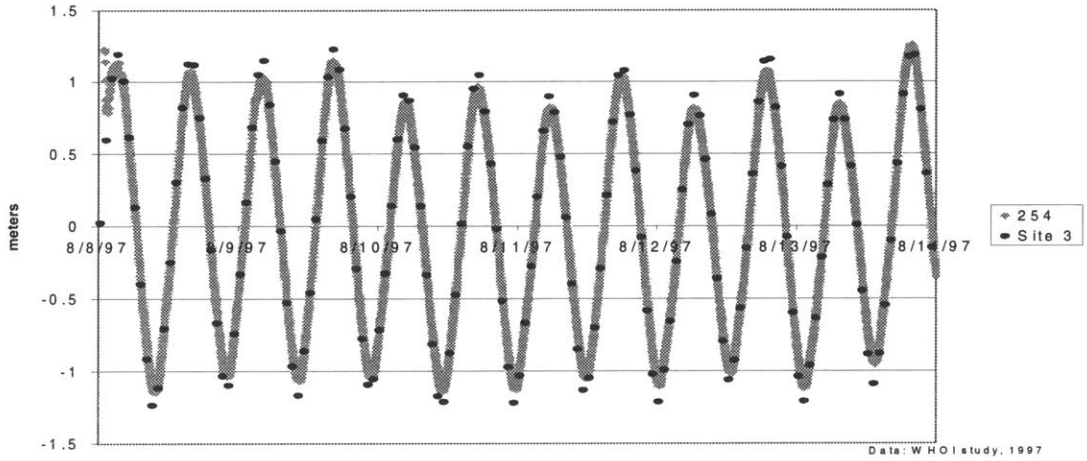

Figure 7.12 Tidal Range Verification near Rte. 3A for Scheme 2 : Manning's n = 0.080

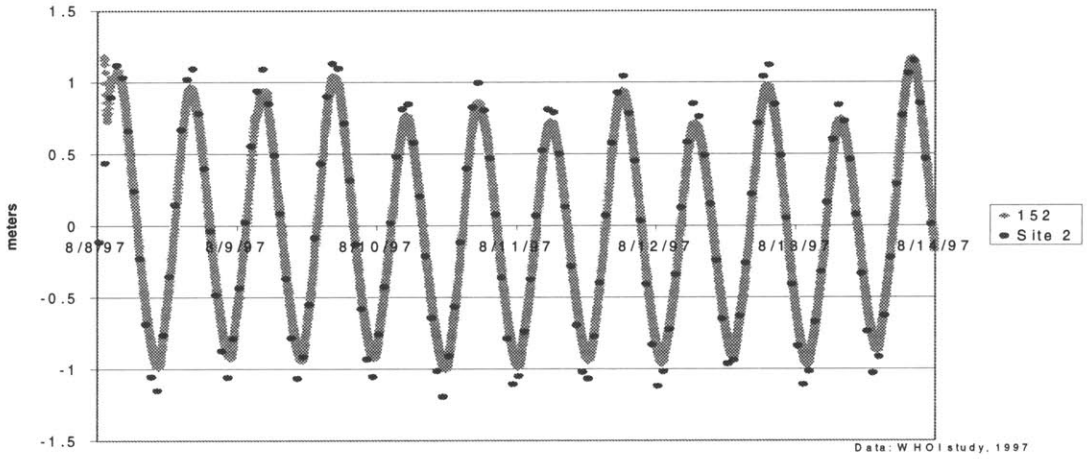

Figure 7.13 Tidal Range Verification near Bridge St. for Scheme 2 : Manning's n = 0.025

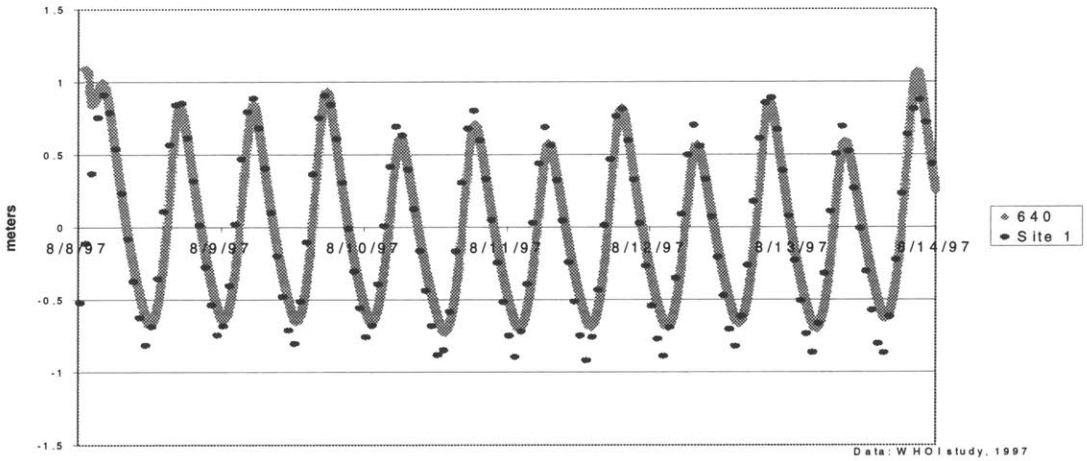

Figure 7.14 Tidal Range Verification near Rte. 3 for Scheme 2 : Manning's n = 0.020

7.6.1 Tidal Range Verification

The model's tidal ranges at the three sites approximate the time series data for the three sites (Figures 7.12-7.14). However, the model consistently underestimates the tidal range at all three sites. This may have to do with the estimates used for determining the tidal boundary condition. At Route 3A, three kilometers upstream of the mouth, the actual average tidal range is 2.21 meters. The average tidal range of the input used for the tidal boundary condition is 2.20 meters. This inconsistency means that the use of the 0.92 factor in reducing Boston Harbor tidal elevations to Scituate Harbor tidal elevations somehow does not quite apply for New Inlet boundary during this time period.

The model does not match the verification (August) data set as well as it matches the calibration (July) data set (Figure 7.15). This is to be expected because calibration involves adjusting parameters such as Manning's n to get a best fit with the data, while verification does not allow for any adjustment.

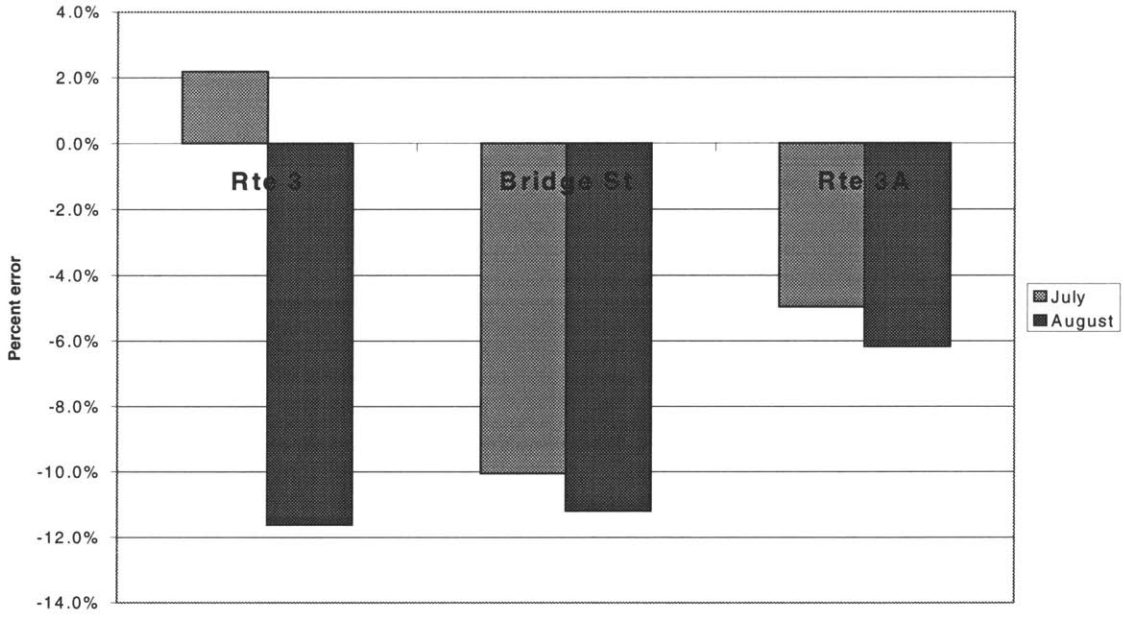

Figure 7.15 Percentage Error of Scheme 2 Tidal Range vs. Calibration Data Set and Verification Data Set

7.6.2 Tidal Lag Verification

The model does similarly for verification of the tidal lags as it does for calibration. Just like the calibration results, the model simulates the high tide lag (Figure 7.16) better than the low tide lag. (Figure 7.17). The model simulates the low tide lag as too long, but there is no discernable pattern to the high tide lag error (Table 7.2).

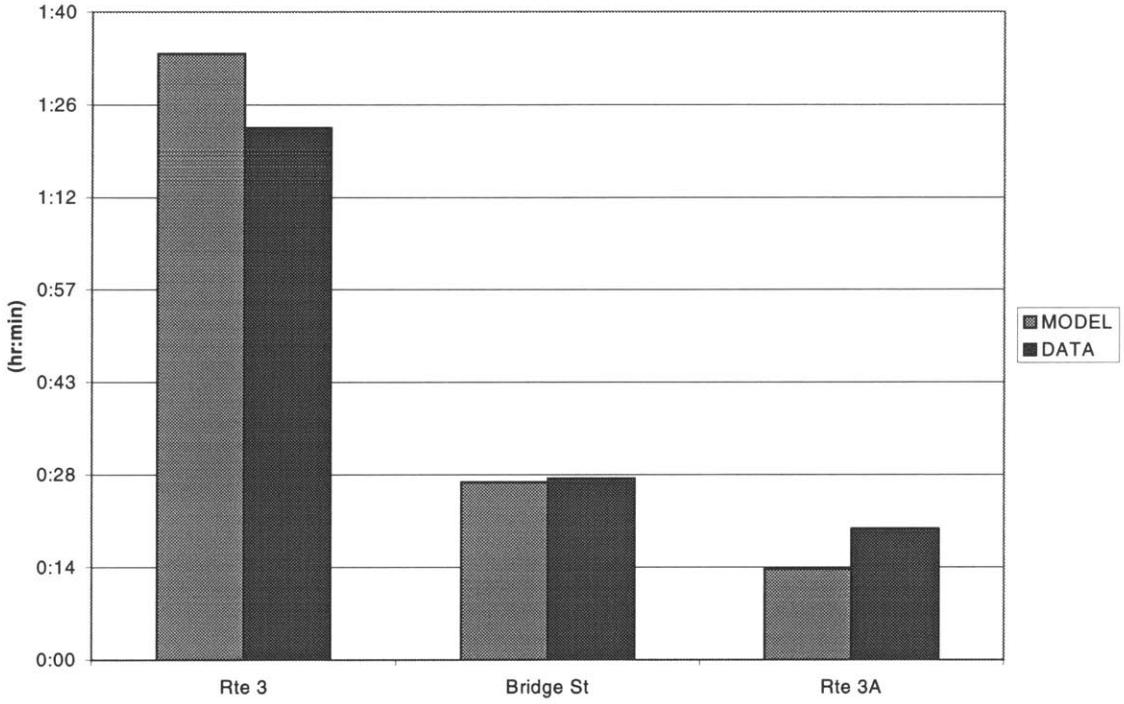

Figure 7.16 Average High Tide Lag August 8-13, 1997 for Scheme 2: Manning's n varies spatially

		High Tide Lag Error		Low Tide Lag Error	
	Kilometers from mouth	July	August	July	August
Route 3A	3	- 0:01	- 0:06	+ 0:21	+ 0:12
Bridge St.	7	+0:04	- 0:01	+ 0:19	+ 0:31
Route 3	14	+0:03	+ 0:11	+ 0:31	+ 0:43

Table 7.2 Errors (hr:min) of Model Lags vs. Calibration and Verification Data

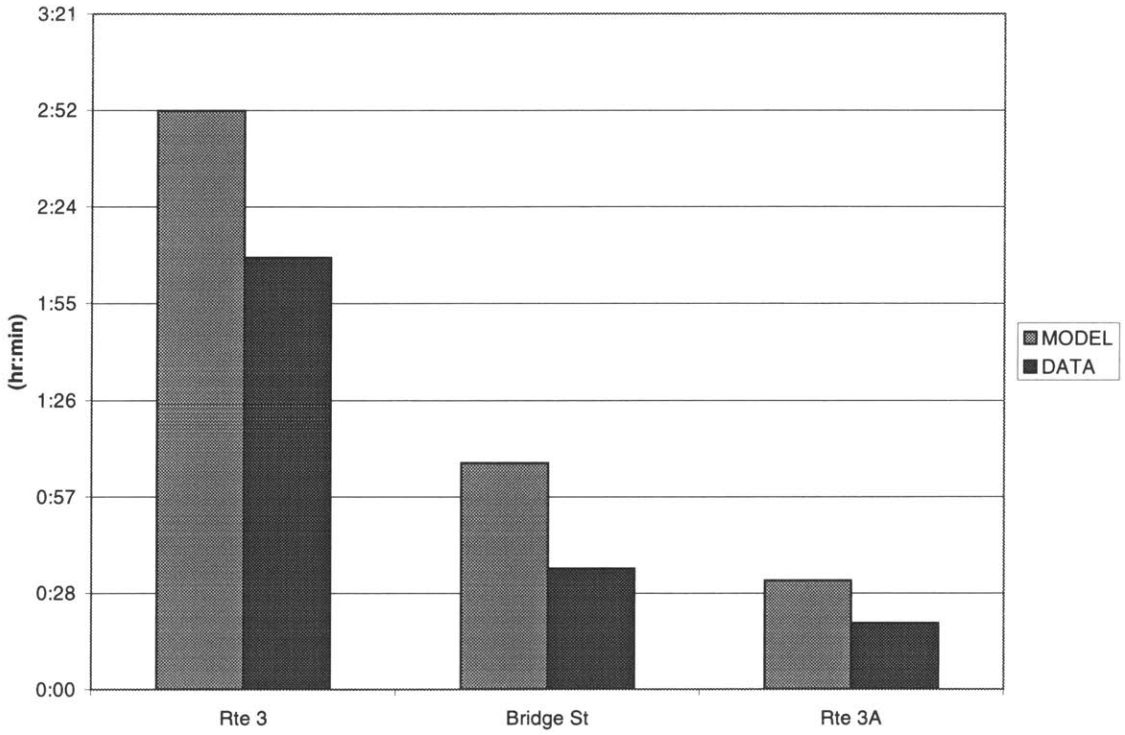

Figure 7.17 Average Low Tide Lag August 8-13, 1997 for Scheme 2: Manning's n varies spatially

7.7 Scheme 2 Discussion

The model calibrates and verifies with a high Manning's n assigned to the mouth and lower and more typical values assigned to the upstream reaches of the rivers. The high Manning's n must account for all the unresolved features of the mouth that add drag to the system and reduce the tidal range. Even though Manning's n is formulated as a depth-averaged result of bottom friction, Manning's n is a calibration tool for unresolved features. Because this scheme only models the lower water channel width, there are many of these unresolved features at the mouth of the river. These include the tidal flats and marshlands in the system that flood at high tide. This increases the channel width and reduces the tidal height. There are constrictions of the low water channel inside the mouth as well as embayments that cause recirculation. All of these

features add drag to the system that must be accounted for by a high Manning's n. In the upstream reaches of the river, however, the low water line is similar to the high water line and the assigned Manning's n can be closer to typical values. This allows velocities in the upstream reaches of the river to calibrate with velocity data.

Using a high Manning's n to represent the sum of the drag at the mouth does have problems. This is most notable when viewing the calibration and verification results for the lag of the low tide up the river. The model consistently overestimates the time it takes for low tide to propagate from the tidal boundary to upstream sites like Bridge St. and Route 3. At low tide, the water is confined to the low water channel so the flow does not encounter many of the features that add drag to the system. The tidal flats and marshlands only affect the flow when it reaches higher elevations. These features add drag that reduces the tidal range and slow down the propagation of the high tide, but do not really affect the low tide flow. A high Manning's n does not represent the low water channel well and the output velocities at low tide in the mouth area are probably too low. As a result, the low tide lags are too large. If the low water channel is defined as separate from the high water features such as tidal flats and marshlands, a lower Manning's n is appropriate. This scheme defines the whole channel by the low water line so Manning's n represents the temporal sum of drag as well as a spatial average.

Despite this problem, the model generally performs well. The model can be used as an input to a water quality model as long as the water quality modeler understands the limitations of this hydrodynamic scheme.

8. Salinity

The second scheme is used to model salinity in the rivers. The model sets the salinity at the ocean boundary as a constant of 35 parts per thousand. The model treats the freshwater sources at the head of the rivers and along the river as either continuity line inflows or element inflows as described in Section 5.2.

8.1 The Initial Condition and Freshwater Flushing

Setting an initial condition for the distribution of salinity is necessary because it takes a long time for the model to eliminate an initial condition of constant salinity in the water body. The estuary actually has a salinity gradient from the ocean salinity at New Inlet to freshwater at the North River tidal head. Only after the model sets up a realistic gradient will its salinity results reflect reality.

A harmonic steady state model run can approximate the amount of time it takes to eliminate the initial condition and reach a realistic salinity gradient. We run a harmonic steady state model by using a harmonic boundary condition with constant range of 2.8 meters at the North River Inlet and constant freshwater inflow approximating July conditions (~0.5 m^3/s). The harmonic representing the changing tidal elevations at the boundary approximates a M2 semi-diurnal curve so that there are 2 cycles per day (Equation 8.1).

$$H = a * \cos(\omega * t + \theta) + \overline{H} \qquad (8.1)$$

where H =tidal elevation above mean lower low water
a = amplitude = 1.4 m
ω = M2 harmonic speed (radians/hr) = 0.5076 rad/hr
t = time (hr)
θ = Phase advance at time 0 = $\pi/4$
$\overline{H}$ = Average tidal elevation above mean lower low water = 1.5 m

The ocean boundary has a constant salinity of 35 ppt so salt is entered into the system with the rising tide. However, starting at an initial condition of zero salinity throughout the estuary, it takes at least two weeks for the salinity in the model to reach harmonic steady state.

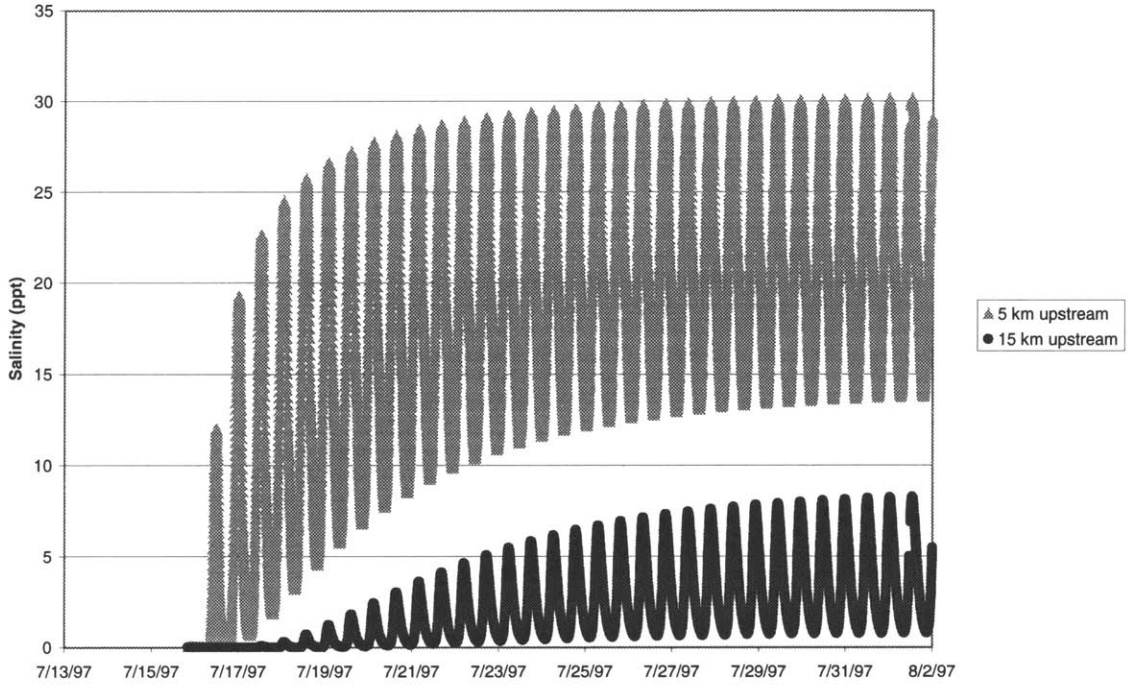

Figure 8.1 Salinity Response to Harmonic Boundary Condition : 5 km and 15 km Upstream

This result is compared to the residence time of freshwater in the estuary using the following formulation (Equation 8.2). This divides the inventory of freshwater by the renewal rate:

$$\tau = \frac{\int f dV}{Q_f} \tag{8.2}$$

where τ = average freshwater residence time
f = freshwater fraction = (ocean salinity-salinity)/ocean salinity
Q_f = freshwater inflow
V = volume represented by freshwater fraction.

Using the average salinity from July to August 1997 (Geyer, 1997) at Route 3A, Bridge St., and Route 3 (Figure 8.1) and rectangular estimates of the cross-section around each point, an inventory of 1.25 million cubic meters of freshwater is calculated (Table 8.1). During this period, the average inflow at Curtis Crossing is about 0.16 m^3/s, and since the North River drainage area is 2.3 times the drainage area of Curtis Crossing, the estimate for freshwater inflow is 0.37 m^3/s.

Site	km upstream	Salinity (ppt)	f	Depth (m)	Width (m)	Δx (km)	fΔV (m^3)
New Inlet	0	35	0	5	150	3	0
Rte. 3A	3	29.1	0.17	5	80	4	204,000
Bridge St	7	22.7	0.35	4	50	7	280,000
Rte. 3	14	9.8	0.72	2	40	1.5	403,000
Tidal Head	20	0	1	2	40	4.5	360,000

Table 8.1 Calculation of Average Freshwater Inventory in North River July-August 1997

The residence time for freshwater in these two dry summer months is about forty days. Both the quasi-steady state model run and the long estimate for residence time point to the need to set initial conditions for the distribution of salinity in the estuary. We accomplish this by setting the salinity at certain nodal coordinates in a text file and using saltic.exe to revise a restart file with interpolated salinity values. Because the initial salinity distribution is not exact, we must be mindful of the time it will take to correct that distribution when modeling salinity.

8.2 Salt Calibration

Along with the pressure data used to calibrate the tidal ranges and lags along the North River, the Woods Hole study monitored salinity at the same points: Rte. 3A, Bridge St., and Rte. 3 (Figure 8.2). We compare these hourly data to model results for salinity at equivalent model nodes. A local high school class has monitored salinity over a day on several occasions, but the goal is to model longer periods of time so Geyer's data set is most appropriate.

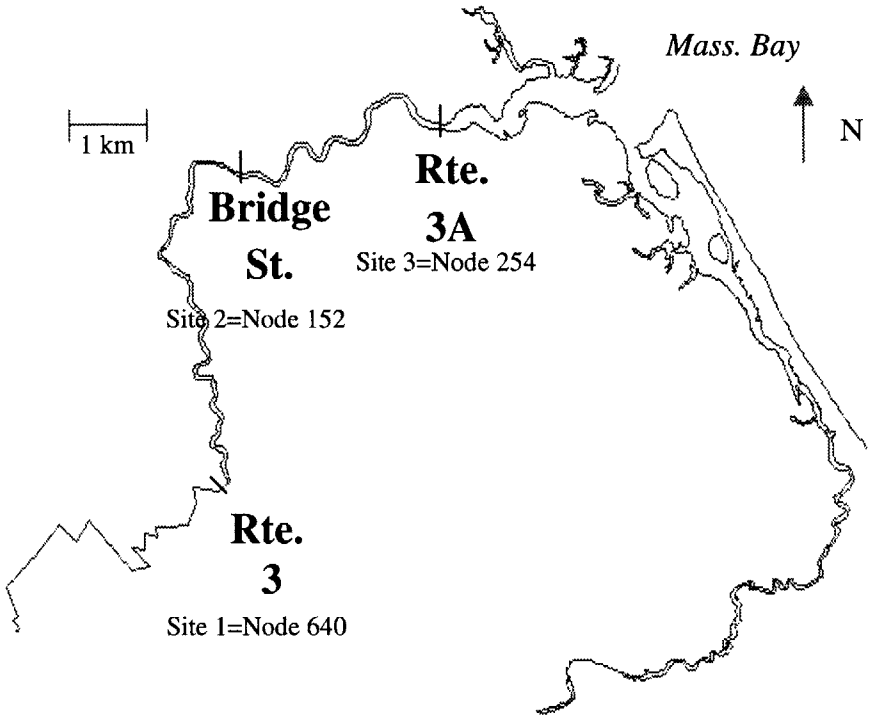

Figure 8.2 Location of North River Salinity Gauge Stations

In order to model the system for comparison, we set initial conditions of salinity along the river based on the salinity measurements at the three points at the start of the model run. For the following comparisons (Figures 8.3-8.5), the initial conditions are based on salinity data for July 15 at 11:19 PM EDT.

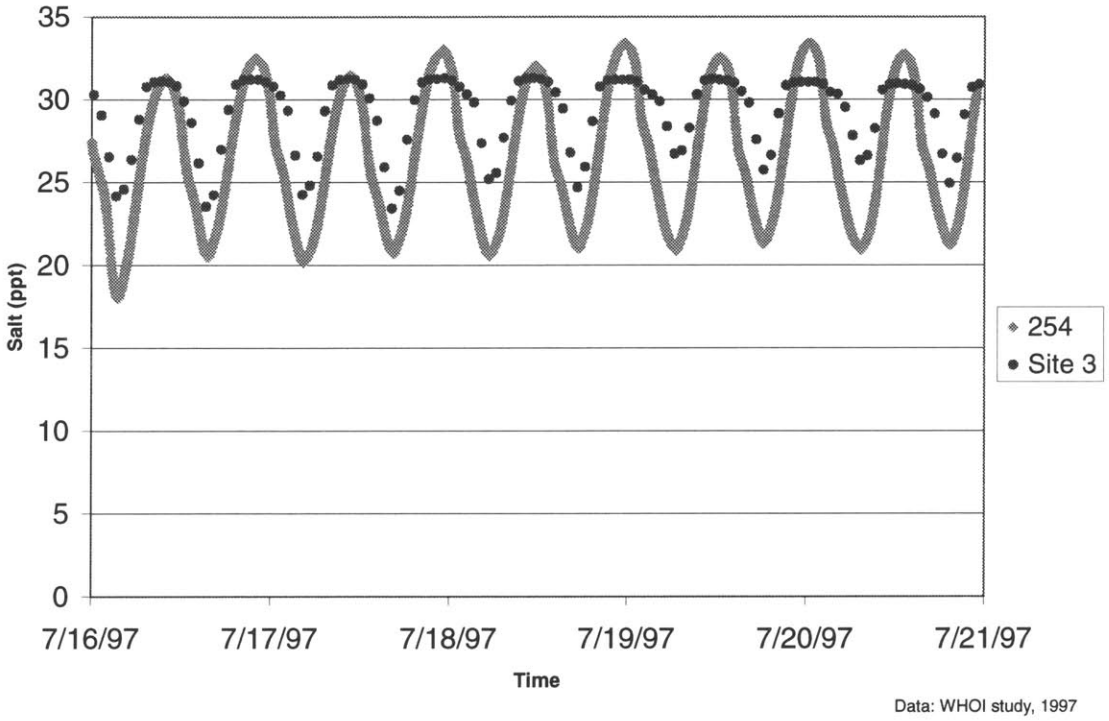

Figure 8.3 Salt Calibration near Rte. 3A for Scheme 2 : Manning's n = 0.080

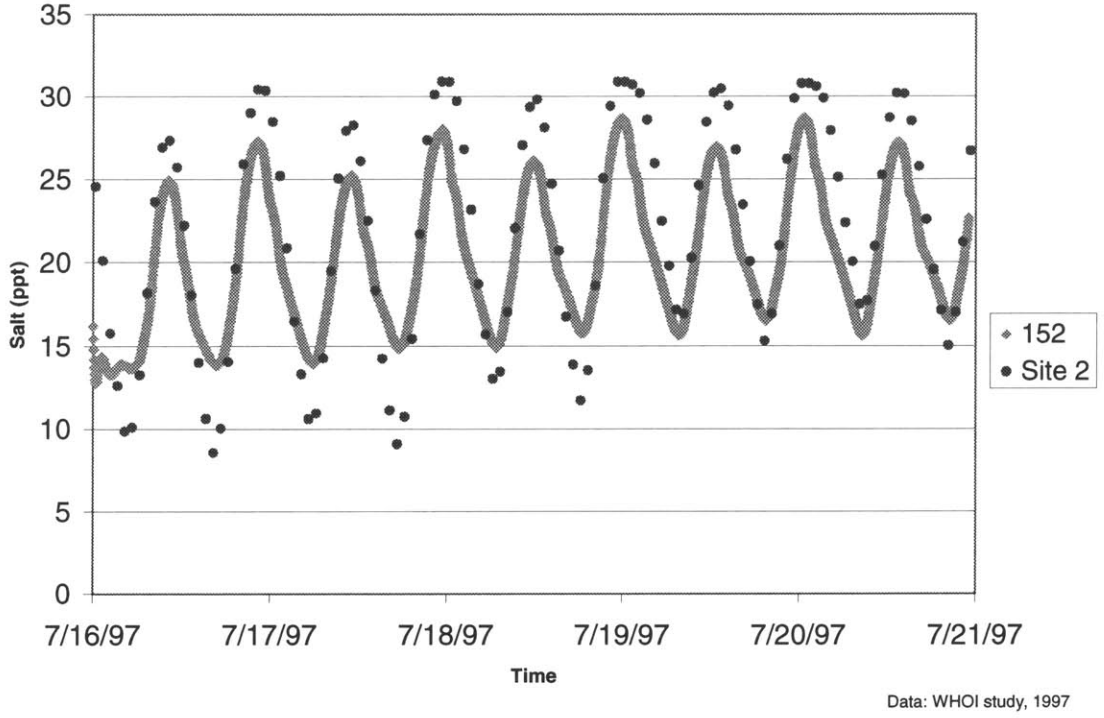

Figure 8.4 Salt Calibration near Bridge St. for Scheme 2 : Manning's n = 0.020

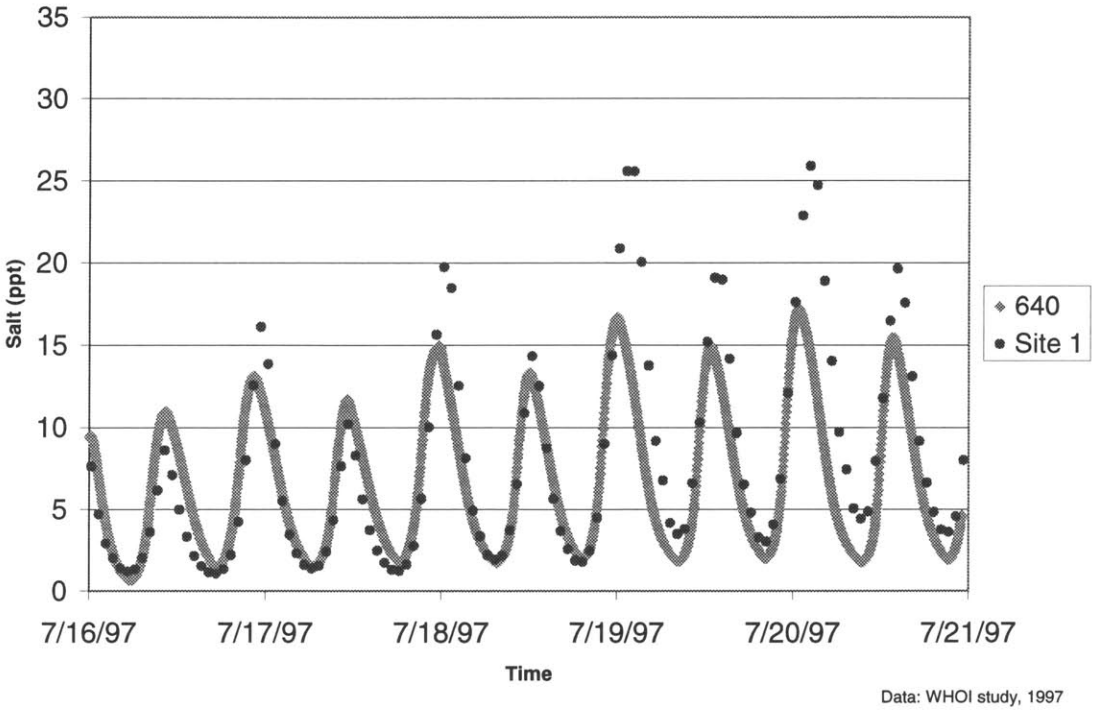

Figure 8.5 Salt Calibration near Rte. 3 for Scheme 2 : Manning's n = 0.025

8.3 Salt Verification

The August data set used for verifying the tidal range and the tidal lags has accompanying salinity measurements. Comparing these measurements to the salinity output of model runs representing August 8-13, 1997 is verification of the salinity model (Figures 8.6-8.8). The initial conditions for verification are based on salinity data for August 8 at 3:19 AM EDT.
There is very similar performance of the salinity model for the August data set as for the July data set.

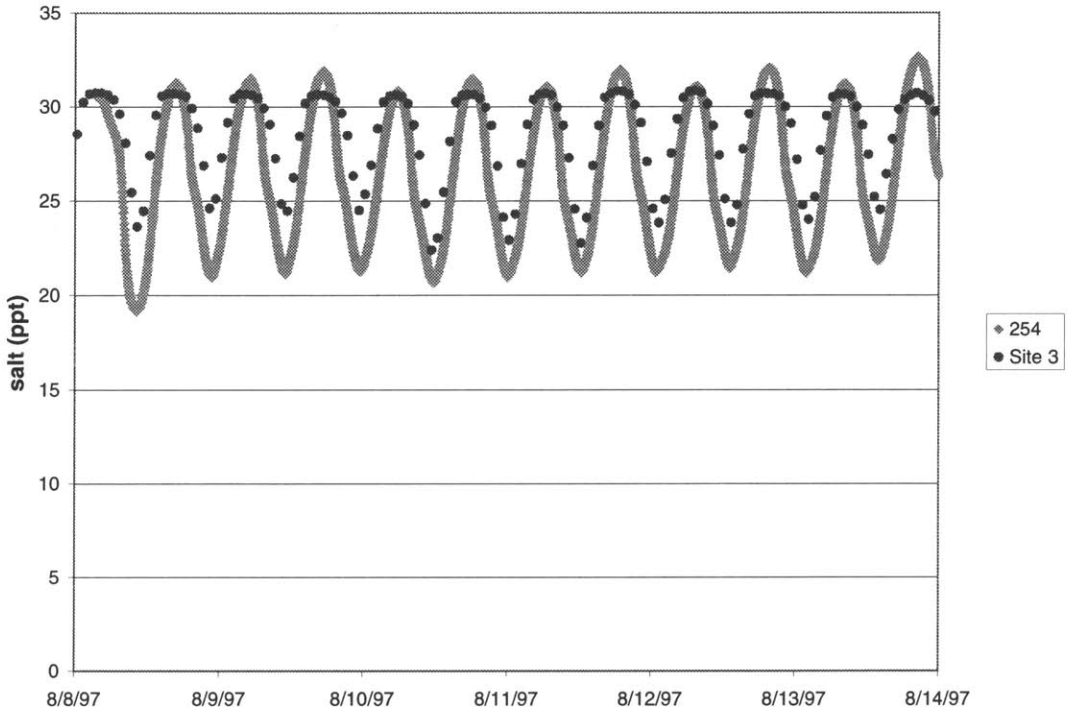

Figure 8.6 Salt Verification near Rte. 3A for Scheme 2 : Manning's n = 0.080

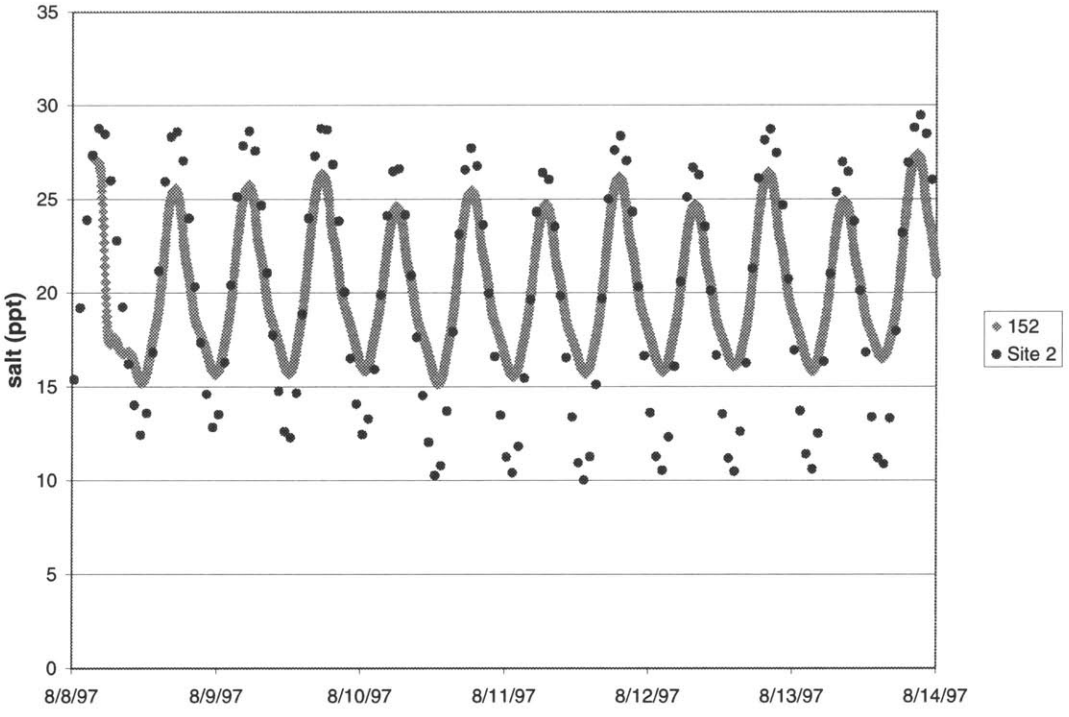

Figure 8.7 Salt Verification near Bridge St. for Scheme 2 : Manning's n = 0.020

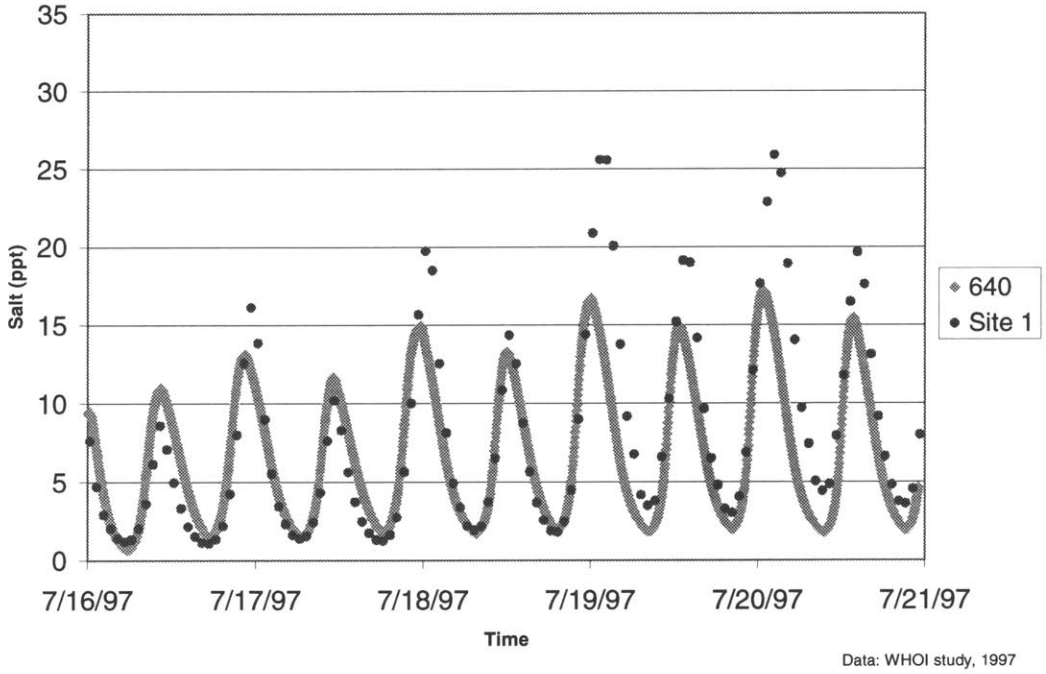

Figure 8.8 Salt Verification near Rte. 3 for Scheme 2 : Manning's n = 0.025

8.4 Salinity Discussion

The salinity results from the model are similar to the salinity data. The results and data match up very well at Rte. 3 (Figures 8.5 and 8.8) – nearest the freshwater head. At Bridge St., the mid-reach point of the three monitoring sites, the salinity range of the model is not quite as large as the salinity range of the data (Figures 8.4 and 8.7). This may indicate the presence of groundwater inflows in the mid-reach stretch of the river. At Rte. 3A, the model's salinity matches the data salinity well at high tide, but at low tide, the model shows lower salinity than the data (Figures 8.3 and 8.6). This is likely a result of this scheme's failure to represent the marshlands. The marshlands flood during high tide and receive salt during that time. However, due to the slower flows in the marshland, the salt is not released to the main channel exactly with the ebb tide. Instead, the marshlands slowly release the salt to the main channel for transport downstream. As a result, the marshlands act as a buffer for salt – keeping the salinity high at low tide.

8.5 Salt-Density Coupling

The calibrated and verified hydrodynamics model does not account for changes in salinity. That is, the hydrodynamics equations of continuity and momentum are not coupled with the salt transport equations. Salt concentrations can affect the hydrodynamics because the density of water is a function of salinity. The main impact of the salinity-density effect occurs when the salt concentrations change in space. This salinity gradient effects a pressure gradient, which enters the momentum equations in the baroclinic pressure term. For the depth-averaged momentum equations (Equations 8.3), this term involves the horizontal pressure gradient.

$$\frac{\partial u}{\partial t}+u\frac{\partial u}{\partial x}+v\frac{\partial u}{\partial y}-fv-\frac{1}{h}\frac{\partial}{\partial x}(h\varepsilon_{xx}\frac{\partial u}{\partial x})-\frac{1}{h}\frac{\partial}{\partial y}(h\varepsilon_{xy}\frac{\partial u}{\partial y})+g\frac{\partial \eta}{\partial x}+\frac{\mathbf{1}}{\boldsymbol{\rho}}\mathbf{g}\boldsymbol{\eta}\frac{\partial \boldsymbol{\rho}}{\partial \mathbf{x}}+\Gamma_{hx}=0 \qquad (8.3a)$$

$$\frac{\partial v}{\partial t}+u\frac{\partial v}{\partial x}+v\frac{\partial v}{\partial y}+fu-\frac{1}{h}\frac{\partial}{\partial x}(h\varepsilon_{yx}\frac{\partial v}{\partial x})-\frac{1}{h}\frac{\partial}{\partial y}(h\varepsilon_{yy}\frac{\partial v}{\partial y})+g\frac{\partial \eta}{\partial y}+\frac{\mathbf{1}}{\boldsymbol{\rho}}\mathbf{g}\boldsymbol{\eta}\frac{\partial \boldsymbol{\rho}}{\partial \mathbf{y}}+\Gamma_{hy}=0 \qquad (8.3b)$$

where g = gravitational acceleration
η= water elevation above a horizontal datum
ρ=density
x,y= horizontal, Cartesian coordinates

When coupled with salt, because salt makes water more dense, this effect should accelerate water moving away from the ocean or decelerate water moving toward the water. RMA-10 allows for coupling of salt transport with the momentum equations. The depth-averaged salt transport equation (Equation 8.4) depends on the hydrodynamic outputs of velocities (u,v) and depth (h).

$$\frac{\partial S}{\partial t}+\mathbf{u}\frac{\partial S}{\partial x}+\mathbf{v}\frac{\partial S}{\partial y}-\frac{1}{\mathbf{h}}\frac{\partial}{\partial x}(\mathbf{h}D_x\frac{\partial S}{\partial x})-\frac{1}{\mathbf{h}}\frac{\partial}{\partial y}(\mathbf{h}D_y\frac{\partial S}{\partial y})-\theta_s=0 \qquad (8.4)$$

In turn, the momentum equations are affected by salinity S through changes in density so RMA-10 iterates until it can best approximate solutions to both the momentum equations and the transport equation. The relationship between salinity and density is defined by an equation of state. RMA-10 uses the following equation of state (Equation 8.5) for salinity (King, 1993).

$$\rho = 999.835\frac{kg}{m^3}[1.0 + \frac{(4.906S - 11.7)}{(6511.7 - 1.906S)} \tag{8.5}$$

where S = salinity in parts per thousand
ρ = density in kilogram per cubic meter

However, turning on the coupling of the equations for this application of the model makes very little difference for tidal range (Figure 8.9) and tidal lag (Figures 8.10-8.11).

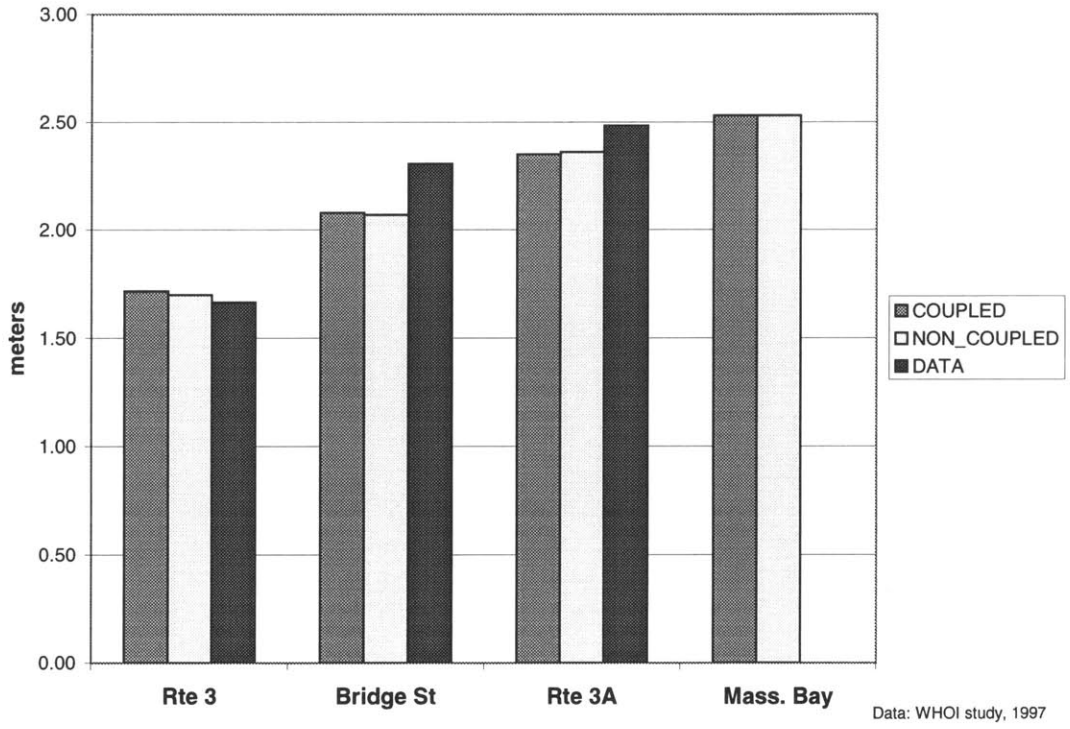

Figure 8.9 Effect on Average Tidal Range July 15-18, 1997 of Coupling Salt and Density

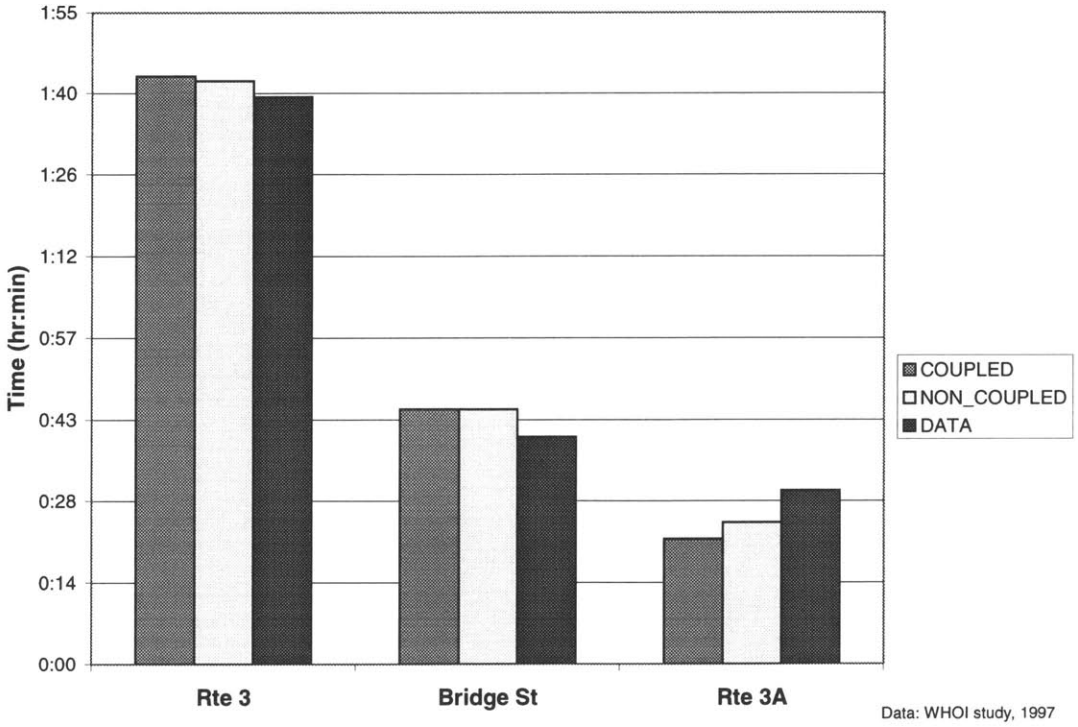

Figure 8.10 Effect on Average High Tide Lag July 15-18, 1997 of Coupling Salt and Density

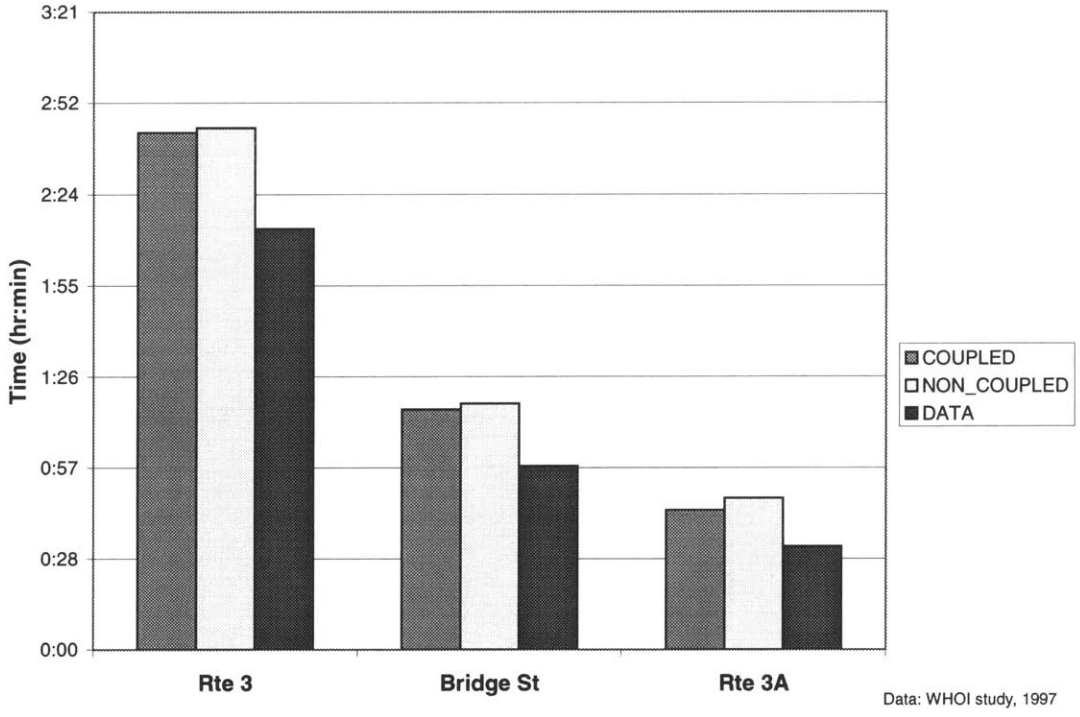

Figure 8.11 Effect on Average Low Tide Lag July 15-18, 1997 of Coupling Salt and Density

9. Scheme 3: Addition of Tidal Flats

Scheme 3 involves modeling the tidal flats. The scheme adds elements to the sides of the main channel represented in the first two schemes. As discussed in Section 4.4, the placement of these tidal flat elements is based on tidal flats represented in USGS topographic maps. This scheme resolves the transverse changes in bottom elevation of the channel better than the first two schemes.

9.1 Wetting and Drying

These tidal flat elements have higher bottom elevations than the main channel and the mean lower low water line. In fact, the bottom elevations assigned to these new elements increase with distance from the main channel to a level higher than the mean water line. As a result, these elements can represent the wetting and drying process of the tidal flats over the tidal cycle. At low tide, the water stays in the main channel represented in the first two schemes. At high tide, the water floods the tidal flats and the channel width increases tremendously.

RMA-10 represents this changing channel cross-section with its drying node implementation (King, 1993). In depth-averaged sections of the model, RMA-10 checks the depths at nodes. If this depth is below a constant set by the modeler (2 cm in this application), the model eliminates any element containing the node from the system. The model determines whether to include a previously dry element in the system with the re-wetting formulation. If the projected depths of all the element's nodes are above a constant set by the modeler (6 cm), the model includes the element. This effect can be seen in Figures 9.1 and 9.2 which show flow in an area dominated by tidal flats, the North River mouth, also known as the Spit. At low tide, the water flows around the tidal flat and the tidal flat is dry (dark grey areas in Figure 9.1). At high tide, the water flows over the tidal flat (Figure 9.2).

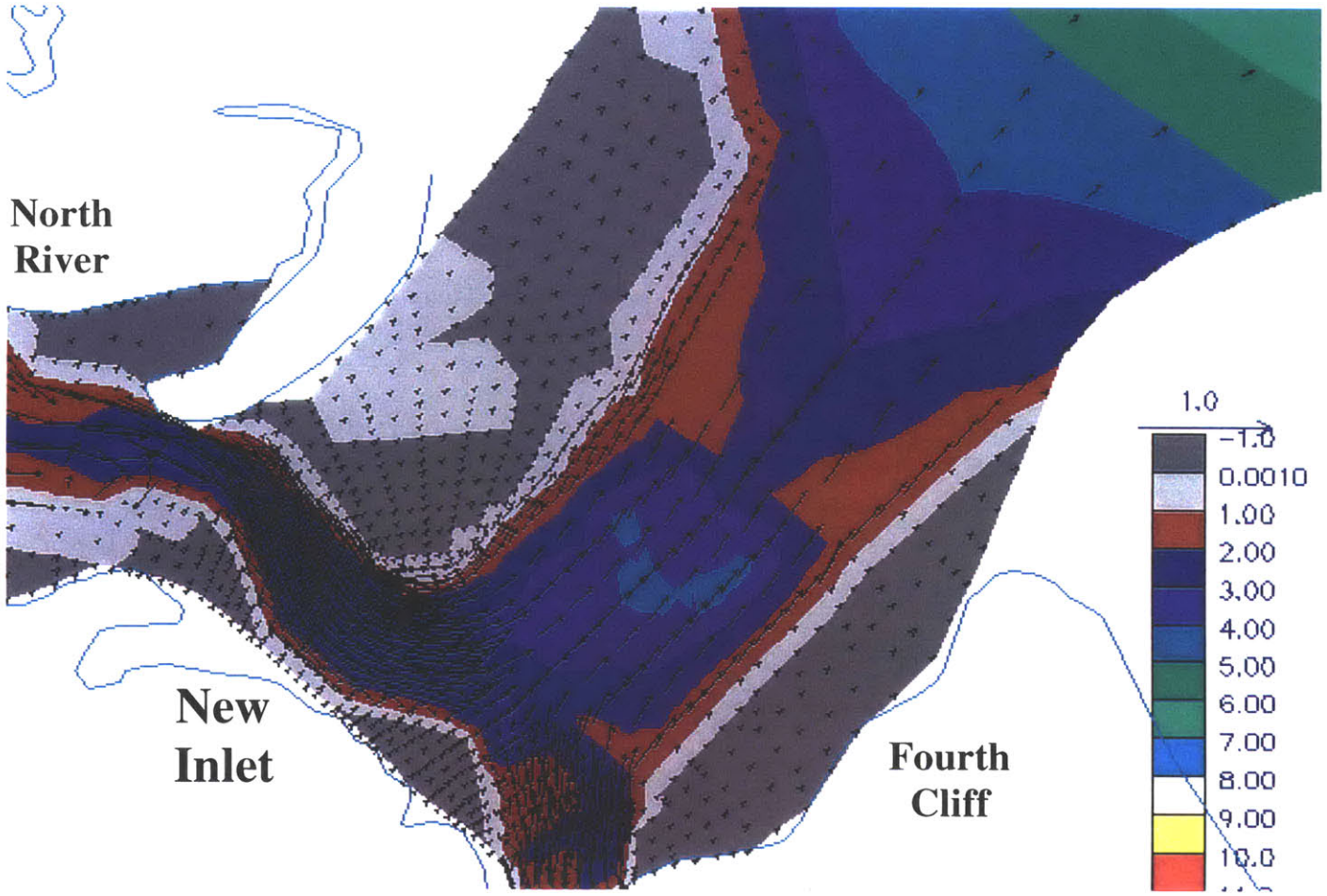

Figure 9.1 Low Tide Flow Around a Dry Tidal Flat (Contours of depth in meters)

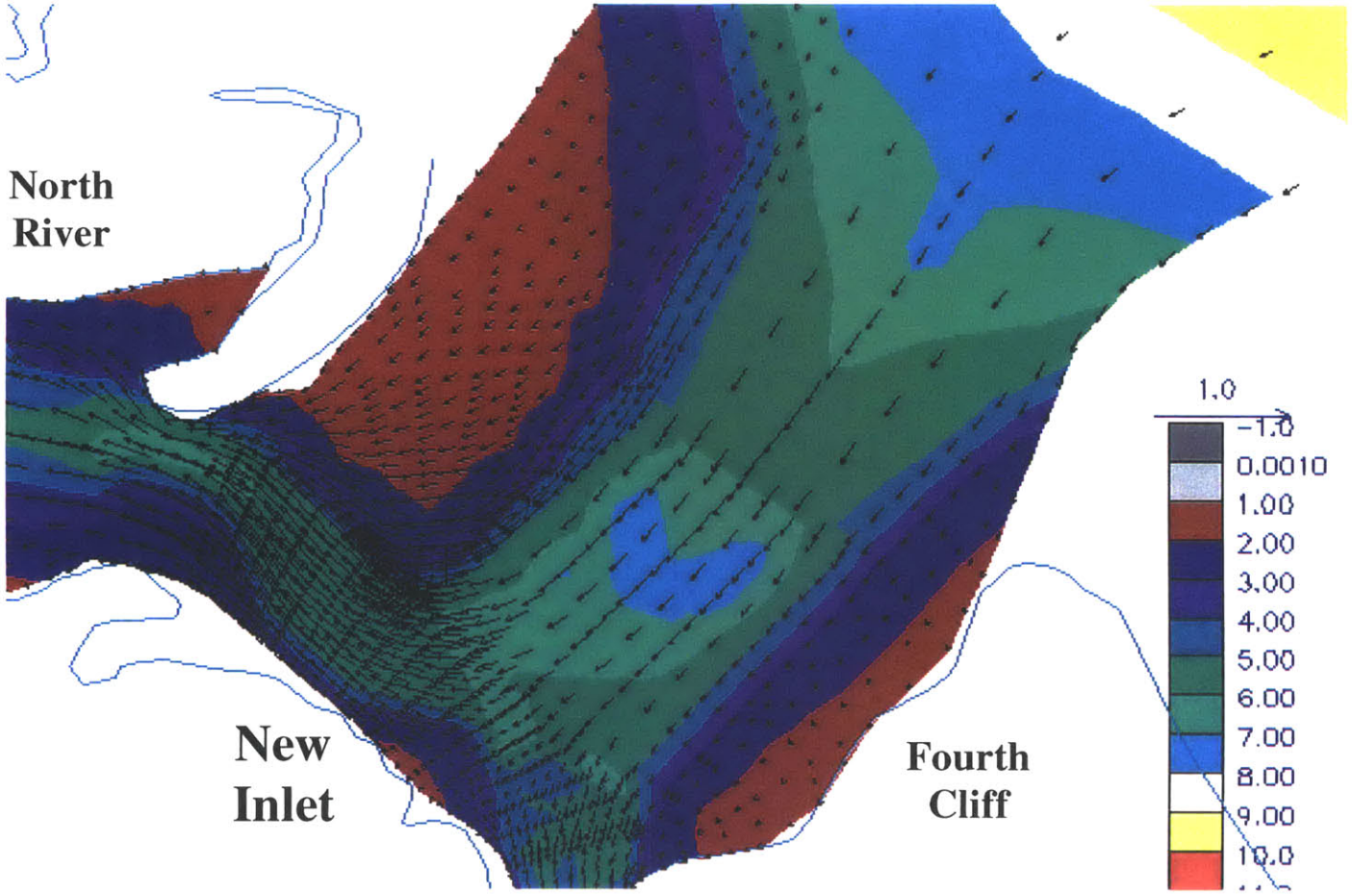

Figure 9.2 High Tide Flow Over a Wet Tidal Flat (Contours of depth in meters)

9.2 Tidal Range Calibration

Using the same calibration process as for the first two schemes, we calibrate Scheme 3 of the model with the Woods Hole time series pressure data. With the resolution of the tidal flats, the Manning's n used near the mouth downstream of Rte. 3A is 0.035 for the main channel and 0.080 for the tidal flats (Figure 9.3). The main channel Manning's n is much closer to typical river values than the Manning's n used in the first two schemes. Like in the second scheme, stretches around Bridge St. and Rte. 3 calibrate with Manning's n values of 0.020 and 0.025 respectively.

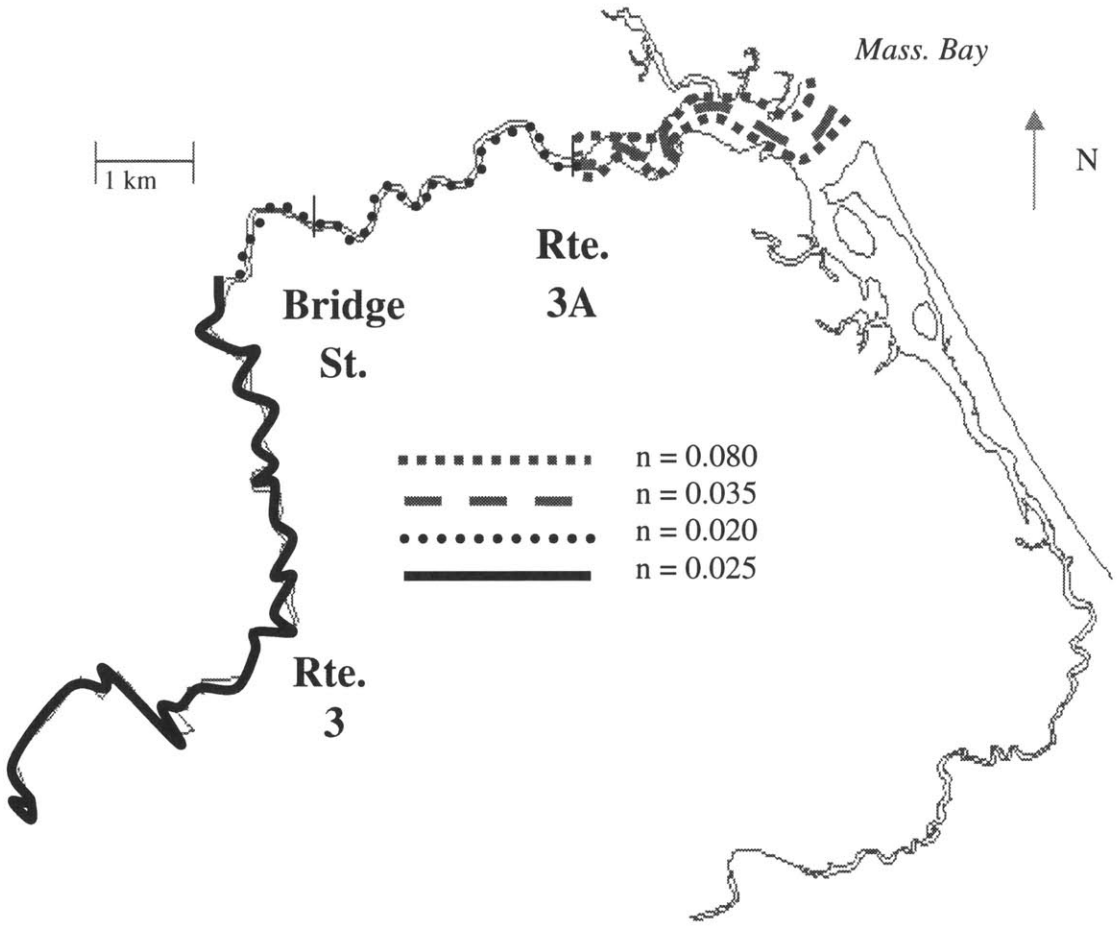

Figure 9.3 Reaches of North River with different Manning's n coefficients for Scheme 3

Figure 9.4 shows that, on the whole, this scheme calibrates with the tidal range data just as well as Scheme 2 does, but with a more realistic Manning's n for the main channel. The high Manning's n used for the tidal flat areas is probably higher than the actual friction provided by the tidal flats themselves. However, this Manning's n helps represent the drag by features still not represented by this schematization. These features include constrictions and the vegetation dense marshlands that flood at high tide.

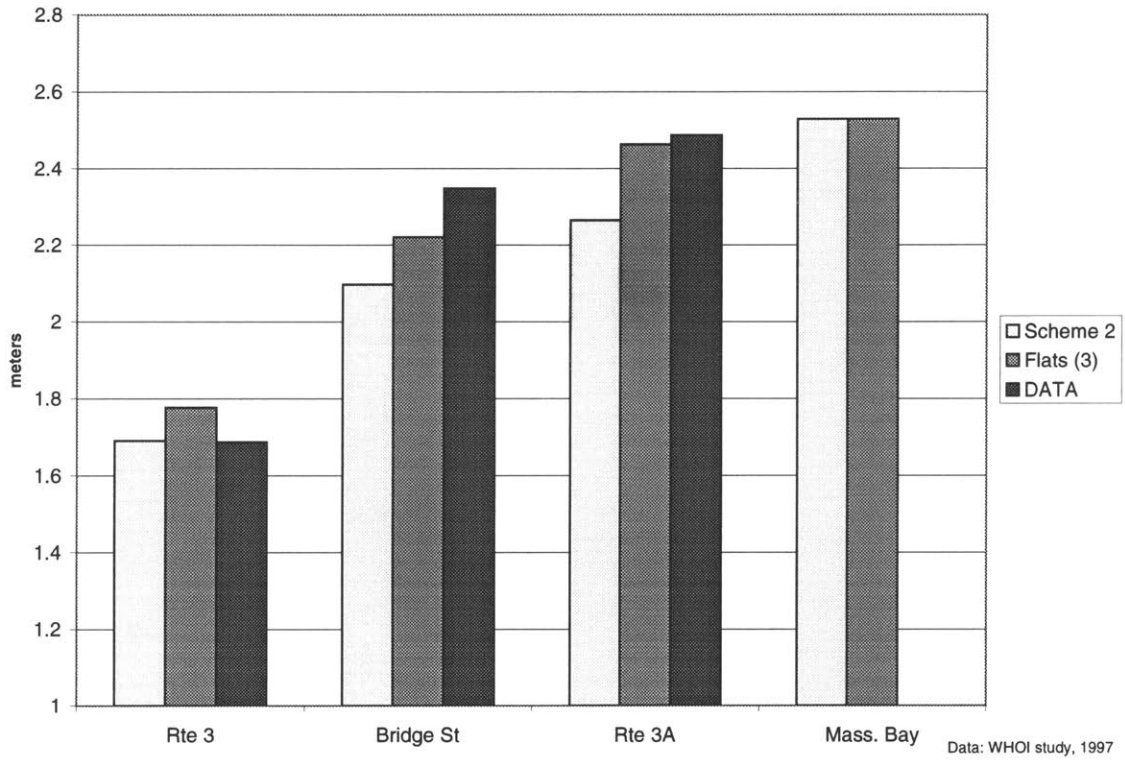

Figure 9.4 Average Tidal Range July 15-18, 1997 for Scheme 2 with no tidal flats and Scheme 3 with flats

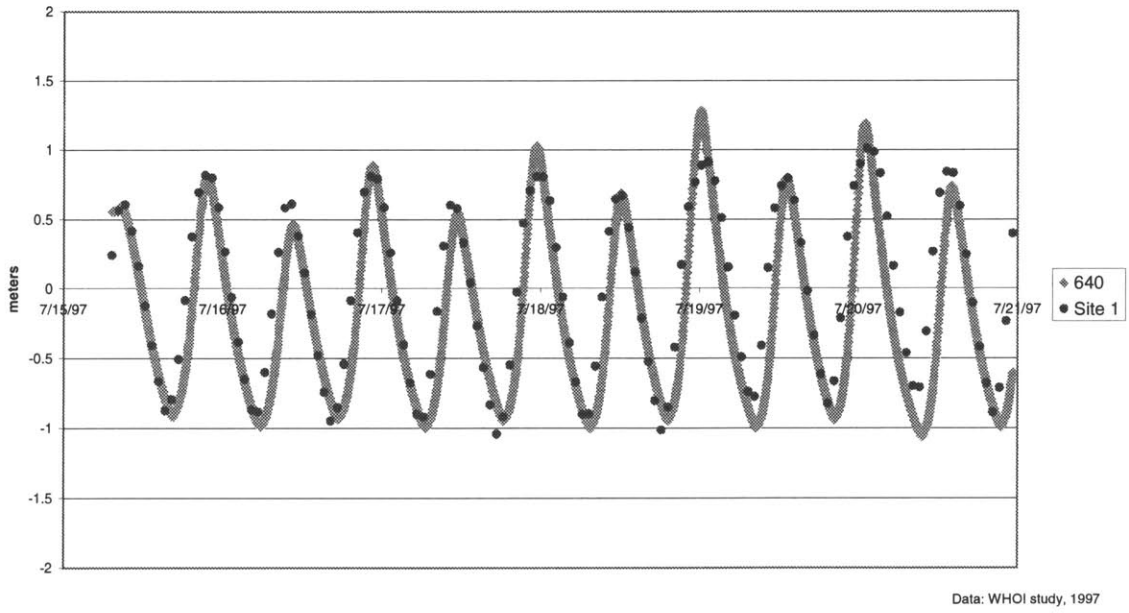

Figure 9.5 Tidal Range Calibration near Rte. 3 for Scheme 3 : Addition of Tidal Flats

Calibration of the depth variation at Route 3 (14 km upstream) reveals the conditions when modeling tidal flats may not be enough to fully represent the contributors to drag in the system. Early in the time series shown in Figure 9.5, the tide is near neap tide and the tidal range is small. During this time period, the model does a fairly good job of approximating the tidal changes at this upstream location. A couple of days later, the tide approaches spring tide and the model's tidal range increases by much more than the data's range does. The large tides on the boundary condition are damped by the system somehow. The marshlands, located at a higher elevation than the tidal flats and lined along the channel for the entire reach of the river, probably affect the flow only for these above-average high tides. These marshlands add significant amount of drag and may damp out spring tidal effects. Further discussion of the drag created by plants in marshlands can be found in Chapter 10.

9.3 Tidal Lag Calibration

The modeling of tidal flats does allow for the main channel friction to be represented more realistically. However, the earlier conjecture that the high Manning's n used for the main channel in Scheme 2 overly increases the low tide lag is not supported by the calibration of

Scheme 3. The use of a lower Manning's n in the main channel in this scheme does not seem to help reduce the low tide lag to values closer to the data (Figure 9.6). The failure of hourly pressure data to identify the time of arrival of the flow peaks seems to be the main culprit for the failure to calibrate the lower tide lag better. Like in Scheme 2, high tide lag calibrates well with the data for Scheme 3 (Figure 9.7).

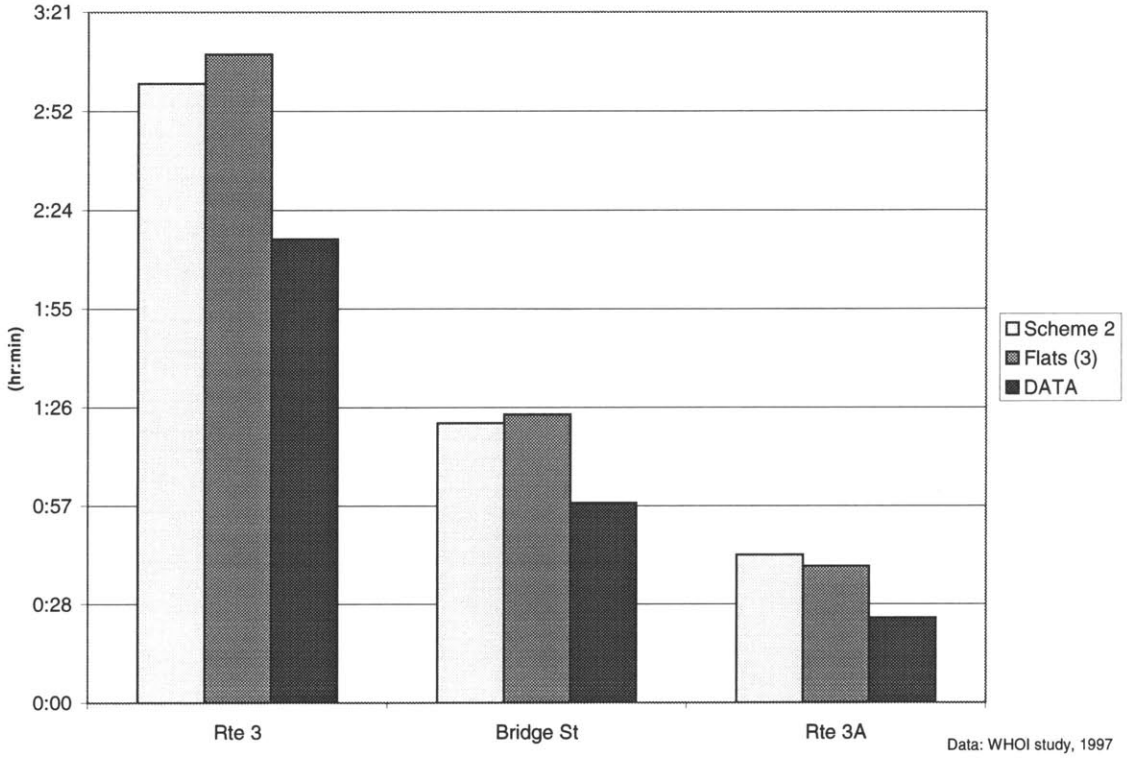

Figure 9.6 Average Low Tide Lag July 15-18, 1997 for Scheme 2 and Scheme 3

9.4 Scalar Transport Modeling

Scheme 3 is unable to model the transport of scalars, such as salt and other water quality constituents of concern. When elements dry up in the flats, scalar concentrations do not converge. This lack of convergence spreads throughout the domain and no values of the concentration output make sense. Therefore, Scheme 3 will be useless from a water quality standpoint until this problem is corrected. However, the hydrodynamic conclusions resulting from calibrating the model are valid without calculating salinity because salt-density coupling has little effect on the hydrodynamics (see Section 8.5).

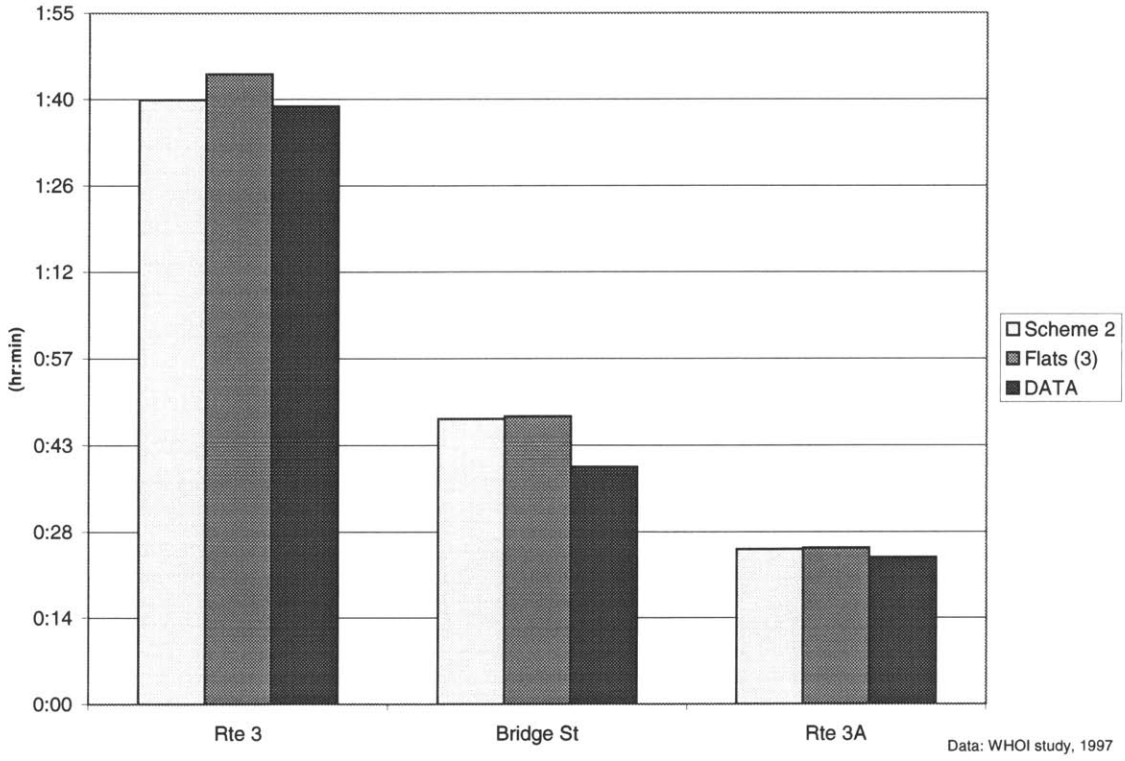

Figure 9.7 Average High Tide Lag July 15-18, 1997 for Scheme 2 and Scheme 3

9.5 Scheme 3 Discussion

The comparison of the results of Scheme 2 and Scheme 3 demonstrates the importance of the features in the mouth area. Without the representation of the mouth features, the model must add drag to the system with a higher bed friction coefficient – Manning's n. The total drag in the mouth is much higher than what would be expected from the channel bottom, because the Manning's n used in the mouth is much higher than typical values for rivers. However, the representation of a feature like the tidal flats allows for the use of a lower and more realistic Manning's n in the mouth. The tidal flats have a significant role in increasing the effective drag on the system. The horizontal resolution provided with the addition of the tidal flats provides a better representation of the flow's physics.

10. Marshlands

One major component of the estuarine system not included in the model is the extensive salt marsh and freshwater wetland area bordering the rivers and their tributaries. These areas flood during high tide, but the wetting and drying of these areas, the drag in these areas, and the scalar transport through these areas are quite different from open channel flow modeled in Schemes 1-3.

10.1 Wetting and Drying

In general, the marshlands are at a higher elevation than the main channel as well as the tidal flats. Therefore, high tidal waters from the rivers overtop the riverbanks and flood the marshlands. However, the marshlands do not quite dry the same way that a tidal flat does. Numerous one-meter wide channels are cut into the marshlands. These channels are about one-meter deep and hold water even as the tide lowers below the elevation of the marshlands. As a result, the marshlands do not exactly dry. RMA-10 has a marsh element formulation that can be used for this situation. This formulation allows for some flow when the water elevation drops below the surface elevation (King, 1998). This approximates the flow in channels cut below the marshland surface. Since there are so many channels, it will be difficult to discretize them so it may be necessary to use this feature of RMA-10 to model flooding and draining of the marsh.

10.2 Drag by Plants

The presence of plants in the marshlands adds drag to the flow. In modeling flow in a treatment wetland with RMA-2, the two-dimensional precursor of RMA-10, Barrett (1996) used a Manning's n of 3. This value is two orders of magnitude higher than the Manning's n used in the main channel of the North and South Rivers. It is also higher than the maximum value allowed for Manning's n in RMA-10, which is 1.

In fact, the drag is of a different character from the friction used in the main channel and the tidal flats. The Manning's n formulation was originally developed where only the channel bottom causes friction. However, in wetlands and marshlands, plants serve as frictional elements that protrude into and through the flow. Burke and Stolzenbach (1983) characterized flow through the marsh grass *Spartina alterniflora*, a grass found in the marshes of the North and South Rivers (Fiske, 1966). The drag force caused by obstructions such as plants is parameterized as follows (Equation 10.1).

$$\Gamma_p = \frac{1}{2}\rho C_d a u^2 \qquad (10.1)$$

where Γ_p = drag force per unit volume by plants
ρ = density of water
C_d= drag coefficient
a = vegetation density, defined as the projected area of obstructions per unit volume
u = flow velocity

Burke and Stolzenbach (1983) found the variation of a, the vegetation density, with respect to the water depth flowing through *Spartina alterniflora*. Therefore, the drag force of *Spartina alterniflora* in the North and South Rivers marshlands can be modeled.

Roig (1994) entered a vegetative friction into RMA-2 for the modeling of marshes in San Francisco Bay. This friction formulation is based on experiments with dowels intended to simulate *Spartina foliosa*, a common plant species in San Francisco Bay. It is suggested that future modeling of flow in the North and South Rivers marshlands enter a new friction term into RMA-10 in the manner of Roig, but use Burke and Stolzenbach's findings for *Spartina alterniflora*. For two-dimensional modeling of the flow though emergent vegetation, as is the case in the North and South Rivers marshlands, the following depth-averaged external traction can be added to RMA-10 (Equations 10.2).

$$\Gamma_{phx} = \frac{1}{2}\rho C_d a_h u\sqrt{(u^2+v^2)} \qquad (10.2a)$$

$$\Gamma_{phy} = \frac{1}{2}\rho C_d a_h v\sqrt{(u^2+v^2)} \qquad (10.2b)$$

where C_d = estimated drag coefficient
Γ_{ph} = depth-averaged drag force per unit volume by plants
ρ = density of water
a_h = depth averaged vegetation density
u,v = depth averaged velocities

This drag formulation is significantly different from the Manning's formulation used in the open channel. The depth-integrated formulations of drag (the depth-averaged formulas multiplied by water depth) make the difference clear (Equations 10.3 and 10.4).

$$h\Gamma_{bhx} = \frac{\rho g n^2 u\sqrt{(u^2+v^2)}}{h^{\frac{1}{3}}} \tag{10.3}$$

$$h\Gamma_{phx} = \frac{h}{2}\rho C_d a_h u\sqrt{(u^2+v^2)} \tag{10.4}$$

where $h\Gamma_{bhx}$ = depth-integrated friction from channel bottom by Manning's formulation
$h\Gamma_{phx}$ = depth-integrated friction from plants
h = water depth
g = acceleration due to gravity
n = Manning's n coefficient

Unlike the Manning formulation where friction decreases with increasing depth, depth-integrated drag through plants increases with water depth. This has implications for damping of high tides that are especially strong, such as a higher high tide or a spring tide.

10.3 Transport through Plants

Transport through the marshland plants must be treated differently from the transport in the open channel. The physical processes that cause diffusion and dispersion are different. Obstructions like plants add the process of mechanical diffusion as well as alter the turbulent diffusion mechanism (Nepf, 1999). However, the problem with lack of convergence for modeling contaminants in flooding and draining elements must be solved before these processes can be included in the model.

Figure 11.1 Features of the Mouth Area

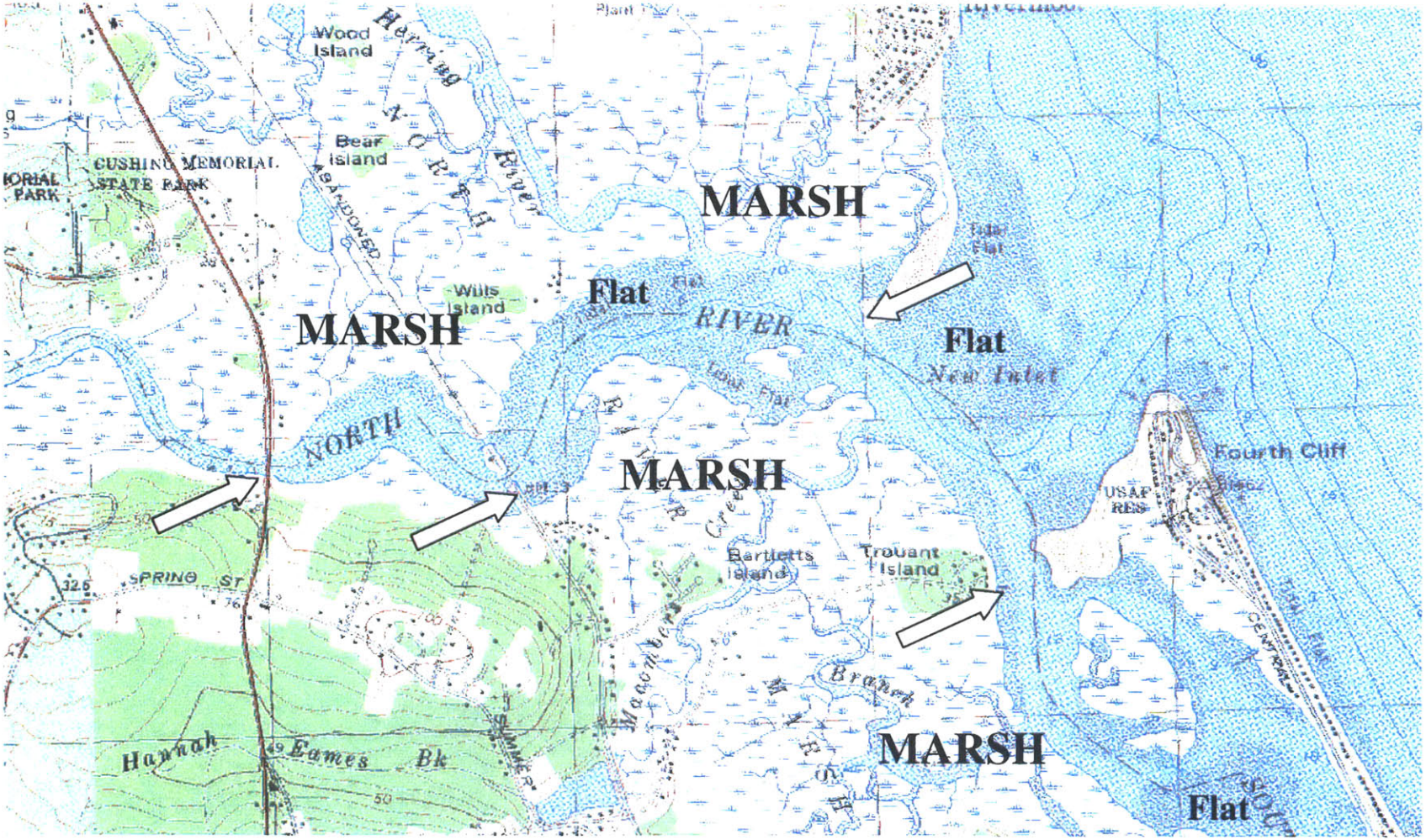

11.Conclusions

11.1 Summary of Results

The development of a hydrodynamics model for the North and South Rivers estuary includes three schemes. Scheme 1 represents only the low water channel of the rivers and does not vary characteristics such as Manning's n over space. Scheme 2 has a similar spatial grid to Scheme 1, but allows for characteristics such as Manning's n to vary over space. Scheme 3 expands the spatial grid to allow for tidal flats that wet and dry over the tidal cycle.

Scheme 1 cannot represent the hydrodynamics of the North and South Rivers. While it is possible to calibrate the tidal range at different points along the North River with a single Manning's n friction coefficient, the resulting upstream velocities are too low to represent velocity accurately. Since a water quality model takes the depths and velocities as independent variables, this scheme is not appropriate for use in a water quality model of the North and South Rivers.

The results from Scheme 2 calibrate and verify with available hydrodynamic data. A high Manning's n friction coefficient is used near the mouth and lower, more realistic coefficients are used upstream. This allows for calibration and verification of the tidal range and tidal lag at three points along the North River and approximates the tidal lag in the South River. In addition, upstream velocities calibrate with data. This scheme is appropriate for use in a water quality model (Lee, 1999).

Scheme 3 has a more refined representation of the hydrodynamics of the mouth with the representation of tidal flats. These tidal flats abut the low water main channel near the mouth and have higher bottom elevations than the main channel so they are not always inundated by water. This scheme calibrates for more realistic Manning's n coefficients for the main channel near the mouth. However, this scheme still does not represent flow through the vegetated

marshlands, which may have a large effect on the system. In addition, Scheme 3 cannot be used for a water quality model, because scalar transport calculations fail to converge when the elements drop out with the wetting and drying of nodes.

11.2 Conclusions of Hydrodynamics

The features of the mouth dominate the system (Figure 11.1). These features include tidal flats, constrictions, embayments, and marshlands. Representing these features is important for accurately representing the flows in the system.

However, if the water quality modeling concerns are located in areas upstream of these features, the representation of these features can be as rough as using a higher Manning's n coefficient. This representation accounts for the drag caused by the mouth features in sum. As a result, the hydrodynamic results for reaches of the upstream reaches are accurate with this rough representation.

For water quality concerns near the mouth, the water quality modeler must exercise caution when using the model that schematizes the mouth as the low water channel with a high Manning's n roughness coefficient. Because this scheme only models the main channel, this model cannot provide water quality predictions for areas dominated by individual features near the mouth. For example, this model does not represent tidal flat areas that flood during high tide. The shallow and intermittent flow in these areas probably results in less dilution of contaminants in these areas. Results from the low water channel scheme for locations near these tidal flats likely underestimate the contaminant concentrations. Since the tidal flats are the locations for shellfishing and swimming, this is a major concern for the North and South Rivers. If the low water scheme predicts high concentrations, the concentrations are probably even higher.

11.3 Future Study

In order to calibrate the model for the South River, time series data of the water depth changes are necessary. Further study of the bathymetry of the upstream reaches of the South River would also aid the model.

Future study of the important mouth area could include further modeling of the flow through the marshlands, modeling of contaminant transport in areas that wet and dry, and expanding the grid to three dimensions at the confluence to account for salt-driven density effects.

References

Adams, E.E. 1999. *1.77 Water Quality Control.* MIT Subject Lecture Notes.

Barrett, K.R. 1996. *Two-Dimensional Modeling of Flow and Transport in Treatment Wetlands: Development and Testing of a New Method for Wetland Design and Analysis.* PhD. Dissertation, Northwestern University.

Baystate Environmental Consultants, Inc. 1991. *Pollution Source Assessment and Recommendations for Mitigation in the North River Watershed.* For the North and South Rivers Watershed Association.

Baystate Environmental Consultants, Inc. 1990. *Water Quality Assessment of the North River and its Tributaries.* For the North and South Rivers Watershed Association.

BSC Group 1987. *North River Water Quality Management Plan.* For the North River Commission.

Burke, R.W. and K.D. Stolzenbach 1983. *Free Surface Flow through Salt Marsh Grass.* MIT Sea Grant College Program 83-216.

Burnett, D.S. 1987. *Finite Element Analysis: From Concepts to Applications.* Addison-Wesley, Reading, MA.

Chow, V.T. 1959. *Open Channel Hydraulics.* McGraw-Hill Co. Inc., New York.

Ditmars, J.D., E.E. Adams, K.W. Bedford, and D.E. Ford 1987. Performance Evaluation of Surface Water Transport and Dispersion Models. *Journal of Hydraulic Engineering.* Vol. 113 No. 8 ASCE 961(20).

Demetracopoulos, A.C., and H.G. Stefan 1983. Transverse mixing in wide and shallow rivers: Case study. *Journal of Environmental Engineering Div.* ASCE 109(3).

Elder, J.W. 1959. The dispersion of marked fluid in turbulent shear flow. *Journal of Fluid Mechanics.* 5(4).

Fischer, H.B., E.J. List, R.C.Y. Koh, J. Imberger, and N.H. Brooks 1979. *Mixing in Inland and Coastal Waters.* Academic Press, San Diego, CA.

Fiske, J.D., C.E. Watson, and P.G. Coates 1966. *A Study of the Marine Resources of the North River.* Massachusetts Division of Marine Fisheries. Monograph Series Number 3.

Geyer, W.R. 1993. Three-Dimensional Tidal Flow Around Headlands. *Journal of Geophysical Research.* 98:955(12).

Geyer, W.R. 1997. North River Dye Study Data (unpublished). Woods Hole Oceanographic Institute.

Geyer, W.R., and R.P. Signell 1992. A Reassessment of the Role of Tidal Dispersion in Estuaries and Bays. *Estuaries*. 15:97(12).

Henderson, F.M. 1966. *Open Channel Flow*. Macmillian, New York.

King I.P. 1998. *A Finite Element Model for Stratified Flow: RMA-10 Users Guide Version 6.5*. University of California Department of Civil and Environmental Engineering, Davis, CA.

King I.P. 1994. *RMAGEN: A Program for Generation of Finite Element Networks, User Instructions, Version 3.3(a)*. University of California Department of Civil and Environmental Engineering, Davis, CA.

King I.P. 1995. *RMAPLT: A Program for Displaying Results from RMA Finite Element Programs, User Instructions, Version 3.0*. University of California Department of Civil and Environmental Engineering, Davis, CA.

King, I.P., 1993. *RMA-10: A Finite Element Model for Three-Dimensional Density Stratified Flow*, Environment Protection Authority, Bankstown, NSW, AWACS Interim Report 93/01/04.

King, I.P., 1997. *RMA-11: A Three Dimensional Finite Element Model for Water Quality in Estuaries and Streams*, University of California Department of Civil and Environmental Engineering, Davis, CA.

King, I.P., 1995. "Strategies for finite element modeling of three dimensional hydrodynamic systems," *Advanced Water Resources*. 8: 68(9).

Koseff, J.R. 1997. Course notes for CEE 161: Open Channel and Pipe Flow. Stanford University.

Lee, S.S. 1999. *Modeling of Fecal Coliform Bacteria in the North and South Rivers*. Master of Engineering Thesis, Massachusetts Institute of Technology.

Lee, S.S., and C.K. Tana, 1999. *The North and South Rivers Modeling Project*. Master of Engineering Project Report, Massachusetts Institute of Technology.

Mackey, P.C., P.M. Barlow, and K.G. Ries 1998. *Relations Between Discharge and Wetted Perimeter and Other Hydraulic-Geometry Characteristics at Selected Streamflow-Gaging Stations in Massachusetts*. U.S. Geological Survey Water-Resources Investigations Report 98-4094.

Metcalf & Eddy 1995. *Final Facilities Plan and Environmental Impact Report for Wastewater Management Volume I*, EOEA No. 5512, WPC-Mass.-887.

Metcalf & Eddy 1995. *Final Facilities Plan and Environmental Impact Report for Wastewater Management Volume II*, EOEA No. 5512, WPC-Mass.-887.

Metcalf & Eddy 1995. *Final Facilities Plan and Environmental Impact Report for Wastewater Management Volume III*, EOEA No. 5512, WPC-Mass.-887.

Nepf, H.M. 1999. Drag, Turbulence and Diffusion in Flow Through Emergent Vegetation. *Water Resources Research.* 35:479(11).

National Ocean Service (NOS) 1988. Retrieve Observed Water Levels and Associated Ancillary Data. WWW at http://www.opsd.nos.noaa.gov/data_res.html .

National Ocean Service (NOS) 1988. Tidal Bench Marks: Boston, Boston Harbor. WWW at http://www.opsd.nos.noaa.gov/bench/ma/8443970.txt.

National Ocean Service (NOS) 1991. Tidal Bench Marks: Scituate, Scituate Harbor. WWW at http://www.opsd.nos.noaa.gov/bench/ma/8445138.txt.

National Ocean Service (NOS) 1999. Tidal Differences and Other Constants. WWW at http://www.opsd.nos.noaa.gov/tab2ec1b.html#10 .

National Ocean Service (NOS) 1997. North River Nautical Chart.

North and South Rivers Watershed Association (NSRWA) 1997. *North & South Rivers Guide*, 3rd edition, Norwell, MA.

North and South Rivers Watershed Association (NSRWA) 1998. *North River Tides*, at http://eco25.mbl.edu/nsrwa/tides.html

Parker, B.B. 1984. *Frictional Effects on the Tidal Dynamics of a Shallow Estuary.* Ph.D Dissertation, The Johns Hopkins University.

Roig, L.C. 1994. *Hydrodynamic Modeling of Flows in Tidal Wetlands.* Ph.D. Dissertation, University of California at Davis.

South River Initiative Recreation and Access Team 1998. *The South River Recreation Guide.*

Stewart, J.P., L.J. Daggett, and R.F. Athow 1985. *Impact of Proposed Runway Extension at Little Rock Municipal Airport on Water-Surface Elevations and Navigation Conditions in Arkansas River.* U.S. Army Corp of Engineers Hydraulics Laboratory.

Sylvan Ascent Inc. 1999. *Topo Depot: 7½-Minute AutoCAD® DWG Maps To Go!* http://www.sylvanmaps.com/topodepo.htm

Thomas, W.A. and W.H. McAnally, Jr. 1985. *Appendix F: User Instructions for RMA-2V, A Two-Dimensional Model for Free-Surface Flows.*

United States Geological Survey 1974. *Duxbury, Massachusetts: 1:25 000-scale topographic map (7.5 X 7.5 Minute Quadrangle).* AMS 6868 II SW – SERIES V 814.

United States Geological Survey 1978. *Hanover, Massachusetts: 1:25 000-scale topographic map (7.5 X 7.5 Minute Quadrangle).* AMS 6868 II SW – SERIES V 814.

United States Geological Survey 1984. *Scituate, Massachusetts: 1:25 000-scale metric topographic map (7.5 X 15 Minute Quadrangle).* Map 42070-B5-TM-025.

United States Geological Survey 1984. *Weymouth, Massachusetts: 1:25 000-scale metric topographic map (7.5 X 15 Minute Quadrangle).* Map 42070-B7-TM-025.

United States Geological Survey 1999. Historical Streamflow Daily Values for Indian Head River At Hanover, Ma (01105730) at WWW http://waterdata.usgs.gov/nwisw/MA/data.components/hist.cgi?statnum=01105730

Wandel, S,W. Jr., and M.A. Morgan 1984. Gazatteer of Hydrologic Characteristics of Streams in Massachusetts – Coastal River Basins of the South Shore and Buzzards Bay. U.S. Geological Survey Water-Resources Investigations Report 84-4288.

Appendix A. Acronyms

BEC	Baystate Environmental Consultants
BSC	The BSC Group
DEP	Massachusetts Department of Environmental Protection
DMF	Massachusetts Division of Marine Fisheries
M&E	Metcalf and Eddy
NOAA	National Oceanic and Atmospheric Administration
NOS	National Ocean Service
NSRWA	North and South River Watershed Association
USGS	United States Geological Survey
WHOI	Woods Hole Oceanographic Institute

Appendix B. Sample Input Files for Scheme 1

B.1 R10 Input File for July 15-17, 1997 : scheme1b.r10

```
OUTFIL  scheme1b
BCFIL   scheme1.alt
INBNGEO scheme1.geo
INBNRST scheme1a.rst
OUTBNRSTscheme1b.rst
OUTBNRESscheme1b.res
INHYD   tribs.hyd
INELEV  tides_b.tid
INELTFL element.hyd
ENDFIL
TI      North and South Rivers where jd=194 is July 14
C0             0       0    1997     195   22.35       0
C1             0       1       0       1       1       1
C2            42   2.461     831    1107       1
C3          1.00    1.00                    0.5    0.02    0.06
C4          20.0     20.     0.0     0.1     0.1    100.     0.0
C5             0       9     0.0     960       2       0      10       0       1
CV       0.02000 0.02000 0.02000    0.20      .2     .25       0
ED1            1   5000.   5000.   5000.   5000.   0.050    1.00    1.00
ED2                4.00    4.00 .000050    0.00
ED1            2   5000.   5000.   5000.   5000.   0.050    1.00    1.00
ED2                4.00    4.00 .000050    0.00
ED1            3   5000.   5000.   5000.   5000.   0.050    1.00    1.00
ED2                4.00    4.00 .000050    0.00
CC1          323     324
CC1         2510    2511    2512
CC1         1882    1883
CC1         1082    1083
CC1          289     473
CC1          538     541
CC1          307     409
CC1          924     931
CC1          550     595
CC1          472     605
CC1          606    1259
CC1          608     609
CC1          610     666
CC1          669     683
CC1         1034    1036    1038
CC1         2513    2514    2515
CC1         2516    2517    2518
CC1         2519    2520    2521
CC1         2522    2523    2524
CC1          577     665     578
CC1         1014    1017    1019
CC1         1022    1025    1028
CC1         1029    1030    1032
ENDGEO
DT
BC
QC             1       0  0.2633   0.426       0     -20      -1       1
QC             3       0 0.12687   6.106   0.000     -20      -1       1
QC             6       0 0.09733   4.785   0.000     -20      -1       1
QC             7       0 0.13208   2.253   0.000     -20      -1       1
QC            10       0 0.00652     1.7   0.000     -20      -1       1
```

```
HC              2        0   2.468    35.0   -20.0      -1       1
EFE           764        0       1 0.0        0.000     -20      -1       1
EFE            94        0       1 0.0        0.000     -20      -1       1
EFE           766        0       1 0.0        0.000     -20      -1       1
EFE           724        0       1 0.00       0.000     -20      -1       1
ENDSTEP
ENDDATA
```

B.2 ALT Boundary Condition Input File for Scheme 1 : scheme1b.alt

```
DT          0.050
BC             10       10       10       10       10       10       10       10       10
ENDSTEP
ENDDATA
```

Appendix C. Sample Input Files for Scheme 2

C.1 R10 Input File for July 15-16, 1997 : both2dt2.r10

```
OUTFIL  both2dt
BCFIL   both2dq.alt
INBNGEO both2dt.geo
INBNRST both2dt1.rst
OUTBNRSTboth2dt2.rst
OUTBNRESboth2dt2.res
INHYD   tribsdr3.hyd
INELEV  tide2dt2.tid
INELTFL element.hyd
ENDFIL
TI      North and South Rivers where jd=194 is July 14
C0            0       0    1997     195   22.05       3
C1            0       1       0       1       1       1
C2           42   2.461     831    1107       1
C3         1.00    1.00                   0.5    0.02    0.06
C4         20.0     20.     0.0     0.1     0.1    100.     0.0
C5            0       9     0.0     240       2       0      10       0       1
CV      0.02000 0.02000 0.02000    0.20      .2     .25       0
ED1           1    5000    5000    5000    5000   0.020    1.00    1.00
ED2                  20     0.1 .000050    0.00
ED1           2    9000    9000    9000    9000   0.080    1.00    1.00
ED2                  20     0.1 .000050    0.00
ED1           3    5000    5000    5000    5000   0.025    1.00    1.00
ED2                  20     0.1 .000050    0.00
CC1         323     324
CC1        2510    2511    2512
CC1        1882    1883
CC1        1082    1083
CC1         289     473
CC1         538     541
CC1         307     409
CC1         924     931
CC1         550     595
CC1         472     605
CC1         606    1259
CC1         608     609
CC1         610     666
CC1         669     683
CC1        1034    1036    1038
CC1        2513    2514    2515
CC1        2516    2517    2518
CC1        2519    2520    2521
CC1        2522    2523    2524
CC1         577     665     578
CC1        1014    1017    1019
CC1        1022    1025    1028
CC1        1029    1030    1032
ENDGEO
DT
BC
QC            1       0  0.2633   0.426       0     -20      -1       1
QC            3       0 0.12687   6.106   0.000     -20      -1       1
```

```
QC            6       0 0.09733   4.785   0.000     -20      -1       1
QC            7       0 0.13208   2.253   0.000     -20      -1       1
QC           10       0 0.00652     1.7   0.000     -20      -1       1
QC           13       0 0.00500     0.6   0.000     -20      -1       0
HC            2       0   2.468    35.0   -20.0      -1       1
EFE         764       0       1 0.0        0.000     -20      -1       1
EFE          94       0       1 0.0        0.000     -20      -1       1
EFE         766       0       1 0.0        0.000     -20      -1       1
EFE         724       0       1 0.00       0.000     -20      -1       1
ENDSTEP
ENDDATA
```

C.2 ALT Boundary Condition Input File for Scheme 2 : both2d.alt

```
DT        0.050
BC           10      10      20      10      10      20      10      10      20
QC           13       0 0.00500     0.6  -5.000     -20      -1
ENDSTEP
ENDDATA
```

C.3 R10 Input File for Salt Coupling July 15-16, 1997 : both2dv2.r10

```
OUTFIL  both2dv
BCFIL   both2dq.alt
INBNGEO both2du.geo
INBNRST both2dv1.rst
OUTBNRSTboth2dv2.rst
OUTBNRESboth2dv2.res
INHYD   tribsdr3.hyd
INELEV  tide2dt2.tid
INELTFL element.hyd
ENDFIL
TI      North and South Rivers where jd=194 is July 14
C0            0       0    1997     195   22.35       3
C1            0       1       0       0       1       1
C2           42   2.461     831    1107       1
C3         1.00    1.00                    0.5    0.02    0.06
C4         20.0     20.     0.0     0.1     0.1    100.     0.0
C5            0       9     0.0     234       2       0      10       0       1
CV      0.02000 0.02000 0.02000    0.20      .2     .25       0
ED1           1    5000    5000    5000    5000   0.020    1.00    1.00
ED2                  20     0.1 .000050    0.00
ED1           2    9000    9000    9000    9000   0.080    1.00    1.00
ED2                  20     0.1 .000050    0.00
ED1           3    5000    5000    5000    5000   0.025    1.00    1.00
ED2                  20     0.1 .000050    0.00
CC1         323     324
CC1        2510    2511    2512
CC1        1882    1883
CC1        1082    1083
CC1         289     473
CC1         538     541
CC1         307     409
CC1         924     931
CC1         550     595
CC1         472     605
CC1         606    1259
CC1         608     609
CC1         610     666
```

```
CC1          669     683
CC1         1034    1036    1038
CC1         2513    2514    2515
CC1         2516    2517    2518
CC1         2519    2520    2521
CC1         2522    2523    2524
CC1          577     665     578
CC1         1014    1017    1019
CC1         1022    1025    1028
CC1         1029    1030    1032
ENDGEO
DT
BC
QC             1       0  0.2633   0.426       0     -20      -1       1
QC             3       0 0.12687   6.106   0.000     -20      -1       1
QC             6       0 0.09733   4.785   0.000     -20      -1       1
QC             7       0 0.13208   2.253   0.000     -20      -1       1
QC            10       0 0.00652     1.7   0.000     -20      -1       1
QC            13       0 0.00500     0.6   0.000     -20      -1       0
HC             2       0   2.468    35.0   -20.0      -1       1
EFE          764       0       1 0.0       0.000     -20      -1       1
EFE           94       0       1 0.0       0.000     -20      -1       1
EFE          766       0       1 0.0       0.000     -20      -1       1
EFE          724       0       1 0.00      0.000     -20      -1       1
ENDSTEP
ENDDATA
```

C.4 R10 Input File for August 8-9, 1997 : aug_8-9.r10

```
OUTFIL  aug_8-9
BCFIL   both2dq.alt
INBNGEO both2du.geo
INBNRST aug_8a1.rst
OUTBNRSTaug_8-9.rst
OUTBNRESaug_8-9.res
INHYD   aug_clq.hyd
INELEV  aug_8-9.tid
INELTFL aug_qei.hyd
ENDFIL
TI      North and South Rivers where jd=194 is July 14
C0             0       0    1997     219     2.3       3
C1             0       1       0       0       1       1
C2            42   2.777     831    1107       1
C3          1.00    1.00                     0.5    0.02    0.06
C4          20.0     20.     0.0     0.1     0.1    100.     0.0
C5             0       9     0.0     914       2       0      10       0       1
CV       0.02000 0.02000 0.02000    0.20      .2     .25       0
ED1            1    5000    5000    5000    5000   0.020    1.00    1.00
ED2                   20     0.1 .000050    0.00
ED1            2    9000    9000    9000    9000   0.080    1.00    1.00
ED2                   20     0.1 .000050    0.00
ED1            3    5000    5000    5000    5000   0.025    1.00    1.00
ED2                   20     0.1 .000050    0.00
CC1          323     324
CC1         2510    2511    2512
CC1         1882    1883
CC1         1082    1083
CC1          289     473
CC1          538     541
CC1          307     409
```

```
CC1          924     931
CC1          550     595
CC1          472     605
CC1          606    1259
CC1          608     609
CC1          610     666
CC1          669     683
CC1         1034    1036    1038
CC1         2513    2514    2515
CC1         2516    2517    2518
CC1         2519    2520    2521
CC1         2522    2523    2524
CC1          577     665     578
CC1         1014    1017    1019
CC1         1022    1025    1028
CC1         1029    1030    1032
ENDGEO
DT
BC
QC             1       0  0.2633   0.426       0     -20      -1       1
QC             3       0 0.12687   6.106   0.000     -20      -1       1
QC             6       0 0.09733   4.785   0.000     -20      -1       1
QC             7       0 0.13208   2.253   0.000     -20      -1       1
QC            10       0 0.00652     1.7   0.000     -20      -1       1
QC            13       0 0.00500     0.6   0.000     -20      -1       0
HC             2       0   2.468    35.0   -20.0      -1       1
EFE          764       0       1 0.0       0.000     -20      -1       1
EFE           94       0       1 0.0       0.000     -20      -1       1
EFE          766       0       1 0.0       0.000     -20      -1       1
EFE          724       0       1 0.00      0.000     -20      -1       1
ENDSTEP
ENDDATA
```

Appendix D. Sample Input Files for Scheme 3

D.1 R10 Input File for July 16-17, 1997 : flat_2b.r10

```
OUTFIL  flat_pd
BCFIL   flat_m.alt
INBNGEO flat_n.geo
INBNRST flat_2a.rst
OUTBNRSTflat_2b.rst
OUTBNRESflat_2b.res
INHYD   tribs_m.hyd
INELEV  flat_m2.tid
INELTFL element.hyd
ENDFIL
TI      tidal flat included
C0            0       0    1997     196   22.05       3
C1            0       1       0       1       1       1
C2           42   2.480     831    1107       1
C3         1.00    1.00                  0.5    0.02    0.06
C4         20.0     20.     0.0     0.1     0.1    100.     0.0
C5            0       9     0.0     480       2       0      10       0       1
CV      0.02000 0.02000 0.02000    0.20      .2     .25       0
ED1           1    5000    5000    5000    5000   0.025    1.00    1.00
ED2                  20     0.1 .000050    0.00
ED1           2    9000    9000    9000    9000   0.035    1.00    1.00
ED2                  20     0.1 .000050    0.00
ED1           3    9000    9000    9000    9000   0.080    1.00    1.00
ED2                  20     0.1 .000050    0.00
ED1           4    9000    9000    9000    9000   0.120    1.00    1.00
ED2                  20     0.1 .000050    0.00
ED1           5    5000    5000    5000    5000   0.020    1.00    1.00
ED2                  20     0.1 .000050    0.00
CC1         323     324
CC1        2510    2511    2512
CC1        1882    1883
CC1        1082    1083
CC1         289     473
CC1         538     541
CC1         307     409
CC1         924     931
CC1         550     595
CC1         472     605
CC1         606    1259
CC1         608     609
CC1         669     683
CC1        1034    1036    1038
CC1        2510    2511    2512
CC1        2513    2514    2515
CC1        2516    2517    2518
CC1        2519    2520    2521
CC1        2522    2523    2524
CC1         577     665     578
CC1        1014    1017    1019
CC1        1022    1025    1028
CC1        1029    1030    1032
```

```
ENDGEO
DT
BC
QC              1        0  0.2633    0.426        0      -20       -1        1
QC              3        0 0.12687    6.106    0.000      -20       -1        1
QC              6        0 0.09733    4.785    0.000      -20       -1        1
QC              7        0 0.13208    2.253    0.000      -20       -1        1
QC             10        0 0.00652      1.7    0.000      -20       -1        1
HC              2        0   2.610     35.0    -20.0       -1        1
EFE           764        0       1 0.0        0.000      -20       -1        1
EFE            94        0       1 0.0        0.000      -20       -1        1
EFE           766        0       1 0.0        0.000      -20       -1        1
EFE           724        0       1 0.00       0.000      -20       -1        1
ENDSTEP
ENDDATA
```

D.2 ALT Boundary Condition Input File for Scheme 3 : flat_m.alt

```
DT          0.050
BC             10       10       10       10       10       10       10       10       10
ENDSTEP
ENDDATA
```

Appendix E. Sample Input Files for Tidal and Inflow Boundary Condition

E.1 Tidal Graph Input File for July 15-16, 1997 : tides2dt2.tid

```
TT tide data for July 15-16 2dt2
CLH              2    1997
HD   195    22.00        0 1.75536      35     -20      -1
HD   195    22.10        0 1.70936      35     -20      -1
HD   195    22.20        0 1.66428      35     -20      -1
HD   195    22.30        0 1.61552      35     -20      -1
HD   195    22.40        0 1.56124      35     -20      -1
HD   195    22.50        0 1.50328      35     -20      -1
HD   195    22.60        0 1.44808      35     -20      -1
HD   195    22.70        0 1.39012      35     -20      -1
HD   195    22.80        0 1.32572      35     -20      -1
HD   195    22.90        0 1.26776      35     -20      -1
HD   195    23.00        0 1.21164      35     -20      -1
HD   195    23.10        0 1.15368      35     -20      -1
HD   195    23.20        0 1.09572      35     -20      -1
HD   195    23.30        0 1.04052      35     -20      -1
HD   195    23.40        0  0.9844      35     -20      -1
HD   195    23.50        0  0.9246      35     -20      -1
HD   195    23.60        0 0.86112      35     -20      -1
HD   195    23.70        0 0.80592      35     -20      -1
HD   195    23.80        0 0.75532      35     -20      -1
HD   195    23.90        0 0.69828      35     -20      -1
HD   196     0.00        0 0.64584      35     -20      -1
HD   196     0.10        0 0.60536      35     -20      -1
HD   196     0.20        0  0.5658      35     -20      -1
HD   196     0.30        0 0.52256      35     -20      -1
HD   196     0.40        0 0.48024      35     -20      -1
HD   196     0.50        0 0.45172      35     -20      -1
HD   196     0.60        0 0.42136      35     -20      -1
HD   196     0.70        0 0.37904      35     -20      -1
HD   196     0.80        0   0.345      35     -20      -1
HD   196     0.90        0 0.32752      35     -20      -1
HD   196     1.00        0 0.31188      35     -20      -1
HD   196     1.10        0 0.29532      35     -20      -1
HD   196     1.20        0 0.28704      35     -20      -1
HD   196     1.30        0 0.29072      35     -20      -1
HD   196     1.40        0 0.29716      35     -20      -1
HD   196     1.50        0 0.30084      35     -20      -1
HD   196     1.60        0  0.3082      35     -20      -1
HD   196     1.70        0 0.32384      35     -20      -1
HD   196     1.80        0 0.33672      35     -20      -1
HD   196     1.90        0 0.34224      35     -20      -1
HD   196     2.00        0  0.3542      35     -20      -1
HD   196     2.10        0 0.37536      35     -20      -1
HD   196     2.20        0 0.39836      35     -20      -1
HD   196     2.30        0 0.41676      35     -20      -1
HD   196     2.40        0 0.43884      35     -20      -1
HD   196     2.50        0  0.4738      35     -20      -1
HD   196     2.60        0 0.51336      35     -20      -1
```

HD	196	2.70	0	0.55108	35	-20	-1
HD	196	2.80	0	0.58236	35	-20	-1
HD	196	2.90	0	0.621	35	-20	-1
HD	196	3.00	0	0.66332	35	-20	-1
HD	196	3.10	0	0.69828	35	-20	-1
HD	196	3.20	0	0.73232	35	-20	-1
HD	196	3.30	0	0.7682	35	-20	-1
HD	196	3.40	0	0.80316	35	-20	-1
HD	196	3.50	0	0.8326	35	-20	-1
HD	196	3.60	0	0.87216	35	-20	-1
HD	196	3.70	0	0.92184	35	-20	-1
HD	196	3.80	0	0.9706	35	-20	-1
HD	196	3.90	0	1.01292	35	-20	-1
HD	196	4.00	0	1.06444	35	-20	-1
HD	196	4.10	0	1.11964	35	-20	-1
HD	196	4.20	0	1.17484	35	-20	-1
HD	196	4.30	0	1.22912	35	-20	-1
HD	196	4.40	0	1.2788	35	-20	-1
HD	196	4.50	0	1.33032	35	-20	-1
HD	196	4.60	0	1.38276	35	-20	-1
HD	196	4.70	0	1.42416	35	-20	-1
HD	196	4.80	0	1.47108	35	-20	-1
HD	196	4.90	0	1.518	35	-20	-1
HD	196	5.00	0	1.56216	35	-20	-1
HD	196	5.10	0	1.6054	35	-20	-1
HD	196	5.20	0	1.6606	35	-20	-1
HD	196	5.30	0	1.71028	35	-20	-1
HD	196	5.40	0	1.75444	35	-20	-1
HD	196	5.50	0	1.8078	35	-20	-1
HD	196	5.60	0	1.87128	35	-20	-1
HD	196	5.70	0	1.92188	35	-20	-1
HD	196	5.80	0	1.9734	35	-20	-1
HD	196	5.90	0	2.02032	35	-20	-1
HD	196	6.00	0	2.07	35	-20	-1
HD	196	6.10	0	2.11416	35	-20	-1
HD	196	6.20	0	2.16476	35	-20	-1
HD	196	6.30	0	2.1988	35	-20	-1
HD	196	6.40	0	2.22916	35	-20	-1
HD	196	6.50	0	2.26136	35	-20	-1
HD	196	6.60	0	2.2954	35	-20	-1
HD	196	6.70	0	2.33312	35	-20	-1
HD	196	6.80	0	2.36256	35	-20	-1
HD	196	6.90	0	2.38924	35	-20	-1
HD	196	7.00	0	2.41132	35	-20	-1
HD	196	7.10	0	2.4242	35	-20	-1
HD	196	7.20	0	2.44812	35	-20	-1
HD	196	7.30	0	2.46652	35	-20	-1
HD	196	7.40	0	2.4702	35	-20	-1
HD	196	7.50	0	2.47848	35	-20	-1
HD	196	7.60	0	2.48032	35	-20	-1
HD	196	7.70	0	2.48032	35	-20	-1
HD	196	7.80	0	2.46928	35	-20	-1
HD	196	7.90	0	2.47112	35	-20	-1
HD	196	8.00	0	2.45916	35	-20	-1
HD	196	8.10	0	2.4564	35	-20	-1
HD	196	8.20	0	2.44352	35	-20	-1
HD	196	8.30	0	2.43616	35	-20	-1
HD	196	8.40	0	2.41684	35	-20	-1
HD	196	8.50	0	2.39936	35	-20	-1
HD	196	8.60	0	2.38372	35	-20	-1
HD	196	8.70	0	2.35796	35	-20	-1
HD	196	8.80	0	2.33496	35	-20	-1
HD	196	8.90	0	2.30276	35	-20	-1

```
HD   196    9.00        0 2.26504      35     -20      -1
HD   196    9.10        0 2.23468      35     -20      -1
HD   196    9.20        0 2.20156      35     -20      -1
HD   196    9.30        0 2.15924      35     -20      -1
HD   196    9.40        0 2.12152      35     -20      -1
HD   196    9.50        0 2.07736      35     -20      -1
HD   196    9.60        0 2.03688      35     -20      -1
HD   196    9.70        0 2.00008      35     -20      -1
HD   196    9.80        0 1.95776      35     -20      -1
HD   196    9.90        0 1.91912      35     -20      -1
HD   196   10.00        0 1.87404      35     -20      -1
```

E.2 Continuity Line Hydrograph Input File for August 7-21, 1997 : aug_clq.hyd

```
TH      August boundary hydrograph jd=218 is August 7, 1997
CLQ             1    1997
QD   218       12       0  0.1472       0      20       0
QD   219       12       0  0.1246       0      20       0
QD   220       12       0  0.1501       0      20       0
QD   221       12       0  0.1614       0      20       0
QD   222       12       0  0.1557       0      20       0
QD   223       12       0  0.1274       0      20       0
QD   224       12       0  0.1472       0      20       0
QD   225       12       0  0.2039       0      20       0
QD   226       12       0  0.1671       0      20       0
QD   227       12       0  0.1699       0      20       0
QD   228       12       0  0.1812       0      20       0
QD   229       12       0  0.3681       0      20       0
QD   230       12       0  0.2718       0      20       0
QD   231       12       0  0.2265       0      20       0
QD   232       12       0  0.3398       0      20       0
CLQ             3    1997
QD   218       12       00.070928       0      20       0
QD   219       12       00.060038       0      20       0
QD   220       12       00.072325       0      20       0
QD   221       12       0 0.07777       0      20       0
QD   222       12       00.075024       0      20       0
QD   223       12       00.061387       0      20       0
QD   224       12       00.070928       0      20       0
QD   225       12       00.098249       0      20       0
QD   226       12       00.080517       0      20       0
QD   227       12       00.081866       0      20       0
QD   228       12       00.087311       0      20       0
QD   229       12       00.177368       0      20       0
QD   230       12       00.130966       0      20       0
QD   231       12       00.109139       0      20       0
QD   232       12       00.163732       0      20       0
CLQ             6    1997
QD   218       12       00.054411       0      20       0       0
QD   219       12       00.046057       0      20       0       0
QD   220       12       00.055483       0      20       0       0
QD   221       12       00.059659       0      20       0       0
QD   222       12       00.057552       0      20       0       0
QD   223       12       00.047092       0      20       0       0
QD   224       12       00.054411       0      20       0       0
QD   225       12       00.075369       0      20       0       0
QD   226       12       00.061766       0      20       0       0
QD   227       12       00.062801       0      20       0       0
QD   228       12       00.066978       0      20       0       0
QD   229       12       00.136063       0      20       0       0
QD   230       12       00.100467       0      20       0       0
```

```
QD   231       12        00.083723       0       20       0       0
QD   232       12        00.125603       0       20       0       0
CLQ             7     1997
QD   218       12        00.073843       0       20       0       0
QD   219       12        00.062506       0       20       0       0
QD   220       12        00.075298       0       20       0       0
QD   221       12        00.080966       0       20       0       0
QD   222       12        00.078107       0       20       0       0
QD   223       12        0 0.06391       0       20       0       0
QD   224       12        00.073843       0       20       0       0
QD   225       12        00.102286       0       20       0       0
QD   226       12        00.083826       0       20       0       0
QD   227       12        0 0.08523       0       20       0       0
QD   228       12        00.090899       0       20       0       0
QD   229       12        00.184657       0       20       0       0
QD   230       12        00.136349       0       20       0       0
QD   231       12        00.113624       0       20       0       0
QD   232       12        00.170461       0       20       0       0
CLQ            10     1997
QD   218       12        00.009716       0       20       0       0
QD   219       12        00.008224       0       20       0       0
QD   220       12        00.009908       0       20       0       0
QD   221       12        00.010653       0       20       0       0
QD   222       12        00.010277       0       20       0       0
QD   223       12        00.008409       0       20       0       0
QD   224       12        00.009716       0       20       0       0
QD   225       12        00.013459       0       20       0       0
QD   226       12        0 0.01103       0       20       0       0
QD   227       12        00.011215       0       20       0       0
QD   228       12        0 0.01196       0       20       0       0
QD   229       12        00.024297       0       20       0       0
QD   230       12        00.017941       0       20       0       0
QD   231       12        0 0.01495       0       20       0       0
QD   232       12        00.022429       0       20       0       0
ENDDATA
```

E.3 Element Inflow Hydrograph Input File for August 7-21, 1997 : aug_qei.hyd

```
TE      August element inflow hydrograph jd=218 is August 7, 1997
QEI           764       1    1997
QE   218       12        00.032063       0       20       0
QE   219       12        00.027141       0       20       0
QE   220       12        00.032695       0       20       0
QE   221       12        00.035156       0       20       0
QE   222       12        00.033915       0       20       0
QE   223       12        0 0.02775       0       20       0
QE   224       12        00.032063       0       20       0
QE   225       12        00.044414       0       20       0
QE   226       12        00.036398       0       20       0
QE   227       12        00.037008       0       20       0
QE   228       12        00.039469       0       20       0
QE   229       12        0 0.08018       0       20       0
QE   230       12        00.059204       0       20       0
QE   231       12        00.049337       0       20       0
QE   232       12        00.074016       0       20       0
QEI           766       1    1997
QE   218       12        00.017003       0       20       0
QE   219       12        00.014393       0       20       0
QE   220       12        00.017338       0       20       0
QE   221       12        00.018644       0       20       0
```

```
QE    222       12        00.017985       0       20       0
QE    223       12        00.014716       0       20       0
QE    224       12        00.017003       0       20       0
QE    225       12        00.023553       0       20       0
QE    226       12        00.019302       0       20       0
QE    227       12        00.019625       0       20       0
QE    228       12        00.020931       0       20       0
QE    229       12        0 0.04252       0       20       0
QE    230       12        00.031396       0       20       0
QE    231       12        00.026163       0       20       0
QE    232       12        00.039251       0       20       0
QEI             94        1    1997
QE    218       12        00.009716       0       20       0
QE    219       12        00.008224       0       20       0
QE    220       12        00.009908       0       20       0
QE    221       12        00.010653       0       20       0
QE    222       12        00.010277       0       20       0
QE    223       12        00.008409       0       20       0
QE    224       12        00.009716       0       20       0
QE    225       12        00.013459       0       20       0
QE    226       12        0 0.01103       0       20       0
QE    227       12        00.011215       0       20       0
QE    228       12        0 0.01196       0       20       0
QE    229       12        00.024297       0       20       0
QE    230       12        00.017941       0       20       0
QE    231       12        0 0.01495       0       20       0
QE    232       12        00.022429       0       20       0
QEI            724        1    1997
QE    218       12        00.009716       0       20       0
QE    219       12        00.008224       0       20       0
QE    220       12        00.009908       0       20       0
QE    221       12        00.010653       0       20       0
QE    222       12        00.010277       0       20       0
QE    223       12        00.008409       0       20       0
QE    224       12        00.009716       0       20       0
QE    225       12        00.013459       0       20       0
QE    226       12        0 0.01103       0       20       0
QE    227       12        00.011215       0       20       0
QE    228       12        0 0.01196       0       20       0
QE    229       12        00.024297       0       20       0
QE    230       12        00.017941       0       20       0
QE    231       12        0 0.01495       0       20       0
QE    232       12        00.022429       0       20       0
ENDDATA
```

Appendix F. Input Files for Steady Harmonic Test

F.1 R10 Input File for Steady Harmonic : harmonic.r10

```
OUTFIL  harmonic
BCFIL   harmonic.alt
INBNGEO both2du.geo
OUTBNRSTharmonic.rst
OUTBNRESharmonic.res
INHARM  harmonic.hmc
ENDFIL
TI      North and South Rivers where jd=194 is July 14
C0            0       0    1997     195   19.05       3
C1            0       1       0       1       1       1
C2           42   2.777     831    1107       1
C3         1.00    1.00                   0.5    0.02    0.06
C4          0.0     20.     0.0     0.1     0.1    100.     0.0
C5            0       9     0.0    2000       2       0      10       0       1
CV      0.02000 0.02000 0.02000    0.20      .2     .25       0
ED1           1    5000    5000    5000    5000   0.020    1.00    1.00
ED2                  20     0.1 .000050    0.00
ED1           2    9000    9000    9000    9000   0.080    1.00    1.00
ED2                  20     0.1 .000050    0.00
ED1           3    5000    5000    5000    5000   0.025    1.00    1.00
ED2                  20     0.1 .000050    0.00
CC1         323     324
CC1        2510    2511    2512
CC1        1882    1883
CC1        1082    1083
CC1         289     473
CC1         538     541
CC1         307     409
CC1         924     931
CC1         550     595
CC1         472     605
CC1         606    1259
CC1         608     609
CC1         610     666
CC1         669     683
CC1        1034    1036    1038
CC1        2513    2514    2515
CC1        2516    2517    2518
CC1        2519    2520    2521
CC1        2522    2523    2524
CC1         577     665     578
CC1        1014    1017    1019
CC1        1022    1025    1028
CC1        1029    1030    1032
ENDGEO
DT
BC
QC            1       0  0.1633   0.426       0     -20      -1       0
QC            3       0 0.12687   6.106   0.000     -20      -1       0
QC            6       0 0.06733   4.785   0.000     -20      -1       0
QC            7       0 0.09208   2.253   0.000     -20      -1       0
QC           10       0 0.00452     1.7   0.000     -20      -1       0
QC           13       0 0.00300     0.6   0.000     -20      -1       0
HC            2       0   2.468    35.0   -20.0      -1       2
EFE         764       0       1 0.2       0.000     -20      -1       0
```

```
EFE            94        0        1 0.2        0.000      -20       -1        0
EFE           766        0        1 0.2        0.000      -20       -1        0
EFE           724        0        1 0.20       0.000      -20       -1        0
ENDSTEP
ENDDATA
```

F.2 ALT Boundary Condition Input File for Steady Harmonic : harmonic.alt

```
DT          0.050
BC             10       10       20       10       10       20       10       10       20
QC              1        0   0.2633    0.426        0      -20       -1
QC              3        0  0.12687    6.106    0.000      -20       -1
QC              6        0  0.09733    4.785    0.000      -20       -1
QC              7        0  0.13208    2.253    0.000      -20       -1
QC             10        0  0.00652      1.7    0.000      -20       -1
QC             13        0  0.00500      0.6    0.000      -20       -1
EFE           764        0        1      0.5    0.000      -20       -1
EFE            94        0        1      0.5    0.000      -20       -1
EFE           766        0        1      0.5    0.000      -20       -1
EFE           724        0        1      0.50   0.000      -20       -1
ENDSTEP
ENDDATA
```

F.3 HMC Harmonic Tidal Input File for Steady Harmonic : harmonic.hmc

```
HARMONIC COEFFICIENTS
 YR MO DA HOUR THOURS C0-TILT
 97  7 15   19     24.00     01.50
    1 = NUMBER OF CONSTITUENTS
    ampltd      speed      equil     kappap        NFR     consti
 1.4000000    0.50589   90.00000 000.00000    1.00000       M2
      35.0       -20.0      -20.0
```